Advanced Technologies for Device-to-device Communications Underlaying Cellular Networks

Yue Wu

Department of Electronic and Eletrical Engineering
University of Sheffield

A thesis submitted in partial fulfilment of the requirements for the degree of
Doctor of Philosophy

Submission Date July 2016

I would like to dedicate this thesis to my loving parents

Declaration

I hereby declare that except where specific reference is made to the work of others, the contents of this dissertation are original and have not been submitted in whole or in part for consideration for any other degree or qualification in this, or any other university. This dissertation is my own work and contains nothing which is the outcome of work done in collaboration with others, except as specified in the text and Acknowledgements. This dissertation contains fewer than 65,000 words including appendices, bibliography, footnotes, tables and equations and has fewer than 150 figures.

Yue Wu
July 2016

Acknowledgements

I am thankful to my supervisors, Dr. Xiaoli Chu and Dr. Wei Liu, who guided me tirelessly throughout my PhD. I want to especially thank my first supervisor, Dr. Xiaoli Chu, for her selfless dedication in helping me with my research works. Dr. Xiaoli Chu and Dr. Wei Liu are both brilliant researchers who were always able to push ideas one step forward, provide valuable suggestions needed to accomplish a task, and share experiences about the research process. I was especially fortunate to work with both of them and benefit from both of their perspectives.

The work in this thesis is the result of collaboration with many other people. A special thanks goes to Dr. Weisi Guo. He contributed in all the works in this thesis. Without his valuable suggestions and comments, there would not be this thesis. Chapter 2 is the joint work with Dr. Weisi Guo, Dr. Siyi Wang, Wuling Liu, Dr. Xiaoli Chu and Prof. Jie Zhang [3], [4]. Chapter 3 is a collaborated works with Dr. Weisi Guo, Haonan Hu, Dr. Xiaoli Chu and Prof. Jie Zhang [11]. Chapter 4 is a joint work with Dr. Siyi Wang, Wuling Liu, Dr. Weisi Guo and Dr. Xiaoli Chu [1]. Chapter 5 is a joint work with Dr. Weisi Guo, Yuan Hu, Long Li, Dr. Xiaoli Chu, Dr. Siyi Wang and Prof. Jie Zhang [2].

Beyond direct collaborators on the works in this thesis, many other people contributed to my graduate work and made the four years PhD studies become an unforgettable experience. I want to thank Dr. Bowei Yang, who provided supercomputer cluster for running the simulations in this thesis. I also want to thank the staff of Iceberg team, who were responsible for maintaining the supercomputer cluster of University of Sheffield. They provide helpful comments on how to optimise my simulations for the cluster and definitely save my life. During the IEEE International Conference on Communications (ICC 15') held in London, 2015, I was very fortunate to meet with Dr. Guanding Yu, who gave me many constructive suggestions on my research works. Over numerous cups of coffee and tea, Mengyang Qiu, Jingxiao Su and Lantian Zhang provided fantastic advice and ideas on my research works. Wuling Liu and Ran Tao were great fun to hang out with and great collaborators on some neat ideas. Finally, the Wireless Communications Group of University of Sheffield was an amazing group which truly inspired me in my four year PhD studies.

I want to thank Prof. Jie Zhang for his constant support to my research works. I am highly grateful for the cheerful encouragement and advice from Ms. Qing Wei and Mr. Yufei Peng. Without such support and encouragement, I can barely finish my PhD studies.

I was also very fortunate to work with Dr. Jiming Chen and Long Li on a joint research project between University of Sheffield and Huawei Technologies Co. Ltd. This project provided me a great opportunity to have an insight in the state-of-art wireless technologies that were deployed in the cellular networks. The conversations with Dr. Jiming Chen and the experts from Huawei also inspired several ideas presented in this thesis.

Last but not least, I want to thank my family and friends for their unwavering support throughout my PhD studies.

Abstract

The past few years have seen a major change in cellular networks, as explosive growth in data demands requires more and more network capacity and backhaul capability. New wireless technologies have been proposed to tackle these challenges. One of the emerging technologies is device-to-device (D2D) communications. It enables two cellular user equipment (UEs) in proximity to communicate with each other directly reusing cellular radio resources. In this case, D2D is able to offload data traffic from central base stations (BSs) and significantly improve the spectrum efficiency of a cellular network, and thus is one of the key technologies for the next generation cellular systems.

Radio resource management (RRM) for D2D communications and how to effectively exploit the potential benefits of D2D are two paramount challenges to D2D communications underlaying cellular networks. In this thesis, we focus on four problems related to these two challenges. In Chapter 2, we utilise the mixed integer non-linear programming (MINLP) to model and solve the RRM optimisation problems for D2D communications. Firstly we consider the RRM optimisation problem for D2D communications underlaying the single carrier frequency division multiple access (SC-FDMA) system and devise a heuristic sub-optimal solution to it. Then we propose an optimised RRM mechanism for multi-hop D2D communications with network coding (NC). NC has been proven as an efficient technique to improve the throughput of ad-hoc networks and thus we apply it to multi-hop D2D communications. We devise an optimal solution to the RRM optimisation problem for multi-hop D2D communications with NC. In Chapter 3, we investigate how the location of the D2D transmitter in a cell may affect the RRM mechanism and the performance of D2D communications. We propose two optimised location-based RRM mechanisms for D2D, which maximise the throughput and the energy efficiency of D2D, respectively. We show that, by considering the location information of the D2D transmitter, the MINLP problem of RRM for D2D communications can be transformed into a convex optimisation problem, which can be efficiently solved by the method of Lagrangian multipliers. In Chapter 4, we propose a D2D-based P2P file sharing system, which is called Iunius. The Iunius system features: 1) a wireless P2P protocol based on Bittorrent protocol in the application layer; 2) a simple centralised routing mechanism for multi-hop D2D communications; 3) an

interference cancellation technique for conventional cellular (CC) uplink communications; and 4) a radio resource management scheme to mitigate the interference between CC and D2D communications that share the cellular uplink radio resources while maximising the throughput of D2D communications. We show that with the properly designed application layer protocol and the optimised RRM for D2D communications, Iunius can significantly improve the quality of experience (QoE) of users and offload local traffic from the base station. In Chapter 5, we combine LTE-unlicensed with D2D communications. We utilise LTE-unlicensed to enable the operation of D2D in unlicensed bands. We show that not only can this improve the throughput of D2D communications, but also allow D2D to work in the cell central area, which normally regarded as a "forbidden area" for D2D in existing works.

We achieve these results mainly through numerical optimisation and simulations. We utilise a wide range of numerical optimisation theories in our works. Instead of utilising the general numerical optimisation algorithms to solve the optimisation problems, we modify them to be suitable for the specific problems, thereby reducing the computational complexity. Finally, we evaluate our proposed algorithms and systems through sophisticated numerical simulations. We have developed a complete system-level simulation framework for D2D communications and we open-source it in Github: https://github.com/mathwuyue/py-wireless-sys-sim .

List of Publications

Publications

[1] Y. Wu, S. Wang, W. Liu, W. Guo, and X. Chu, "Iunius: A cross-layer peer-to-peer system with device-to-device communications," *IEEE Transactions on Wireless Communications*, vol. 15, no. 10, pp. 7005–7017, Oct. 2016.

[2] Y. Wu, W. Guo, H. Yuan, L. Li, S. Wang, X. Chu, and J. Zhang, "Device-to-device meets LTE-unlicensed," *IEEE Communications Magazine*, vol. 54, no. 5, pp. 154–159, May 2016.

[3] Y. Wu, W. Liu, S. Wang, W. Guo, and X. Chu, "Network coding in device-to-device (D2D) communications underlaying cellular networks," *2015 IEEE International Conf. Commun. (ICC)*, pp. 2072–2077, Jun. 2015.

[4] Y. Wu, S. Wang, W. Guo, X. Chu, and J. Zhang, "Optimal resource management for device-to-device communications underlaying SC-FDMA systems," *2014 9th International Symposium on Communication Systems, Networks Digital Signal Processing (CSNDSP)*, pp. 569–574, Jul. 2014.

[5] S. Qiu, W. Guo, B. Li, Y. Wu, X. Chu, S. Wang, and Y. Y. Dong, "Long range and long duration underwater localization using molecular messaging," *IEEE Transactions on Molecular, Biological and Multi-Scale Communications*, vol. 1, no. 4, pp. 363–370, Dec. 2015.

[6] B. Yang, Y. Wu, X. Chu, and G. Song, "Seamless handover in software-defined satellite networking," *IEEE Communications Letters*, vol. 20, no. 9, pp. 1768–1771, Sep. 2016.

[7] S. Wang, W. Guo, Z. Zhou, Y. Wu, and X. Chu, "Outage probability for multi-hop d2d communications with shortest path routing," *IEEE Communications Letters*, vol. 19, no. 11, pp. 1997–2000, Nov. 2015.

[8] W. Guo, S. Wang, Y. Wu, J. Rigelsford, X. Chu, and T. O'Farrell, "Spectral- and energy-efficient antenna tilting in a hetnet using reinforcement learning," *Wireless Communications and Networking Conference (WCNC), 2013 IEEE*, pp. 767–772, Apr. 2013.

[9] B. Yang, G. Song, Y. Chen, Y. Zheng, and Y. Wu, "Qos-aware indiscriminate volume storage cloud," *Concurrency and Computation: Practice and Experience*, 2016.

[10] B. Yang, G. Song, Y. Zheng, and Y. Wu, "Qosc: A qos-aware storage cloud based on hdfs," *2015 International Symposium on Security and Privacy in Social Networks and Big Data (SocialSec)*, pp. 32–38, Nov. 2015.

Submitted

[11] Y. Wu, W. Guo, H. Hu, X. Chu, and J. Zhang, "Location-based radio resource management for device-to-device communications," *IEEE Trans. Commun.*, Jul. 2016.

[12] Y. Wu, B. Yang, W. Guo, X. Chu, S. Wang, and H. Zhang, "A software-defined network protocol for device-to-device communications: Challenges, solutions and business model," *IEEE Network*, Jul. 2015.

[13] R. Tao, Y. Wu, B. Yang, X. Chu, and J. Zhang, "Small cell throughput optimization with in-band wireless backhaul," *IET Electronic Letters*, Jul. 2016.

Table of contents

List of Figures

List of Tables

List of Abbreviations

3GPP 3rd Generation Partnership Project.

AWGN additive white Gaussian noise.

B&B branch-and-bound.

BS base station.

CA context aware.

CC conventional cellular.

CCA clear channel assessment.

COT channel occupancy time.

D2D device-to-device.

DF decode-and-forward.

DL downlink.

FDD frequency division duplex.

GPSR greedy perimeter stateless routing.

HD half duplex.

IAR interference avoidance routing.

LBT listen-before-talk.

LP linear programming.

LTE Long-Term Evolution.

LTE-U LTE-unlicensed.

MCS modulation and coding scheme.

MINLP mixed integer nonlinear programming.

NC network coding.

OFDMA orthogonal frequency-division multiple access.

P2P peer-to-peer.

QoE quality of experience.

QoS quality of service.

RAT radio-access technology.

RB resource block.

RRM radio resource management.

SC-FDMA single carrier frequency division multiple access.

SINR signal to interference and noise ratio.

SPPP spatial Poisson Point Process.

SPR shortest-path-routing.

UE user equipment.

UL uplink.

Chapter 1

Introduction

Recent years we have seen an explosive growth in data demand which requires an evolution of current cellular network. As a result, a wide range of new wireless technologies have been developed for such challenge. Millimetre wave mobile communication is proposed to enable cellular user equipment (UE) to communicate at an extreme high frequency (30GHz – 300GHz), so that it may utilise more bandwidth and thus improve the system throughput [14]. Hyper-dense small cells deployment is under test to meet the "1000x mobile data traffic challenge" by Qualcomm and other institutes [15]. Massive MIMO is proposed as an evolution from conventional point-to-point MIMO in order to help concentrate energy into ever smaller regions of space to manifestly improve the throughput and radiated energy efficiency [16]. LTE-unlicensed is developed to allow cellular UE sharing unlicensed frequency bands with Wi-Fi [17]. Finally, device-to-device (D2D) communication is proposed to offload local data traffic from cellular base stations (BSs) and improve cellular spectrum efficiency by enabling two UEs in proximity to communicate with each other directly reusing cellular radio resources.

In this thesis, we focus on developing advanced technologies to improve the performance of D2D communications, which is one of the key technologies in the next generation network as aforementioned. In this chapter, we would first introduce the concept of D2D communications, following by concluding the paramount challenges in D2D communications. Then we discuss the state-of-art researches in D2D communications. Finally we summarise our achievements and present the structure of this thesis.

1.1 D2D Communications

Direct communication technology is not a new concept. There already exists several wireless technologies which allow two UEs to communicate each other directly. Two

conventional direct communication technologies are Bluetooth [18] and WiFi-direct [19]. In Internet-of-Thing (IoT), Zigebee protocol is proposed for machine-to-machine (M2M) communication [18]. In addition, new technologies such as HiperLan2 are proposed for fast local area direct communications [20]. The potential of these direct communications that can offload local data traffic from cellular network and improve the throughput of cellular UEs are studied in [21], [22]. However, all the aforementioned technologies are operated in unlicensed bands and without infrastructure support. This causes three problems: 1) cannot improve the spectrum efficiency of cellular network; 2) not able for efficient interference management; and 3) connecting to each other requiring manual settings [23].

To tackle such problems, a new kind of direct communication technology, D2D communications underlaying cellular network is proposed [23]. D2D communications enable two cellular UEs in proximity to communicate with each other directly by reusing the licensed band. Thus D2D can improve the cellular spectrum efficiency and efficient interference management is possible to be applied to it. In addition, for BS-assisted D2D communications, the peer discovery and link establishment can be set up by BS without manual settings.

The prototype of D2D communication is proposed in [24], [25], which was called FlashLinq. The authors realised the D2D prototype utilising field-programmable gate array (FPGA) board and tested the throughput of a simple system consisting only one pair of D2D UEs [25]. A more detailed introduction of the concept of D2D communications is firstly published in [23]. The authors presented the overview of D2D communications and summarised some early works in this area. Based on the works of Flashlinq, LTE-Direct was proposed by Qualcomm, which was the first industrial experimental D2D network [26]. Recently, D2D communication is well known as one of the key technologies in 5G and its industrial standardisation is in progress conducted by 3GPP organisation [27].

Although the BS in the cellular network will not involve into the data transmissions between a pair of D2D UEs, it might help in the progress of peer discovery, link establishment and radio resource management (RRM) for D2D communications [23]. In this case, it is called BS-assisted D2D communications (or network-assisted D2D, controlled D2D) [23], [28]. Otherwise, it is called autonomous D2D communications [28]. LTE-Direct proposed by Qualcomm is an autonomous D2D system [26]. However, in many existed researches, authors considered BS-assisted D2D communications, as the assistance from central BS may provide more efficient peer discovery, link managements and RRM for D2D communications [23], [28]–[33]. In this thesis, we also consider BS-assisted D2D communications.

Based on how D2D reuses cellular resources, it can be grouped into two types: D2D communications underlaying cellular network and D2D communications overlaying cellular network [28]. For D2D communications underlaying cellular network, D2D may share the

same radio resources with CC UEs [23], [28]; while for D2D communications overlaying cellular network, D2D and CC UEs would exclusively share the radio resources [28]. Most of the current researches focus on D2D underlaying cellular network as intuitively it can better exploit the spectrum efficiency of cellular networks. There exists several researches on mode selection of D2D, which compare the advantages and disadvantages of these two modes under different scenarios [34]–[36].

1.2 Challenges in D2D Communications

There are several paramount challenges in D2D communications. Peer discovery and link establishment are the first two challenges for setting up D2D communications [23], [29]. For autonomous D2D communication, it requires D2D UEs to broadcast message, search potential peers and set up the links all by themselves [23], [26]. In [37], the authors suggested to utilise Dynamic Source Routing (DSR) for peer discovery in autonomous D2D communications, which requires the D2D UEs to flood discovery message periodically for peer discovery. The authors argued that such mechanism can efficiently find D2D pairs in local area. For BS-assisted D2D communications, BS may help D2D UEs broadcast the connection messages and set up the communication links [23], [30]. In [38], the authors proposed an efficient centralised peer discovery schemes for D2D communications based on graph theory. In [23], [29] the authors discussed how the core network may involve in the link establishment of D2D communications. Then in [39], the authors proposed a signalling mechanism for D2D link establishment. We note that, these two problems draw major research interests from the industry and is under standardisation process organised by 3GPP [27].

After the D2D link is set up, interference management and radio resource management (RRM) then become the most problems for D2D communications [23], [32]. For D2D communications underlaying cellular networks, the D2D UEs reuse the cellular radio resources and thus may cause the interference to the CC UEs and vice versa. Such mutual interference may significantly jeopardise both D2D and CC communications. A proper RRM for D2D communications is the most efficient approach to this problem [23], [32], [40]. Furthermore, although for D2D overlaying cellular networks there is no mutual interference between D2D and CC communications, the D2D occupies part of the radio resources. Thus a proper RRM is also critical for D2D communications overlaying cellular network [41]. It can be concluded that, a well-designed RRM scheme for D2D is critical in improving its performance (e.g., throughput, energy efficiency and etc.) while maintaining the performance of CC UEs [28], [32]. We note that, there have already existed extensive researches in RRM

for D2D communications and this thesis also focus on this area. There are several other techniques that may deal with the interference management for D2D and thus improve its performance, including cooperative communications [3], [42], [43], beamforming for D2D UEs [44], interference alignment [45] and interference cancellation for D2D communications [44], [46]. In addition, MIMO is expected to further improve the throughput of D2D communications [47]. However, there are several limitations of these techniques. [3] and [43] are only for multi-hop D2D. [44] and [47] require new hardware components on devices, while [45] requires new signal structure of D2D communications, wherein the signals from D2D UEs are designed to be aligned in the orthogonal space of CC links. Finally, [46] requires the D2D receiver having the knowledge of the interfered source, and [42] requires the D2D transmitter having the knowledge of the CC transmitting source.

There are some new challenges for D2D communications in next generation cellular networks. In [33] introduces a game-theory approach for the research of business value of D2D communications. We note that there may have four major emerging challenges for D2D in the next generation network [32], [48], [49].

D2D with millimetre wave (mmWave). mmWave is proposed for the next generation networks for very high data rate networks, as it enables cellular UEs operating at high frequency. It is quite suitable for D2D communications as it targets at short-range communications. It has unique propagation model and thus require new researches in how to combine D2D with mmWave network [50].

D2D with hyper-dense small cells. Current researches focus on D2D coexisting with macro cells, which the system model is relatively simple [23], [32]. The mutual interference situations for both D2D and CC UEs will be much more complicated if taking hyper-dense small cells into consideration. In addition, mode selection between CC small cell communications or D2D communications becomes a new problem to the system [51].

D2D with new core network infrastructure and applications. We see the evolution of core network in recent years. New technologies such as virtual network function (NFV) and software-defined network (SDN) have been applied into current core network. We note that, new protocols should be designed for D2D communications in order to extend the capabilities of D2D and make it compatible for future core network. We have seen the researches in area is in the ascendant [52], [53].

1.3 Related Works

In this thesis, we focus on the radio resource management and developing new technologies for D2D communications. In this section, we would summarise the state-of-art researches in these areas.

As mentioned in [40], the joint power control and subchannel allocation problem for D2D communications can be generally modelled as mixed integer nonlinear programming (MINLP) problem and solved by branch-and-bound algorithm [54]. However, MINLP problem is a NP-hard problem and lack of efficient algorithm to solve it. Thus assumptions are applied to the system model to reduce the problem complexity.

Early works include [34], [55]–[58], in which the authors consider a simplified system consisting of only a single cell with one D2D pair and one CC UE. More general scenarios consisting of multiple cells and arbitrary numbers of CC UEs and D2D pairs were considered in [3], [4], [59]–[62]. In [4], [59], the authors propose BS-assisted centralised RRM schemes for D2D communications in orthogonal frequency-division multiple access (OFDMA) and single-carrier FDMA (SC-FDMA) systems respectively. In [60] the authors propose a two-stage, semi-distributed RRM for D2D communications, while in [61] the authors further presents a distributed RRM scheme based on spatial Poisson point process (SPPP) analysis. In [62], the authors analyse the trade-off between the energy efficiency and the transmission delay of D2D communications, and propose an optimal RRM scheme to achieve the Pareto optimal for the trade-off based on fractional programming and Lyapunov optimisation. The authors propose RRM schemes for conventional multi-hop D2D communications and multi-hop D2D with network coding (NC) in [37] and [3] respectively. Furthermore, in [63], the authors demonstrated the spectral efficiency and energy efficiency of multi-hop D2D with physical network coding (NC), direct D2D and CC communications via central BS. The mobility of D2D UEs are considered in [64], [65]. In [64] the authors give the theoretical boundary of energy efficiency of D2D communications considering the UEs movements. In [65], the author proposed a algorithm for UEs to choose between CC and D2D communications according to their moving velocity. Non-orthogonal subchannel allocation for D2D communications is considered in [66]. The authors assume that multiple D2D communications can share same subchannels and formulate the power control problem for D2D as a convex problem. Advanced system models of D2D communications are considered in [67]–[69]. In [67], the authors propose an analytic framework for D2D communications based on spatial Poisson Point Process (SPPP). In [68], the authors propose an optimal RRM scheme for D2D communications coexisting of heterogeneous network based on game theory. In [69], the authors consider the QoS-delay requirement instead of the SINR requirement for the CC UEs and propose an optimal RRM scheme for D2D

communication while guaranteeing the effective capacity requirement (i.e., the QoS-delay requirement) of CC communications. These works give insight into RRM and interference management for D2D communications and significantly improve the throughput performance of D2D communications while guaranteeing the quality of service (QoS) requirement of conventional cellular (CC) UEs.

Instead of the numerical optimisation approach for the joint power control and subchannel allocation problem for D2D communications, game theory can be utilised to solve the problem. As the QoS requirement of CC UEs should always be fulfilled, the RRM problem for D2D communications is formulated as a Stackelberg game. A Stackelberg equilibrium or a more general Nash equilibrium then can be achieved [70]–[74]. If we consider a non-cooperative game model of the RRM problem for D2D communications, then a pseudo distributed RRM scheme can be derived for D2D communications [66], [73], [75]. For the BS-assisted D2D communications, as the BS can act as a central coordinator for the radio resource usage for both CC and D2D UEs, the RRM problem for D2D can be further formulated as a coalition game [76], [77]. In [78], the authors assume that the BS is aware of the channel state of CC UEs and the locations of the D2D UEs. Then the authors model the subchannel assignments for D2D UEs as a minimum-weighted partitioning and the power control problem for the D2D as a multi-agent learning game. Based on these, the authors present a hybrid centralised-distributed RRM scheme for D2D communications.

1.4 Summary of Results

Our works are based on the current researches and take one more step. The thesis focus on enhancing the quality of service (QoS) and of device-to-device (D2D) communications underlaying cellular networks. Specifically, the thesis strives to enhance the performance (e.g., throughput, energy efficiency and etc.) of D2D communications while guaranteeing the QoS requirement of conventional cellular user equipments (UEs) in different scenarios. Two major methods are utilised: 1) apply different advanced wireless communications techniques to D2D communications, and 2) develop related optimal radio resource management (RRM) schemes for D2D communications.

The thesis mainly consists of five research topics in D2D communications:

1. Optimisation of RRM schemes for D2D communications and its underlaying cellular networks.

2. Network coding (NC) in D2D communications.

3. Location-based analysis in D2D communications.

4. Novel peer-to-peer (P2P) system based on D2D communications, including a new application layer P2P protocol and a joint design of routing algorithm and RRM for multi-hop D2D communications.

5. How to apply LTE-unlicensed into D2D communications.

1.5 Thesis Plan

The thesis is organised as follows. Chapter 2 introduces the RRM schemes for D2D communications, focus on enhancing the throughput of D2D underlaying SC-FDMA system [4] and multi-hop D2D with NC [3]. Chapter 3 then gives a comprehensive analysis of key performance metrics of D2D communications in a geometrical perspective [11]. Chapter 4 proposes Iunius, a novel P2P system based on D2D communications and evaluates how this system can significantly enhance the QoS of cellular UEs [1]. Chapter 5 demonstrates how advanced wireless technology, such as LTE-unlicensed, can further boost the performance of D2D communications [2]. Finally, we conclude our works and discusses possible future works in Chapter 6.

Chapter 2

Optimised Radio Resource Management for D2D: MINLP Approach

2.1 Introduction

In this chapter, we present fundamental designs of RRM schemes for D2D communications. We start from considering the optimal RRM problem for single-hop D2D underlaying Single Carrier Frequency Division Multiple Access (SC-FDMA) system, and further considering optimal RRM scheme for multi-hop D2D with network coding (NC) and cache.

As we mentioned in Chapter 1, RRM scheme is crucial for enhancing the performance of D2D communications while maintaining the QoS requirement for CC communications. Profound researches have been conducted to propose optimal RRM schemes for D2D communications under different assumptions. However, we note that, before our work [4] has been published, there is few researches considering the RRM scheme for D2D underlaying SC-FDMA system. We believe this problem is important, as SC-FDMA is the UL access scheme in the 3GPP-Long Term Evolution (LTE) standard, and D2D is better to reuse UL resources other than DL resources as discussed in [29]. In addition, in previous works, authors utilised Shannon capacity formula when to calculate the throughput in their optimisation problems [34], [55], [56], [59], [79], [80], which is not precise in systems that utilise realistic modulation schemes [81]. In our work, we leverage an empirical formula proposed in [81], which takes capacity saturation of real modulation schemes into consideration while maintaining tractable characteristic, to calculate the throughput. We would see in the following discussions that our proposed scheme provides a substantial improvement in the total throughput of D2D communications without compromising the QoS requirements of CC UEs.

Then we take a step further, considering the RRM scheme for multi-hop D2D with NC and caching capability at UEs. Simple RRM scheme is proposed for multi-hop D2D in [37]. However, such scheme is either optimal nor considering cooperative techniques for multi-hop communications. In [32], the authors demonstrated the potential to apply NC, an efficient cooperative techniques which can reduce the amount of transmissions in multi-hop communications, into D2D communications. We propose a practical solution to realise it and a related optimal RRM for multi-hop D2D with NC enabled.

In this chapter, we do centralised RRM for D2D communications, which we always assume all the channel state information (CSI) are known to the BS.

2.2 Radio Resource Management for D2D in SC-FDMA System

In this section, we optimise the resource management of CC UEs and D2D communications that use uplink resources in a SC-FDMA system. We study this problem from two aspects, power control and RB allocation. We first consider the general optimisation of power control for both D2D UEs and CC UEs assuming resource blocks (RBs) have been pre-allocated to them. The UE data rate will be calculated by utilising a curve-fitting based modulation and coding scheme (MCS) proposed in [81]. A realistic multi-cells system model that contains an arbitrary number of CC UEs and D2D communication pairs is considered. A power control optimisation algorithm is proposed to maximise the D2D communication throughput while maintaining the QoS of CC UEs. We then propose an optimal RB allocation scheme for D2D links taking all SC-FDMA RB allocation restrictions into consideration. Combining these two designs together leads to a composite optimal resource management mechanism for the D2D communications. Our approach overcomes the limitations in the aforementioned works and our results show that the throughput of D2D communications can be significantly improved under certain QoS constraints for CC UEs.

2.2.1 System Model

We consider a multi-cell environment, where each cell optimises its own radio resources with awareness of intra- and inter-cell interference measurements. For each cell, we consider a multi-user system where N_C CC UEs ($C_1, C_2, \ldots, C_{N_C}$) and N_D D2D pairs (N_D D2D transmitters, $D_1^T, \ldots, D_{N_D}^T$ and N_D D2D receivers, $D_1^R, \ldots, D_{N_D}^R$) exist, and a BS located at the center of the cell, as illustrated in Fig. 2.1. We focus on the uplink employing SC-FDMA with the transmission bandwidth B divided into K orthogonal RBs. We assume that the D2D

communications may reuse all uplink frequency bands and the resource allocations for the D2D communications and the cellular communications are independent. As specified in [82], the RB allocation in SC-FDMA should be obligated to two restrictions:

1. *adjacency*, that is when multiple RBs are allocated to one UE, they should be adjacent; and

2. *exclusivity*, which indicates that any RB can only be allocated to at most one CC UE and/or one D2D pair in a cell.

In terms of power allocation, the transmit power of each UE for a RB is limited to $P_{\max}$. The total transmit power of a D2D link should be no larger than $P^{\dagger}_{\max}$.

We consider a channel model consisting distance based path loss, multipath fading and shadowing. Thus the channel gain g of a link can be expressed as:

$$g = \kappa d^{-\alpha} \cdot \|h\|^2 \cdot \zeta, \tag{2.1}$$

where κ is a constant determined by the environment [82], α is the path loss distance exponent, d is the distance between the transmitter and receiver, h is the Rayleigh fading coefficient and ζ is the shadowing gain with log-normal distribution.

The interference scenario is depicted in Fig. 2.1. A D2D transmitter generates interference to the BS and the corresponding D2D receiver suffers from the interference generated by CC UEs which utilise the same RBs as the D2D link. Assume the RB allocation is predetermined. Then for a RB k which is allocated to CC UE $i(k)$ and D2D pair $j(k)$, the received signal to interference and noise ratio (SINR) at the BS can be written as:

$$\gamma_k^{j(k)} = \frac{g_k^{i(k)} P_k^{i(k)}}{g_k^{j(k)i(k)} P_k^{j(k)} + I_k^{i(k)} + N_0} \tag{2.2}$$

where $g_k^{i(k)}$ and $g_k^{j(k)i(k)}$ represent the channel gain (as defined in (2.1)) of the cellular uplink and the interference link from $j(k)^{\text{th}}$ D2D transmitter to BS respectively, $P_k^{i(k)}$ and $P_k^{j(k)}$ are the transmit power of $i(k)^{\text{th}}$ CC UE and the $j(k)^{\text{th}}$ D2D transmitter for k^{th} RB respectively, $I_k^{i(k)}$ is the inter-cell interference power, N_0 is the additive white Gaussian noise (AWGN) power.

The received SINR of the k^{th} RB at the $j(k)^{\text{th}}$ D2D receiver can be written as:

$$\gamma_k^{j(k)} = \frac{g_k^{j(k)} P_k^{j(k)}}{g_k^{i(k)j(k)} P_k^{i(k)} + I_k^{j(k)} + N_0} \tag{2.3}$$

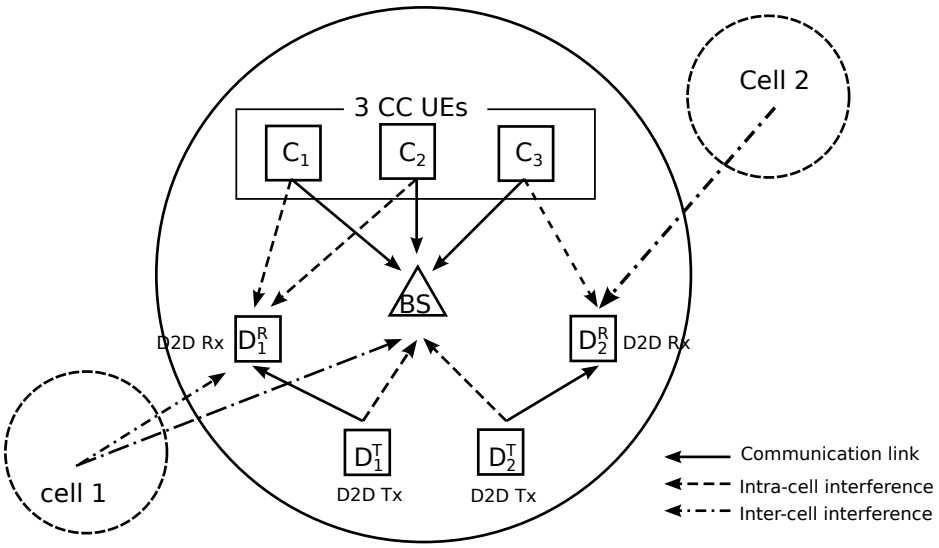

Fig. 2.1 System model of D2D communications underlaying cellular network where $N_C = 3$ CC UEs and $N_D = 2$ D2D pairs share the uplink resources. The intra-cell interference includes the interference from D2D transmitters to the BS and the interference from the CC UEs to the D2D receivers.

where $g_k^{j(k)}$ and $g_k^{i(k)j(k)}$ represent the channel gain (as defined in (2.1)) of the D2D link and the interference link from $i(k)^{\text{th}}$ CC UE to the $j(k)^{\text{th}}$ D2D receiver respectively, and $I_k^{j(k)}$ is the inter-cell interference to the D2D receiver.

The objective is to maximise the total throughput of D2D communications, while guaranteeing that every CC UE has an uplink SINR no less than γ_t to satisfy the QoS requirement. To compute the UE's data rate in terms of its SINR, we apply the result from [81], which describes the relation between the SINR and the data rate more precisely than using the Shannon's capacity formula. As mentioned above, the D2D pairs leverage all cellular uplink RBs. Thus their total throughput ($R_D^{\dagger}$) is equal to the total throughput of all RBs, i.e.

$$R_D^{\ddagger} = \sum_{k=1}^{K} a \arctan\left(\frac{\gamma_k^{j(k)} + b}{c}\right) \tag{2.4}$$

where $a\arctan((\gamma + b)/c)$ is the data–rate formula proposed in [81], and the parameters a, b and c are determined by the actual MCS and channel model. Its specific advantage over Shannon capacity formula is that it considers capacity saturation of real modulation schemes. And its advantage over alternative saturate capacity formula is that it is very tractable in optimisation frameworks. According to [81], the parameters a, b and c for combined adaptive MCS (adaptive modulation from QPSK to 64QAM, along with turbo coding) for LTE are $a = 2.27, b = 13, c = 40$ (for SINR from -6dB to 40dB), which are used in this work. Based

on (2.4), the optimisation problem is formulated as

$$\text{OPT:} \quad \underset{\boldsymbol{P}_C,\boldsymbol{P}_D}{\arg\max}\, a \sum_{k=1}^{K} \arctan\left(\frac{\gamma_k^{j(k)}+b}{c}\right) \tag{2.5}$$

subject to:

$$0 \le P_k^{i(k)} \le P_{\max}, \qquad 0 \le P_k^{j(k)} \le P_{\max} \tag{2.6}$$

$$\sum_{l\in\mathscr{K}_{j(k)}} P_l^{j(k)} \le P_{\max}^{\dagger}, \qquad \forall j(k) \in \{1,2,\ldots,N_D\} \tag{2.7}$$

$$\gamma_k^{j(k)} \ge \gamma_t, \qquad \forall k \in \{1,2,\ldots,K\} \tag{2.8}$$

where $\boldsymbol{P}_C$ and $\boldsymbol{P}_D$ are transmit power vectors for CC UEs and D2D transmitters respectively, $\mathscr{K}_{j(k)}$ is the set of RBs assigned to D2D link $j(k)$ and γ_t is the uplink SINR threshold of a CC UE. Inequation (2.6) is the fundamental power allocation constraint for both CC UEs and D2D transmitters [82]. Inequation (2.7) defines the total power budget constraint for each D2D transmission. Inequation (2.8) is the QoS constraint for each CC UE.

Solving the optimisation problem (2.5) subject to the constraints (2.6), (2.7) and (2.8) is a challenging task, as it is difficult to verify whether $R_D^{\ddagger}$ is concave or not [83]. In Subsection 2.2.2 we will propose an analytical characterization of the optimal solution to (2.5).

2.2.2 Optimal Power Management

In this section we focus on solving the power management optimisation problem (2.5). We will show that (2.5) can be transformed into a concave problem which has a closed form solution. As a first step, note that from (2.2) we have $P_k^{i(k)} = (\gamma_k^{i(k)}(g_k^{j(k)i(k)}P_k^{j(k)} + I_k^{i(k)} + N_0))/g_k^{i(k)}$ and substituting it in (2.3) we have

$$\gamma_k^{j(k)} = \frac{g_k^{i(k)} g_k^{j(k)} P_k^{j(k)}}{g_k^{i(k)j(k)}\gamma_k^{i(k)}(g_k^{j(k)i(k)}P_k^{j(k)} + I_k^{i(k)}) + g_k^{i(k)}(I_k^{j(k)} + N_0)} \tag{2.9}$$

Since $R_D^{\ddagger}$ defined in (2.5) is monotonically increasing in $\gamma_k^{j(k)}$ ($\forall k \in \{1,\ldots,K\}$), and from (2.9) we can see that $\gamma_k^{j(k)}$ is monotonically decreasing in $\gamma_k^{j(k)}$ for fixed $P_k^{j(k)}$ ($\forall k \in \{1,\ldots,K\}$), the $\gamma_k^{j(k)}$ should be γ_t to achieve the optimal solution while maintain the QoS

constraints (2.8). Combining this result with (2.9) we obtain

$$\gamma_k^{j(k)} = \frac{g_k^{i(k)} g_k^{j(k)} P_k^{j(k)}}{g_k^{i(k)j(k)} \gamma_t (g_k^{j(k)i(k)} P_k^{j(k)} + I_k^{i(k)}) + g_k^{i(k)} (I_k^{j(k)} + N_0)} \tag{2.10}$$

which can be proved to be a concave function in $P_k^{j(k)}$ and the optimal power solution can be solved by Lagrangian multipliers and Karush-Kuhn-Tucker (KKT) conditions[81], [83], [84]. Introducing the Lagrange multipliers, $\boldsymbol{\lambda}$, corresponding to constraints in (2.7), and KKT multipliers, $\boldsymbol{\mu}, \boldsymbol{\nu}$, corresponding to constraints in (2.6), we obtain the following optimal power solution ($P_k^{i(k)*}$, $P_k^{j(k)*}$)

$$\begin{aligned} P_k^{i(k)*} &= \frac{\gamma_t (g_k^{j(k)i(k)} P_k^{j(k)*} + I_k^{i(k)} + N_0)}{g_k^{i(k)}} \\ P_k^{j(k)*} &= \frac{-\omega_k^* + \sqrt{(\omega_k^*)^2 - 4\rho_k^* \phi_k^*}}{2\rho_k^*} \end{aligned} \tag{2.11}$$

where ρ_k^*, ϕ_k^*, ω_k^* are defined in (2.12) [1]

$$\begin{aligned} \rho_k^* &= c(g_k^i g_k^j)^2 + 2bc g_k^i g_k^j g_k^{ij} g_k^{ji} \gamma_t + (b g_k^{ij} g_k^{ji} \gamma_t)^2 \\ \phi_k^* &= (c g_k^{ij} \gamma_t + g_k^{ji})^2 + (b^2 + c^2) \left(g_k^{ij} \gamma_t (I_k^i + N_0) + g_k^i (I_k^j + N_0) \right)^2 \\ &\quad - \frac{ac (g_k^i)^2 g_k^j \left(g_k^{ij} \gamma_t (I_k^i + N_0) + g_k^i (I_k^i + N_0) \right)}{g_k^i (\lambda_j + \nu_k) + \mu_k \gamma_t g_k^{ji} g_k^{ji}} \\ \omega_k^* &= 2 \left(g_k^{ij} \gamma_t (I_k^i + N_0) + g_k^i (I_k^j + N_0) \right) \left((b^2 + c^2) g_k^{ij} g_k^{ji} \gamma_t + bc g_k^i g_k^j \right) \end{aligned} \tag{2.12}$$

The Lagrange multipliers and KKT multipliers can be solved from the complimentary slackness conditions [83], [84]:

$$\lambda_{j(k)} \Big(\sum_{l \in \mathscr{K}_{j(k)}} P_l^{j(k)*} - P_{\max}^{\dagger} \Big) = 0 \tag{2.13}$$

$$\mu_k \Big(\frac{\gamma_t (g_k^{j(k)i(k)} P_k^{j(k)*} + I_k^{i(k)} + N_0)}{g_k^{i(k)}} - P_{\max} \Big) = 0 \tag{2.14}$$

$$\nu_k (P_k^{j(k)*} - P_{\max}) = 0 \tag{2.15}$$

[1] The index k of $i(k)$ and $j(k)$ in (2.12) is dropped for simplicity.

Since $\lambda_{j(k)} > 0$, we get

$$\sum_{l \in \mathscr{K}_{j(k)}} P_l^{j(k)*} = P_{\max}^{\dagger}, \quad \forall j(k) \in \{1, \ldots, N_D\} \tag{2.16}$$

and if $\mu_k \neq 0$ or $\nu_k \neq 0$ we obtain

$$\begin{aligned} P_k^{i(k)*} &= \frac{\gamma_t (g_k^{j(k)i(k)} P_k^{j(k)*} + I_k^{i(k)} + N_0)}{g_k^{i(k)}} \\ P_k^{j(k)*} &= \min \left\{ P_{\max}, \frac{1}{g_k^{j(k)i(k)}} \left(\frac{g_k^{i(k)} P_{\max}}{\gamma_t} - I_k^{i(k)} - N_0 \right) \right\} \end{aligned} \tag{2.17}$$

otherwise when $\mu_k = 0$ and $\nu_k = 0$, $\lambda_{j(k)}$ can be derived from solving (2.11) and (2.16). This is a polynomial equation which is difficult to solve algebraically. Note that finding numerical solution for a polynomial equation has been widely studied in numerical analysis research and efficient algorithms have been proposed [85]. For the purpose of illustration in this paper, we simply use the built-in Matlab function *fsolve* to solve the problem, which performs Levenberg-Marquardt and trust-region-reflective methods to find the numerical solution.

We see that (2.17) is a "greedy" power allocation scheme for D2D communications. With this scheme the D2D communications transmit at the maximum power within the power per RB constraint (2.6) and the QoS constraint for CC UEs (2.8), and thus have the maximum throughput of D2D communications. However this solution might be infeasible due to the total transmit power constraint, i.e. there is no $\lambda_{j(k)} > 0$ can satisfy (2.16). In this case, $\mu_k = 0$, $\nu_k = 0$ and $\lambda_{j(k)}$ is derived from (2.16) whereby the power allocation for D2D communications shown in (2.11) can be interpreted as a combination of *channel-inversion* and *water-filling* [81].

From these discussions, we are finally able to conclude the power management scheme for the CC UEs and D2D transmitters. With a specific RB allocation scheme for cellular and D2D communications, where RB k is allocated to CC UE $i(k)$ and D2D pair $j(k)$ in the network, the optimal transmit powers of UE $i(k)$ and UE $j(k)$ for RB k $(P_k^{i(k)*}, P_k^{j(k)*})$ are given by

- (2.17) if it is feasible;
- otherwise derive $\lambda_{j(k)}$ from (2.16) for $\mu_k = 0, \nu_k = 0$ and the power control scheme is shown in (2.11).

2.2.3 Optimal Resource management scheme

In preceding sections we considered the power management scheme for CC UEs and D2D communications. Specifically, we proposed an optimal power control scheme assuming that the RBs have been properly allocated to CC UEs and D2D links. Most of previous work on resource allocation for D2D communications underlaying cellular network typically focused on a single subchannel selection problem, whereby a D2D pair is restricted to be assigned only one subchannel in a transmission time interval [57], [79]. In this section, we focus on the resource allocation for D2D communications in the SC-FDMA system, which is a multi-user multi-subchannel allocation problem.

We assume that RBs have been assigned to CC UEs in advance. This assumption is applicable to the case where some resource allocation scheme of SC-FDMA system is employed for CC UEs. Let $\mathscr{K}_j$ denote the set of RBs assigned to D2D pair j. Due to the RB adjacency restriction, we require the K RBs to be divided into exactly N_D ordered sets, wherein each set has n_j adjacent RBs, and such that $K = n_1 + n_2 + \cdots + n_{N_D}$. Without loss of generality, we assume that n_j is pre-determined. In this case, there are $N_D!$ possible RB allocations. To get an idea of how complex this is, assuming the 3GPP-LTE test case of $N_D = 10$ D2D pairs [82], this would require searching through over 3.6 million possible RB allocations. Thus this straightforward approach is apparently not practical.

Our approach is to use dynamic programming to solve the problem. This approach is based on recursion and eliminates any redundant computation in the recursion process. The algorithm can be simply explained as follows: the recursion process divides the problem into several subproblems each with a smaller search space. In each sub-call, we solve a subproblem by 1) directly obtaining the solution from the solution table if possible; otherwise 2) using dynamic programming algorithm and storing the solution into the solution table.

Algorithm 1 is the pseudo-code for our algorithm. Ordered set $\{\mathscr{K}_{Avail}\}$ and n (Line 1) indicate the available groups of RBs to be allocated in each sub-call and the cardinality of the set respectively, thus the recursion process stops as soon as $n = 1$ (Lines 2–10). The *solutionTable* (Line 1) is empty at the beginning and is used to store the subresults. The function **getFromSolutionTable** (Lines 5, 17) achieves the pre-stored subresult from *solutionTable*. The optimal power control scheme proposed in Section 2.2.2 is implemented in the function **OptPowerCtrlThroughput** (Lines 7, 22), wherein the input is a RB allocation scheme and the output is the optimal throughput. In the pseudo-code we define three operators $\leftarrow, \ominus, \oplus$ on the ordered sets (Lines 15–28), which perform getting an element, removing a specific element and adding a specific element to the set respectively.

function RBALLOCATION($\{\mathscr{K}_{Avail}\}$,n,solutionTable)
  if $n = 1$ **then**
    $t \leftarrow \{\mathscr{K}_{Avail}\}$
    if $R(t) \in$ *solutionTable* **then**
      $R(t) \leftarrow$ **getFromSolutionTable**(t)
    else
      $R(t) \leftarrow$ **OptPowerCtrlThroughput**(t)
      solutionTable$\leftarrow R(t) \oplus$ *solutionTable*
    end if
    return $[R(t), t]$
  end if

  $R_{\max} \leftarrow 0$
  $optAllocationSet \leftarrow emptySet$
  for all $t \leftarrow \{\mathscr{K}_{Avail}\}$ **do**
    if $R(\{\mathscr{K}_{Avail}\} \ominus t) \in$ *solutionTable* **then**
      $[R(\{\mathscr{K}_{Avail}\} \ominus t), allocationSet] \leftarrow$ **getFromSolutionTable**$(\{\mathscr{K}_{Avail}\} \ominus t)$
    else
      $[R(\{\mathscr{K}_{Avail}\} \ominus t), allocationSet] \leftarrow$ **getRBAllocation**$(\{\mathscr{K}_{Avail}\} \ominus t, n-1,$ *solutionTable*)
      solutionTable$\leftarrow R(\{\mathscr{K}_{Avail}\} \ominus t) \oplus$ *solutionTable*
    end if
    $R(t) \leftarrow$ **OptPowerCtrlThroughput**(t) + R$(\{\mathscr{K}_{Avail}\} \ominus t)$
    if $R(t) > R_{\max}$ **then**
      $R_{\max} \leftarrow R(t)$
      $optAllocationSet \leftarrow t \oplus allocationSet$
    end if
  end for
  return $[R_{\max}, optAllocationSet]$
end function

Algorithm 1. Dynamic programming for RB allocation of D2D communications.

It can be proved that the total number of calculations of our approach is dramatically reduced from $N_D!$ to $N_D 2^{N_D-1} + \frac{N_D(N_D+1)}{2} - 1$ [86]. That is, with $N_D = 10$ as mentioned above, our approach would only require 5174 operations to find the optimal solution.

2.2.4 Simulation Results

In our simulation, the system simulated is a network containing 19 hexagonal cells, wherein each cell has 3 sectors. The channel model is simulated as Urban Micro (UMi) and the related path loss model is described in Table B.1.2.1–1 in [82]. CC UEs and D2D transmitters are uniformly distributed in the central cell. For each D2D transmitter, its

Table 2.1 Simulation Parameters

Parameter	**Value**
Inter site distance	500m
Uplink bandwidth	10MHz
Number of RBs	25
Noise power(N_0)	-121dBm
Pathloss exponent (α)	$1.5, 2, 2.5, 3, 3.5, 4, 4.5$
Maximum transmitting power ($P_{\max}$)	23dBm
D2D radius	20m
Number of CC UEs (N_C)	10
Number of D2D pairs (N_D)	10
QoS constraint for CC UEs (γ_t)	8.75dB
Multipath fading	Rayleigh distribution with the scale parameter of 0.5
Shadowing	Log-noraml distribution with standard deviation of 4dB

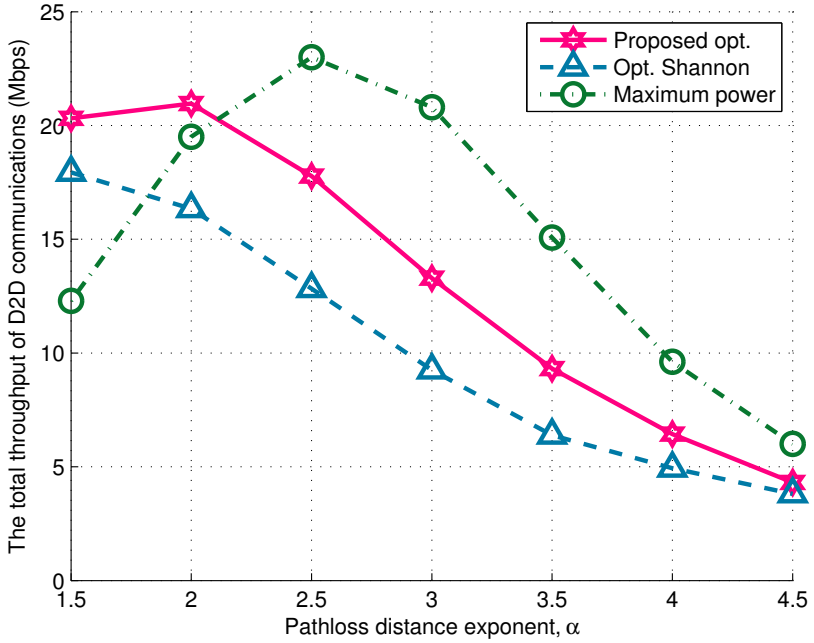

Fig. 2.2 Total throughput of D2D communications with different power control schemes and RR RB allocation scheme in SC-FDMA systems

corresponding receiver is uniformly distributed in a circle centred at the D2D transmitter with a radius of 20m. Other simulation parameters are summarized in Table 2.1.

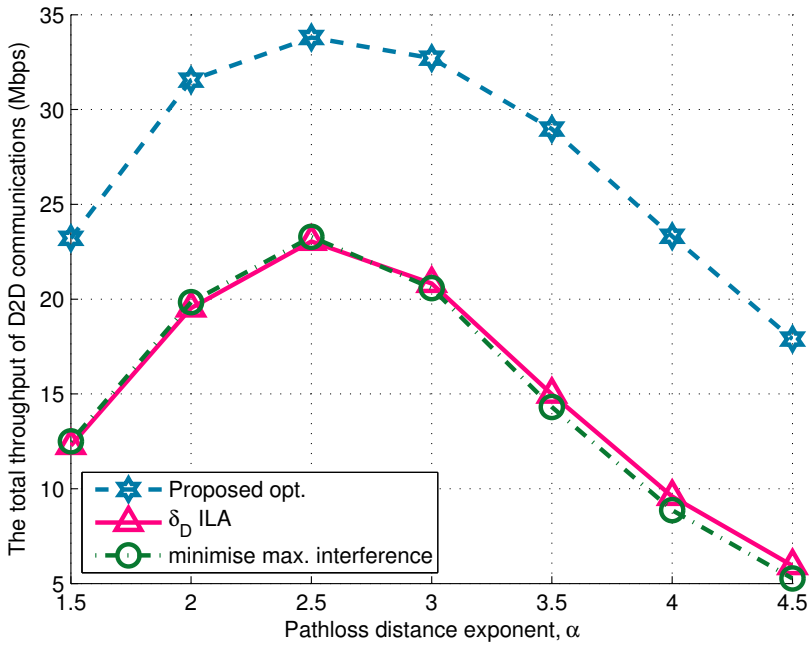

Fig. 2.3 Total throughput of D2D communications with different RB allocation schemes in SC-FDMA systems. The transmit power of each UE is 23 dBm.

We first evaluate the performance of the proposed power control scheme. In terms of RB allocation, we use round robin (RR) scheme for both CC UEs and D2D pairs, in which each UE is assigned an equal number of adjacent RBs in turn. We denote the pathloss distance parameter as α. We compare our results with the algorithm proposed in [80] and the simple power management which allows both CC UEs and D2D transmitters to operate at the maximum power level. In [80], the authors solved a similar power control optimisation problem for D2D communication as we do in this work, except that they utilised the Shannon capacity for the data rate of D2D communications. Fig. 2.2 shows the performance of different schemes in different pathloss environments. It can be observed that our scheme outperforms the optimal Shannon capacity power control scheme [80] in all interference scenarios and achieves at most 25% improvement. For $1.5 < \alpha < 2.2$ the proposed power control scheme outperforms the other two schemes, but for $\alpha > 2.2$ it is worse than the simple maximum power scheme. This is because the simple maximum power management scheme does not guarantee the QoS of CC UEs, and in large pathloss environments the transmit power of D2D communications should be significantly limited to guarantee the QoS requirement of CC UEs.

In Fig. 2.3, we compare the performance of our proposed RB allocation scheme with two other subchannel allocation schemes in different pathloss environments. We assume

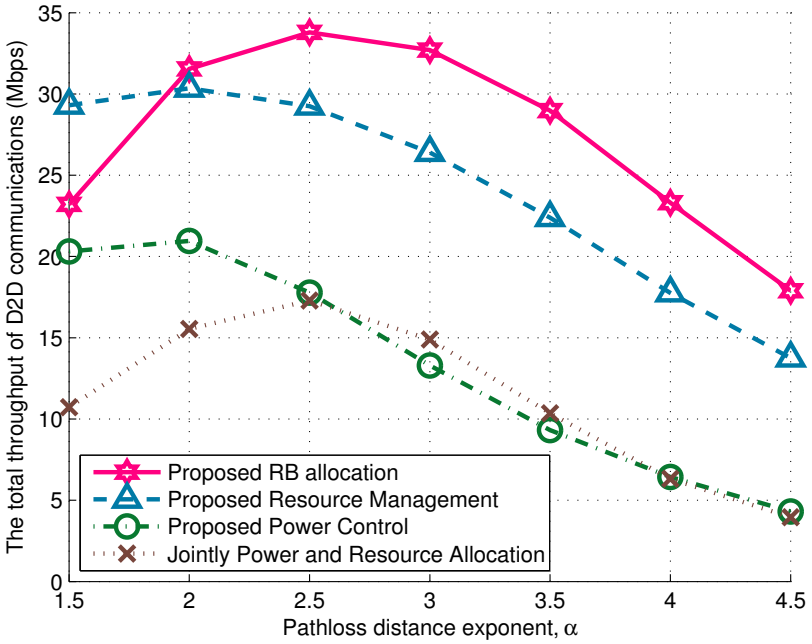

Fig. 2.4 Total throughput of D2D communications with proposed resource management scheme, proposed power control scheme, proposed RB allocation scheme and the jointly power and resource allocation scheme proposed in [34], in SC-FDMA systems.

every UE uses the maximum allowed transmit power $P_{\max} = 23$ dBm for a RB and there is no total transmit power restriction for D2D communications. For all values of α our scheme achieves significant improvement of total throughput of D2D communications compared with the δ_D-ILA scheme [79] and the minimised maximum interference scheme [57]. For $\alpha \geq 3.5$ in particular, improvement of 100% can be achieved with our proposed RB allocation scheme. We also include an approximate average computational time measurements for the proposed RB allocation scheme leveraging *tic-toc* method in Matlab. We see that dynamic programming is approximately 1400x more efficient than the exhaustive search algorithm.

Finally we evaluate the performance of our proposed optimal resource management scheme for D2D communications, which consists of the power control scheme in Section 2.2.2 and the RB allocation scheme in Section 2.2.3. From Fig. 2.4, it can be seen that our proposed resource management scheme significantly outperforms the existing jointly power and resource allocation scheme [34] in the uplink SC-FDMA system. This is mainly because we consider a more general scenario and remove the assumption that one D2D pair shares the same resources with only one CC UE in [34]. The improvement of throughput of D2D communications is more significant in a large pathloss environment, as we can see that for $\alpha = 4.5$ our proposed resource management scheme achieves almost 150% improvement.

It is worth noting that this improvement is achieved under the QoS constraint of CC UEs. If such QoS constraint of CC UEs can be ignored, then for $\alpha \geq 2$ the proposed RB allocation scheme with maximum transmit power for both CC UEs and D2D transmitters obtains the highest total throughput of D2D communications and for $\alpha = 2.5$ the total throughput reaches the maximum value of almost 35 Mbps. Finally, we can observe that for $1.5 \leq \alpha \leq 2.5$, the proposed power control scheme results in a substantial improvement in total throughput of D2D communications when compared to the existing jointly power and resource allocation scheme [34]. In larger path loss environments, our proposed power control scheme achieves roughly the same total throughput of D2D communications as the existing scheme [34], but with a reduced complexity.

2.2.5 Conclusion

A resource management mechanism is devised for D2D communications in co-existence with a multi-cell and multi-user SC-FDMA cellular network. The paper proposes two sub-routines: power control scheme and RB allocation scheme. We leverage on a tractable capacity formula devised for realistic modulation and coding schemes and consider a general system model. As a result, our analysis shows that our power control scheme has a better performance in terms of total throughput of D2D communications compared to previous works. The optimal RB allocation scheme for D2D communications is devised with a much reduced complexity compared to exhaustive search. It is shown that the proposed resource management scheme can achieve a total throughput of D2D communications of 30 Mbps in a moderate pathloss environment while guaranteeing a QoS requirement for other CC UEs, as well as significantly outperforms previous works in all pathloss environments.

2.3 Radio Resource Management for D2D with Network Coding

This section discusses the optimal RRM for multi-hop D2D with network coding (NC). We apply NC into multi-hop D2D communications and develop an optimised RRM mechanism for the resulting system. We consider a two-way relay model for D2D communications re-using uplink (UL) radio resources of a cellular network, which may have an arbitrary number of CC UL UEs. The proposed RRM scheme optimises both power control and subchannel assignment to maximise the throughput of D2D communications under QoS constraints for CC UL UEs. In addition, we investigate the impact of caching capabilities at the D2D relay on the system performance. Finally, we compare the data transmission performance of our proposed NC-D2D system supported by the optimised RRM mechanism with that of the multi-hop D2D system and the associated RRM in [37].

2.3.1 System Model

We consider D2D communications reusing UL radio resources of a multi-cell system as depicted in Fig. 2.5, where each cell performs its own RRM based on intra- and inter-cell interference measurements. There are N_C CC UL UEs uniformly distributed in the coverage area of a BS, each communicating directly with the BS. A pair of D2D UEs, D_a and D_b, are communicating with each other via relay UE D_R within the coverage area of the BS. The UL system bandwidth is orthogonally divided into K subchannels, each with a bandwidth B. Without loss of generality, we assume that each subchannel is exclusively assigned to one CC UL UE, i.e., $N_C = K$. This assumption is just for the simplicity in theoretical analysis and can be removed in practical implementations as we will show in Section 2.3.4. Furthermore, we assume that each UL subchannel can be re-used by at most one D2D transmitter. Finally, we assume that the RRM for D2D communications is controlled by the BS.

We consider a channel model consisting of distance dependent path loss, multipath fading and shadowing. Thus the channel gain g of a link can be expressed as:

$$g = \kappa d^{-\alpha} \|h\|^2 \zeta, \tag{2.18}$$

where κ is an environment related constant [82], α is the path loss distance exponent, d is the distance between the transmitter and receiver, h is the Rayleigh fading coefficient, and ζ denotes the log-normal distributed shadowing.

We apply NC to the D2D communications. Each NC transmission consists of two steps. In the first time slot, D_a and D_b send data packets S_a and S_b to the relay D_R, respectively.

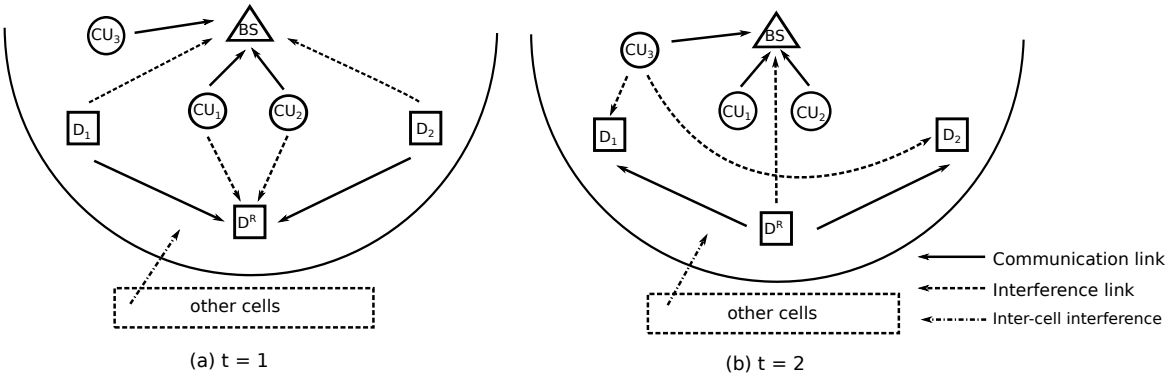

Fig. 2.5 Network system model. D2D UEs D_a and D_b are communicating with each other via a relay D_R re-using CC UL resource. Three CC UL UEs (CU_1,CU_2 and CU_3) have UL communications with BS. Subfigure (a) illustrates the links model in the first time slot and Subfigure (b) illustrates the links model in the second time slot.

Then in the second time slot, D_R performs the XOR operation on the two received packets and broadcasts the XOR result. D_a and D_b can obtain each other's packet by performing XOR on the packet received from the relay and the packet that they transmitted in the first step [87], [88], i.e.:

$$S_b = S_a \oplus (S_a \oplus S_b), \qquad S_a = S_b \oplus (S_a \oplus S_b). \tag{2.19}$$

The interference scenario during each step is shown in Fig. 2.5. In the first step, the two D2D transmitters generate interference to CC UL communications while the D2D relay D_R suffers from the interference caused by CC UL UEs (see in Fig. 2.5 (a)). Without loss of generality, assuming that subchannel $i\,(i \in \{1,\cdots,K\})$ is allocated to CC UL UE i, the signal to interference plus noise ratio (SINR) of CC UL UE i in time slot 1 can be expressed as

$$\gamma_c^{1,i} = \frac{g_c^{1,i} p_c^{1,i}}{\chi_a^i g_{a,c}^i p_a^i + \chi_b^i g_{b,c}^i p_b^i + I_c^{1,i} + N_0}, \tag{2.20}$$

where $p_c^{1,i}, p_a^i$ and p_b^i are the transmit power of CC UL UE i for a subchannel, D2D transmitters D_a and D_b, respectively, $g_c^{1,i}$ is the channel gain (as defined in (2.18)) of the link from CC UL UE i to the BS in time slot 1, $g_{a,c}^i$ and $g_{b,c}^i$ are the channel gains (as defined in (2.18)) of the interference links from D_a and D_b to the BS, respectively, $I_c^{1,i}$ is the inter-cell interference power received by the BS in subchannel i in time slot 1, N_0 is the additive white Gaussian noise (AWGN) power over a subchannel, and $\chi_j^i\,(j = a,b)$ are the indicators of subchannel

assignment for D_a and D_b respectively, which are defined as

$$\chi_j^i = \begin{cases} 1, & \text{if subchannel } i \text{ is allocated to } D_j, \\ 0, & \text{otherwise.} \end{cases} \tag{2.21}$$

Note that $\chi_a^i + \chi_b^i \leq 1, \forall i \in \{1, \cdots, K\}$.

If subchannel i is allocated to $D_j\,(j = a, b)$, the SINR in subchannel i at D_R can be written as

$$\gamma_{j,r}^i = \frac{g_{j,r}^i p_a^i}{g_{c,r}^i p_c^{1,i} + I_r^i + N_0}, \tag{2.22}$$

where $g_{j,r}^i$ and $g_{c,r}^i$ represent the channel gains (as defined in (2.18)) of the links from D_j and the CC UL UE i to D_R respectively, and I_r^i is the inter-cell interference power received by D_R in subchannel i.

To employ NC into the D2D communications, it is required that the D2D relay D_R can correctly decode the packets received from $D_j\,(j = a, b)$, i.e.,

$$\gamma_{j,r}^i \geq \beta, \tag{2.23}$$

where β is the SINR threshold required for correctly decoding at D_R. This is typically achieved in decode-and-forward relay systems [89]–[91].

In the second step, assuming that subchannel i is allocated to CC UL UE i and D_R broadcasts in subchannel i to D_a and D_b if $\chi_r^i = 1$ (otherwise $\chi_r^i = 0$), then D_R generates interference to CC UL UE i while D_a and D_b are interfered by CC UL UE i. The SINR of CC UL UE i in time slot 2 can be written as

$$\gamma_c^{2,i} = \frac{g_c^{2,i} p_c^{2,i}}{\chi_r^i g_{r,c}^i p_r^i + I_c^{2,i} + N_0}, \tag{2.24}$$

where $p_c^{2,i}$ and p_r^i are the transmit power of CC UL UE i and D2D relay D_R for a subchannel respectively, $g_c^{2,i}$ and $g_{r,c}^i$ are the channel gains (as defined in (2.18)) of the links from CC UL UE i and from D_R to the BS respectively, and $I_c^{2,i}$ is the inter-cell interference power received by the BS in subchannel i in time slot 2.

The SINRs at $D_j\,(j = a, b)$ are given by

$$\gamma_{r,j}^i = \frac{g_{r,j}^i p_r^i}{g_{c,j}^i p_c^{2,i} + I_j^i + N_0}, \tag{2.25}$$

where $g^i_{r,j}$ and $g^i_{c,j}$ represent the channel gains (as defined in (2.18)) of the links from D_R to D_j and from CC UL UE i to D_j respectively, and I^i_j is the inter-cell interference power received by D_j in subchannel i in time slot 2.

The upper bound of the achievable data rate of CC UL UE i in the first time slot:

$$R^{1,i}_c = B\log_2(1+\gamma^{1,i}_c). \tag{2.26}$$

The upper bound of the achievable data rate of CC UL UE i in the second time slot is as follows

$$R^{2,i}_c = B\log_2(1+\gamma^{2,i}_c). \tag{2.27}$$

The upper bound of the achievable data rate $R_{j,r}$ of the transmission from $D_j\,(j=a,b)$ to D_R in time slot 1 is given by

$$R_{j,r} = B\sum_{i=1}^{K}\chi^i_j\log_2(1+\gamma^i_{j,r}). \tag{2.28}$$

We assume that the duration t of a time slot is short enough that the channel state remains constant over t. Thus the number of data bits that are available to be broadcast by relay D_R in time slot 2 is given by

$$S^1_d = \min\{R_{a,r}t + d_a, R_{b,r}t + d_b\}, \tag{2.29}$$

where d_a and d_b are respectively the number of data bits previously received from D_a and D_b but have not been processed by the relay. Note that d_a and d_b can be set to 0 if there is no cache at the D2D relay D_R. We note that although (2.29) cannot be achieved in a realistic system, it can be seen as an upper bound approximation to the actual number of data bits the system can transmit.

In the second time slot, the transmission rate $R_{r,j}\,(j=a,b)$ of the link between D_R and D_j is given by

$$R_{r,j} = B\sum_{i=1}^{K}\chi^i_r\log_2(1+\gamma^i_{r,j}). \tag{2.30}$$

Thus the total number of data bits exchanged between D_a and D_b during the two time slots of a NC transmission can be written as

$$S^{\dagger}_d = 2\min\left\{\min\{S^1_d, R_{r,a}t\}, \min\{S^1_d, R_{r,b}t\}\right\}. \tag{2.31}$$

2.3.2 Problem Formulation

Base on the above system model, we formulate the RRM as an optimisation problem. Note that in the D2D underlaying cellular UL scenario, the channel allocation and transmit power of each CC UL UE is pre-determined and would not be changed when D2D communications take place. We aim to maximise the throughput of D2D communications in each NC transmission cycle without violating the QoS constraints of CC UL UEs. Thus the RRM optimisation problem can be formulated as follows

$$OPT: \quad \underset{\boldsymbol{p}_j, \boldsymbol{\chi}_j (j=a,b,r)}{\arg\max} \quad S_d^{\dagger} \tag{2.32}$$

subject to,

$$\chi_a^i + \chi_b^i \leq 1, \quad \forall i \in \{1, \cdots, K\} \tag{2.33}$$

$$\delta_j^i \leq p_j^i \leq p_{\max}, \quad \forall i \in \{1, \cdots, K\},\ j = a, b \tag{2.34}$$

$$0 \leq p_r^i \leq p_{\max}, \quad \forall i \in \{1, \cdots, K\} \tag{2.35}$$

$$R_c^{1,i} \geq \upsilon_i, R_c^{2,i} \geq \upsilon_i, \quad \forall i \in \{1, \cdots, N_C\} \tag{2.36}$$

where $\boldsymbol{p}_j$ and $\boldsymbol{\chi}_j\,(j = a, b, r)$ are transmit power vectors and subchannel assignment indicator vectors for D_j respectively, each vector is of size $K \times 1$, $\delta_j^i\,(j = a, b)$ is the minimum transmit power for D_j to satisfy the SINR requirement defined in (2.23), $p_{\max}$ is the maximum transmit power of a D2D UE can leverage, and υ_i is the QoS requirement for the i^{th} CC UL UE.

2.3.3 Radio Resource Management Mechanism

In this section, we will propose an optimal RRM mechanism for NC-D2D communications underlaying cellular networks by solving the optimisation problem *OPT* defined in (2.32).

The two steps in a NC transmission cycle are independent from each other. Thus the *OPT* defined in (2.32) can be divided into two sub-problems *OPT 1* for the first step and *OPT 2* for the second step:

$$\begin{aligned} OPT\ 1: \quad & \underset{\boldsymbol{p}_j, \boldsymbol{\chi}_j (j=a,b)}{\arg\max} \quad S_d^1 \\ \text{s.t.} \quad & (2.33)\text{–}(2.36) \end{aligned} \qquad \begin{aligned} OPT\ 2: \quad & \underset{\boldsymbol{p}_r, \boldsymbol{\chi}_r}{\arg\max} \left\{ \min\{R_{r,a}, R_{r,b}\} \right\} \\ \text{s.t.} \quad & (2.34) \text{ and } (2.36) \end{aligned}$$

We first solve the sub-problem *OPT 1*. Since the exclusive constraint (2.33) ensures that there is at most one D2D transmitter interfering the CC UL UE in subchannel i, substitut-

ing (2.20) and (2.26) into (2.36) and solving it for p_j^i, we have the following transmit power constraint for $D_j\,(j=a,b)$ in subchannel i:

$$p_j^i \le \frac{1}{g_{j,c}^i}\left(\frac{g_c^{1,i}p_c^{1,i}}{2^{\frac{v_i}{B}}-1} - I_c^{1,i} - N_0\right) \triangleq p_j^{i,*}. \tag{2.37}$$

Base on (2.34) and (2.37), we update the transmit power constraints for $p_j^i\,(j=a,b)$:

$$\delta_j^i \le p_j^i \le \min\{p_{\max}, p_j^{i,*}\} \triangleq \overline{p}_j^i. \tag{2.38}$$

According to (2.22), (2.28) and (2.29), for any given $\boldsymbol{\chi}_j\,(j=a,b)$, S_d^1 is strictly increasing in $\boldsymbol{p}_j$ and reaches its maximum value when the maximum transmit power is allocated for the assigned subchannel, i.e.,

$$p_j^i = \begin{cases} \overline{p}_j^i, & \chi_j^i = 1 \text{ and } \delta_j^i \le \overline{p}_j^i \\ 0, & \chi_j^i = 0 \text{ or } \delta_j^i > \overline{p}_j^i \end{cases} \tag{2.39}$$

Following (2.39), we reformulate the sub-problem *OPT 1* as follows.

$$\textit{MILP-OPT 1}: \quad \arg\max_{\boldsymbol{\chi}_{j\,(j=a,b)}} x \tag{2.40}$$

$$\text{s.t.} \quad x \le R_{j,r}t + d_j, \quad j=a,b \tag{2.41}$$

$$(2.33) \text{ and } (2.39) \tag{2.42}$$

where x is a continuous variable. *MILP-OPT 1* follows the form of a mixed integer linear programming (MILP) problem. Several efficient algorithms have been proposed to solve MILP problems [92], [93]. In this paper, we leverage the widely used *branch-and-bound* algorithm [92] to solve *MILP-OPT 1*. Exploring a variety of optimal/sub-optimal/heuristic MILP solving algorithms and evaluating their efficiency and applicability to our problem is beyond the scope of this paper.

The *branch-and-bound* (B&B) algorithm for solving *MILP-OPT 1* is presented in Fig. 2.6. Function *RRM_Step1* calls the function *B&B_Search* to form a *B&B tree* [92], the nodes of which are the elements of the vector $\boldsymbol{\chi}_j\,(j=a,b)$, and search through the *B&B tree*. In line 2, the vector of visited nodes ($\boldsymbol{\chi}_a$) and the incumbent maximum value of x in (2.40) (*maxVal*) are given the initial values of $\varnothing$ and 0, respectively. For each node visited, *B&B_Search* solves the linear programming (LP) relaxation with $\boldsymbol{\chi}_a$, which relaxes the integer constraint (2.21) to $0 \le \chi_j^i \le 1$ for *MILP-OPT 1*, and predicts the upper bound of the node (x_{LP}). A branch will be pruned in any of the following three cases: 1) the LP relaxation problem is infeasible;

1: **function** RRM_STEP1
2: $\boldsymbol{\chi}_j^*(j=a,b) \leftarrow$ B&B_SEARCH($\varnothing$, 0)
3: **return** $\boldsymbol{\chi}_j^*$
4: **end function**
5:
6: **function** B&B_SEARCH($\boldsymbol{\chi}_a$, maxVal)
7: $x_{LP}, \boldsymbol{\chi}_j^{LP}(j=a,b)) \leftarrow$ Solve LP relaxation of (2.40) with $\boldsymbol{\chi}_a$
8: **if** LP relaxation is infeasible **then**
9: **return** *prune branch*
10: **end if**
11: **if** $\boldsymbol{\chi}_j^{LP} \in \mathbb{Z}^+$ **then**
12: **if** $x_{LP} >$ maxVal **then**
13: maxVal $\leftarrow x_{LP}$
14: $S^* \leftarrow \boldsymbol{\chi}_j^{LP}$
15: **end if**
16: **return** *prune branch*
17: **end if**
18: **if** $x_{LP} \leq$ maxVal **then**
19: **return** *prune branch*
20: **end if**
21: **if** LEN($\boldsymbol{\chi}_a$)$< 2K$ **then**
22: B&B_SEARCH($(\chi_m = 0) \rightarrow \boldsymbol{\chi}_a$, maxVal)
23: B&B_SEARCH($(\chi_m = 1) \rightarrow \boldsymbol{\chi}_a$, maxVal)
24: **end if**
25: **return** S^*
26: **end function**

Fig. 2.6 Branch-and-bound algorithm for solving *MILP-OPT 1*.

2) the LP relaxation problem has an integer optimum solution; and 3) the upper bound of the branch is no larger than the incumbent maximum value (lines 8–20). If no pruning condition is met and the number of visited nodes is less than $2K$ (line 21), then an arbitrary unvisited node χ_m in $[\boldsymbol{\chi}_1, \boldsymbol{\chi}_2]/\boldsymbol{\chi}_a$ is attached with new branches leading to two successor nodes: $\chi_m = 0$ and $\chi_m = 1$ and the function *B&B_Search* is called for these two successor nodes respectively (lines 22–24). The algorithm recursively repeats these procedures until the solution of *MILP-OPT 1* is found.

In the worst case, the *branch-and-bound* algorithm would require 2^K calls of *B&B_Search* to solve the problem, but it has been proven to be practically efficient in most cases [92]. In our numerical experiments, the *branch-and-bound* routine arrives at the optimal solution within 20 calls of *B&B_Search*, and the LP relaxation problem typically converges within 100 iterations for $K = 50$.

Table 2.2 Simulation Parameters

Parameter	**Value**
Inter-site distance	500m
D2D radius	$10, 20, 30, 40, 50$m
SINR threshold (β)	0dB
Number of CC UL UEs (N_C)	5
NC time slot (t)	10ms
Uplink bandwidth	10MHz
Number of subchannels (K)	50
Noise power(N_0)	-121dBm
Pathloss exponent (α)	$1.5, 2, 2.5, 3, 3.5, 4$
Maximum transmit power ($p_{\max}$)	6dBm
Multipath fading	Rayleigh distribution with the scale parameter of 0.5
Log-normal shadowing	Standard deviation of 4dB

Next, we solve the sub-problem *OPT 2*. Similar to sub-problem *OPT 1*, by substituting (2.24) and (2.27) into (2.36) and solving it for p_r^i, we obtain the following transmit power constraint for the D2D relay:

$$p_r^i \leq \frac{1}{g_{r,c}^i}\left(\frac{g_c^{2,i} p_c^{2,i}}{2^{\frac{v_i}{B}}-1} - I_c^{2,i} - N_0\right) \triangleq p_r^{i,*}. \tag{2.43}$$

According to (2.30), if all available subchannels are allocated to the D2D relay, $R_{r,a}$ and $R_{r,b}$ might arrive at their maximum values. In addition, both $R_{r,a}$ and $R_{r,b}$ are strictly increasing functions of p_r^i. Thus, combining with (2.35), the optimal solution to *OPT 2* is given by

$$\chi_r^i = 1 \text{ and } p_r^i = \min\{p_{\max}, p_r^{i,*}\}, \quad i \in \{1, \cdots, K\} \tag{2.44}$$

The proposed optimal RRM mechanism for NC-D2D communications underlaying cellular UL can be summarised as:

- Before NC-D2D transmission begins, inter-cell interference plus noise power is estimated at the D2D receivers and the BS [29]. Channel gains g can be estimated using methods proposed in [29], [37].

- In time slot 1 of NC transmission, the transmit powers of D_a and D_b are defined in (2.39), and their subchannel assignments are obtained by the algorithm given in Fig. 2.6.

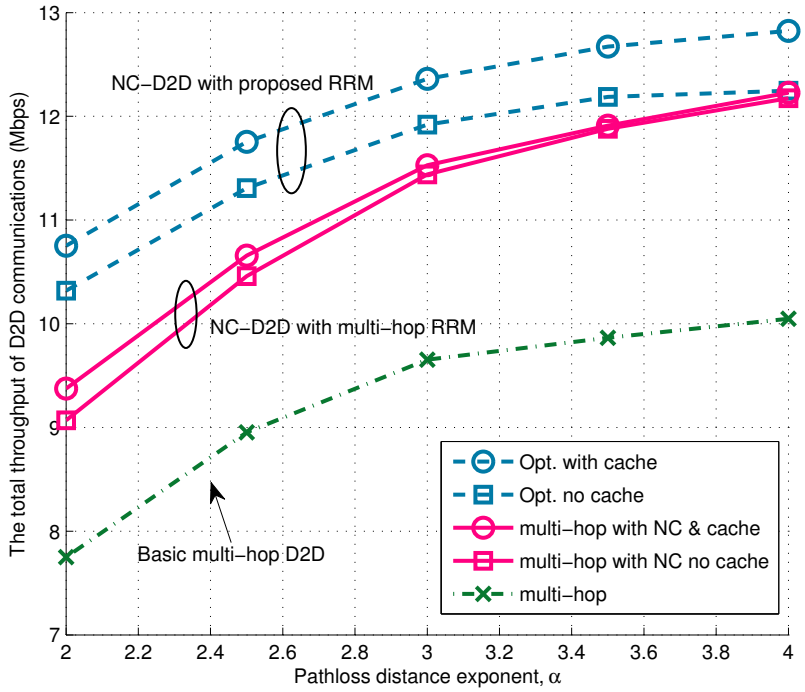

Fig. 2.7 D2D throughput versus path loss exponent. D2D radius is set as 20 m.

- In time slot 2 of NC transmission, all available subchannels are allocated to D_R and the corresponding transmit power follows (2.44).

2.3.4 Simulation Results

In this section, we present simulation results to evaluate the performance of the proposed NC-D2D RRM mechanism. The simulated network contains 19 hexagonal cells, each having 3 sectors. We evaluate the performance of the central cell, where $N_C = 5$ CC UL UEs and one D2D relay D_R are uniformly distributed in it. D_a and D_b are uniformly distributed in a circle centred at the D_R with a specific radius (called D2D radius and given in Table 2.2). For the other 18 cells, each cell contains 5 uniformly distributed CC UL UEs and their interference effects to the central cell UEs are simulated. We adopt the Urban Micro (UMi) channel model and the path loss model in Table B.1.2.1–1 of [82]. Other major simulation parameters are summarised in Table 2.2.

Two metrics are used in performance evaluation: the total throughput of D2D communications defined as $S_d^{\dagger}/(2t)$; and the transmission time required for D_a and D_b to exchange 1000 Mbits of data. As we can see in the subsequent discussions, with caching capabilities at D2D relay being used in NC-D2D transmissions, the typical inverse relationship between

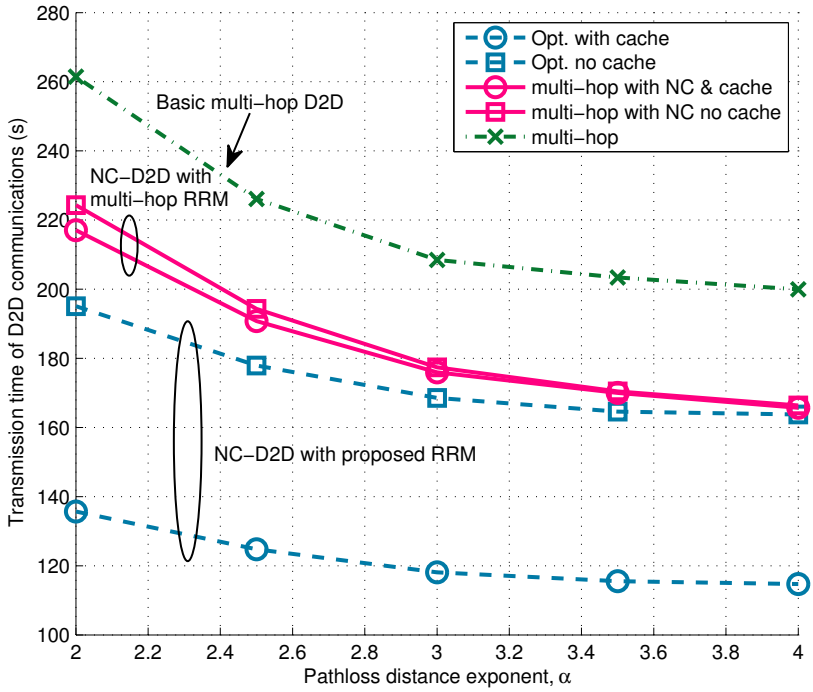

Fig. 2.8 D2D transmission time required to exchange 1000 Mbits in different path loss environment. D2D radius is set to 20m.

throughput and transmission time may not always hold. We compare the performance of our proposed NC-D2D RRM mechanism with two other schemes: the multi-hop D2D RRM mechanism in [37], and NC-D2D communications supported by the RRM mechanism in [37]. The RRM mechanism proposed in [37] can be summarised as: 1) the uplink CC UE transmits at a power level that keeps its SINR at $\eta\beta_C$ when the D2D communication is absent, where β_C is the QoS requirement for CC UEs and $\eta > 1$ is a control parameter; and 2) the D2D UE transmits at a power level that keeps the SINR of its interfered CC UE above β_C. For NC-D2D communications, we consider two scenarios: D_R with an unlimited cache, and D_R with no cache (i.e., d_a and d_b are set to 0 in (2.29)). The QoS constraint υ_i for each CC UL UE is uniformly distributed in the range $(0, \upsilon_c^i)$, where υ_c^i is the maximum data rate CC UL UE can achieve if the D2D communication is absent at the moment.

Fig. 2.7 shows the throughput of D2D communications versus pathloss exponents α, where the D2D radius is set at 20m. It can be seen that our proposed NC-D2D RRM mechanism outperforms the other two schemes for all pathloss exponents considered. This is because our proposed RRM optimizes the transmit power and subchannel assignments for the NC transmissions of D2D UEs. Since a larger α indicates a more isolated environment, the

throughput of D2D communications increases with α for all considered schemes. Compared to the conventional multi-hop D2D communications, NC-D2D achieves $15\% - 20\%$ improvement of throughput with the same RRM mechanism deployed. In addition, the availability of cache at the relay can always improve the throughput of NC-D2D communications, with more significant improvement under our proposed RRM as compared to the mutli-hop RRM in [37]. We note that, the trends of the throughput of D2D communications versus the path loss exponent α are different in Fig. 2.4 and Fig. 2.7. This is first because the two systems utilise different RB allocation schemes. For Fig. 2.4 the SC-FDMA system requires the allocated RBs for D2D communications are adjacent, while such limitation is removed for Fig. 2.7. This difference also shows how the path loss exponent affects the received signal power and the interference power of D2D communications is quite different in different scenarios. From Fig. 2.4, we can conclude that the path loss exponent has more effect on the received signal power of the D2D communications and thus the data rate of the D2D decreases as α increases in D2D underlaying SC-FDMA system. However, in Fig. 2.7 we see that the path loss exponent has more effect on the interference power of NC-D2D thus its data rate increases as α increases. The insight of how path loss exponent may affect the received signal power and the interfered signal power of D2D communications is worth of future researches.

Fig. 2.8 plots the total transmission time for D_a and D_b to exchange 1000 Mbits of data versus pathloss exponent α. It can be seen that NC can reduce the required transmission time of D2D communications for a given RRM. Our proposed NC-D2D RRM mechanism achieves the shortest transmission time among all schemes for all pathloss exponents considered. The cache capability at the D2D relay dramatically reduces the transmission time when our proposed RRM mechanism is deployed, while it is not that significant with the multi-hop RRM mechanism of [37]. First, the caching capabilities can reduce the number of re-transmissions. Second, our proposed RRM mechanism is designed to take into account caching at the relay, which is an improvement over multi-hop RRM mechanism in [37]. In all scenarios, the transmission time decreases as α increases. This is because the throughput of D2D communications increases when α increases, as the D2D links are more isolated from CC ULs. When the cache is available at the relay, our proposed NC-D2D algorithm can reduce the transmission time by $60\% - 85\%$ compared to the multi-hop RRM for D2D communications without NC and by $33\% - 57\%$ compared to NC-D2D with the multi-hop RRM mechanism.

In Figs. 2.9 and 2.10, we plot the throughput of D2D communications and time consumption for exchanging 1000 Mbits, respectively, versus the D2D radius, where pathloss exponent $\alpha = 3$. These two figures show that the total throughput of D2D communications

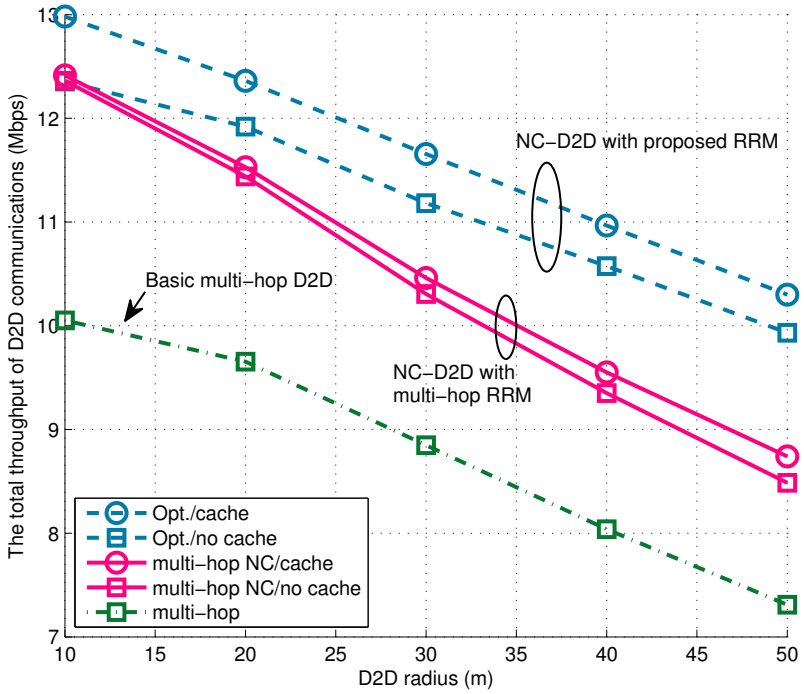

Fig. 2.9 D2D throughput with different D2D radius in a moderate path loss environment ($\alpha = 3$).

decreases and the transmission time increases as the D2D radius increases. This is because as the D2D radius increases, D_a, D_b and D_R are more likely to be far apart from each other. Moreover, the performance improvements offered by our proposed RRM mechanism over the multi-hop RRM scheme in [37] become more evident for NC-D2D communications as the D2D radius increases. As we can see in Fig. 2.10, with our proposed NC-D2D RRM mechanism and caching at the D2D relay, a maximum 100% reduction in transmission time can be achieved compared to the conventional multi-hop D2D communications. This result indicates the necessity of our proposed RRM mechanism for multi-hop D2D communications with source UE and destination UE being relatively far apart.

2.3.5 Conclusion

In this section, we have investigated the potential benefit of employing network coding (NC) to multi-hop D2D communications underlaying cellular networks. We focus on the two-way relay model, and have proposed an optimal RRM mechanism tailored for NC-D2D communications. The proposed RRM mechanism maximises the throughput of D2D communications while guaranteeing the QoS requirements of CC UL UEs. Our simulation

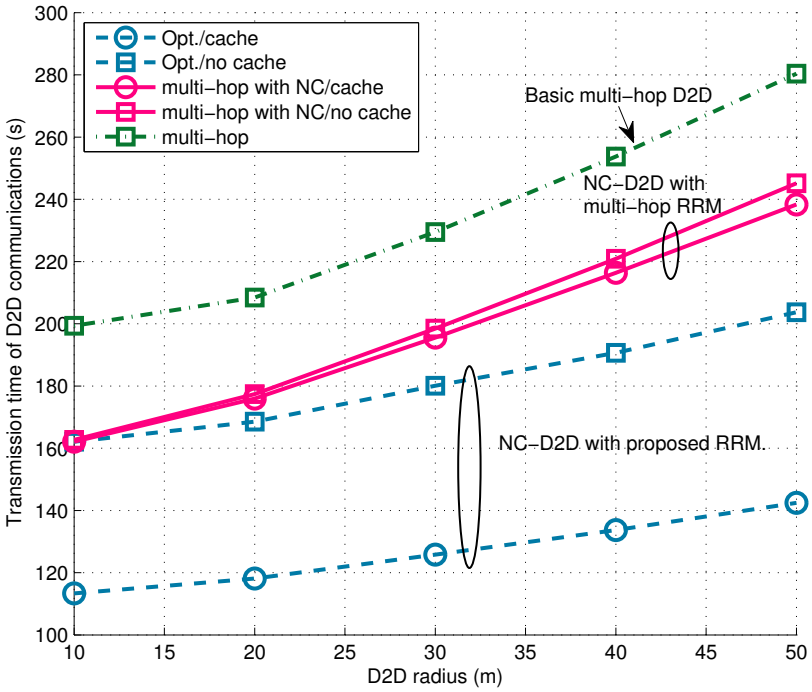

Fig. 2.10 D2D transmission time required for exchanging 1000 Mbits with different D2D radius in a moderate path loss environment ($\alpha = 3$).

results have shown that as compared to the conventional multi-hop D2D communications, NC-D2D supported by our proposed RRM mechanism can significantly improve the throughput and reduce the transmission time (maximum of 100%) for a given large file size. Moreover, the availability of cache at the D2D relay can further improve the system performance.

Chapter 3

Location-based Radio Resource Management for D2D

3.1 Introduction

Remind in the previous chapter, we demonstrate how optimal RRM may significantly boost the performance of D2D communications while guaranteeing the performance of CC communications. The proposed algorithms require accurate channel state information of multiple channels and solving an NP-hard mixed integer nonlinear programming (MINLP) problem. However, the impact of user location on both the RRM and the resulting D2D–CC coexistence performance has not been sufficiently studied.

In this chapter, we propose a novel location-based analytical framework for D2D communication reusing UL cellular resources, where inter-cell interference is modeled using SPPP [67], [94]–[96]. The proposed analytical framework gives insights in how the D2D transmitter's location in a cell may affect its performance and the optimal RRM for it. We first identify the key constraints (i.e., the maximum transmit power and transmission distance) of D2D communications as a function of the D2D's transmitter's location in a cell, so that the QoS of CC UL UEs can be guaranteed. Then we propose two low complexity RRM schemes, which jointly optimise the channel allocation and power control of D2D communications for maximizing the D2D throughput and energy efficiency. Finally, we demonstrate that the D2D throughput and the energy efficiency highly depend on the location of its transmitter in a cell and we discuss the trade-off between throughput and energy efficiency for D2D communications sharing the UL cellular resources.

The rest of the chapter is organized as follows. In Section 3.2 we present the system model and problem formulation. Then we derive the maximum allowed transmit power,

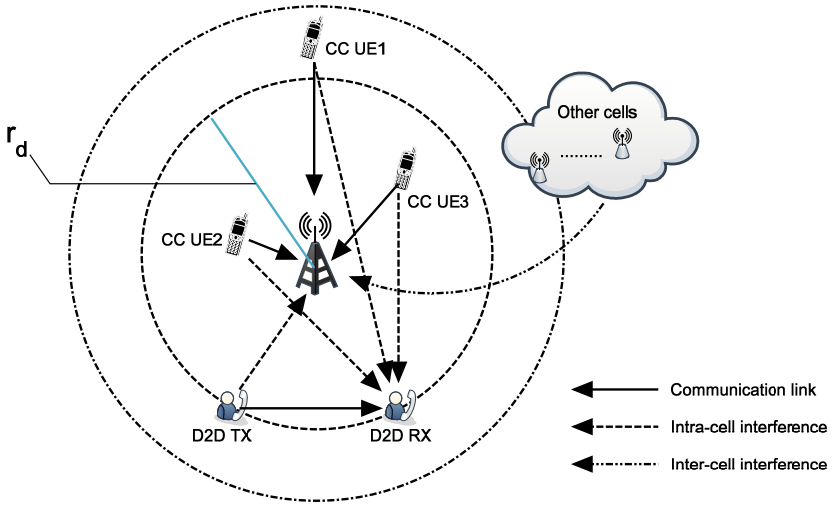

Fig. 3.1 System model. There are $N_C = 3$ CC UEs and one D2D pair in the center macro cell. The distance from D2D transmitter to the center BS is r_d.

the constraints of the usable channels and the maximum radius of D2D communications in Section 3.3. We propose two optimal location-based RRM mechanisms for D2D communications in Section 3.4 and analyse the performance in terms of throughput and energy efficiency in Section 4.5. Conclusions are presented in Section 4.6.

3.2 System Model and Problem Formulation

3.2.1 System Model

In this chapter, we consider BS-assisted D2D communications [29], [37] reusing UL cellular resources [29] in a system that contains multiple heterogeneous cells. We focus on the performance analysis of the central macro-cell of radius r, where there are one D2D pair and N_C CC UL UEs uniformly distributed in it (see Fig. 3.1). We assume that the N_C CC UL UEs are allocated to N_C orthogonal subchannels and the D2D pair is allowed to reuse all of the N_C subchannels. The bandwidth of each subchannel is B. We assume that the location of each UE in a cell is known by the BS [37]. The communication links and the intra-cell interference links are illustrated in Fig. 3.1. We assume the UL UEs in other cells (including both macro-cell UEs and small-cell UEs) are distributed following a SPPP with density λ [67], [97]. These UEs act as the sources of inter-cell interference to the CC UL and D2D communications in the central macro-cell. We note that the distance between a D2D receiver and an inter-cell interferer can be as short as 0 in a heterogeneous network [97]. Each UE has a maximum total transmit power $P_{\max}$.

We define the channel gain g as:

$$g = \kappa |h|^2 d^{-\alpha}, \tag{3.1}$$

where h is the fading coefficient following Rayleigh distribution, d is the distance between the transmitter and the receiver, and α and κ are the path loss distance exponent and the path loss adjusted constant that takes carrier frequency and environment related factors into consideration [82], respectively.

We assume the CC UL UEs utilise a distance-proportional fractional power control scheme following the discussion in [97]. The UL transmit power P_C^i of the i^{th} CC UL UE is given by [97]:

$$P_C^i = \bar{p}(d_C^i)^{\alpha\varepsilon}, \qquad \varepsilon \in [0,1], \quad \bar{p} \in (0, P_{\max} r^{-\alpha\varepsilon}], \tag{3.2}$$

where d_C^i is the distance between the i^{th} CC UL UE and the BS, and ε is an adjustment parameter defined in [97]. For a larger ε, the transmit power of CC UE is more related to its distance to the serving BS.

We consider the signal-to-interference ratio (SIR) in this chapter. The noise power at a subchannel with a practical bandwidth B [1] is negligible comparing to the interference power. The SIR γ_D^n of the D2D link in the n^{th} subchannel is given by:

$$\gamma_D^n = \frac{g_D^n P_D^n}{\sum\limits_{l \in \mathscr{I}_D^n} g_{l,D}^n P_{l,D}^n + g_{C,D}^n P_C^n}, \tag{3.3}$$

where P_D^n, P_C^n and $P_{l,D}^n$ are the transmit power levels in the n^{th} subchannel of the D2D transmitter, the CC UE utilising the n^{th} subchannel (as defined in (3.2)) in the same cell, and the interfering UEs in the l^{th} neighboring cell, respectively, g_D^n, $g_{C,D}^n$ and $g_{l,D}^n$ are the channel gains (as defined in (3.1)) of the D2D link, the intra-cell link from CC UE to the D2D receiver, and the inter-cell interference links from UE in the l^{th} neighboring cell to the D2D receiver, respectively. The transmit power of UEs in other cells is unknown to the central cell. In worst case, all interfering UEs transmit at their maximum power level, i.e.,

$$P_{l,D}^n = P_{\max}, \quad \forall l \in \mathscr{I}_D^n, \forall n = 1, \cdots, N_C \tag{3.4}$$

[1] A subchannel in the current LTE/LTE-advanced system is normally a RB, which has bandwidth of 180 KHz

Similarly, we have the SIR γ_C^n for the CC UL UE utilising the n^{th} subchannel

$$\gamma_C^n(P_D^n) = \frac{g_C^n P_C^n}{\sum\limits_{k \in \mathscr{I}_C^i} g_{k,C}^n P_{\max} + g_{D,C}^n P_D^n} \tag{3.5}$$

where g_C^n, $g_{D,C}^n$ and $g_{k,C}^n$ are the channel gain (as defined in (3.1)) of the CC communication link, the intra-cell interfered link from D2D transmitter to the CC UE, and the inter-cell interfered links, respectively.

We consider the achievable data rate of D2D communications. For D2D communications at n^{th} subchannel, it is

$$T_n = B \log_2(1 + \gamma_d^n) \tag{3.6}$$

For the power consumption of each UE, we consider its total transmit power P_{transmit} and circuit power P_{circ}. We assume P_{circ} is static [98]. Thus the total power consumption for an UE can be represented as

$$P_{\text{total}} = P_{\text{circ}} + P_{\text{transmit}} \tag{3.7}$$

Denote χ_D^n as the subchannel allocation indicator for the D2D communications

$$\chi_D^n = \begin{cases} 1, & \text{if subchannel } n \text{ is allocated to D2D communications,} \\ 0, & \text{otherwise.} \end{cases} \tag{3.8}$$

Then the energy efficiency of the D2D communications can be calculated as

$$F(\boldsymbol{P}_D, \boldsymbol{\chi}_D) = \frac{\sum\limits_{n=1}^{N_C} \chi_n T_n}{\boldsymbol{\chi}_D' \boldsymbol{P}_D + P_{\text{circ}}} \tag{3.9}$$

where $\boldsymbol{\chi}_D$ is the n-by-1 vector of χ_D^n, $\boldsymbol{P}_D$ is the n-by-1 vector of the transmit power P_D^n for the D2D communications at n^{th} subchannel.

3.2.2 Optimisation Problem Formulation

In this work, we consider two major optimisation problems for D2D communications: 1) maximising the throughput; and 2) maximising the energy efficiency.

We formulate the throughput optimisation problem for D2D communications as:

$$\textit{OPT1}: \ \arg\max_{\boldsymbol{P}_D, \boldsymbol{\chi}_D} \sum \chi_D^n T_n \tag{3.10}$$

subject to,

$$0 \leq P_D^n \leq P_{\max}^n \tag{3.11}$$

$$\boldsymbol{\chi}' \boldsymbol{P}_D \leq P_{\max} \tag{3.12}$$

where $P_{\max}^n$ is the maximum allowed transmit power for the D2D communications at the n^{th} subchannel and is further discussed in Section 3.3.

We consider the optimisation problem for energy efficiency in D2D communications as

$$OPT2\text{: } \arg\max_{\boldsymbol{P}_D, \boldsymbol{\chi}_D} F(\boldsymbol{P}_D, \boldsymbol{\chi}_D) \tag{3.13}$$

subject to,

$$\sum_{n}^{N_C} \chi_n T_n \geq \Phi_D \tag{3.14}$$

$$\text{and (3.11), (3.12).} \tag{3.15}$$

where Φ_D is the data rate requirement of D2D communications. We note that (3.14) is the QoS requirement of D2D communications.

3.3 Constraints in the D2D Communications

In this section, we discuss the constraints (in terms of the maximum transmit power and transmission range) of D2D communications from a geometric perspective.

We first give Lemma 3.3.1, which shows the exponential expectation of the integration of all the inter-cell interference power at subchannel i. This lemma will be utilised in the proof of the propositions and conclusions in this section.

Lemma 3.3.1. *Suppose the set $\mathscr{I}_C^i$, which contains all the inter-cell CC UL UEs that utilise subchannel i and are distributed in an area following SPPP with density λ. The Rayleigh fading power $|h|^2$ following an exponential distribution with mean $1/\mu$, then the exponential expectation of the integration of all the inter-cell interference power at subchannel i is*

$$\mathbb{E}\left\{\exp\left(-s\sum_{k\in\mathscr{I}_C^i} P|h_{k,C}^i|^2 (d_{k,C}^i)^{-\alpha}\right)\right\} = \exp\left(-\frac{2\lambda\pi^2(\mu/sP)^{-2/\alpha}\csc(2\pi/\alpha)}{\alpha}\right), \quad \textit{for any } \alpha > 2 \tag{3.16}$$

Proof.

$$\mathbb{E}\left\{\exp\left(-s\sum_{k\in\mathscr{I}_C^i} P_{\max}|h_{k,C}^i|^2(d_{k,C}^i)^{-\alpha}\right)\right\} \tag{3.17}$$

$$=\mathbb{E}\left\{\prod_{k\in\mathscr{I}_C^i}\exp\left(-sP_{\max}|h_{k,C}^i|^2(d_{k,C}^i)^{-\alpha}\right)\right\} \tag{3.18}$$

$$\overset{(a)}{=}\exp\left(-\int_0^\infty 2\lambda\pi r\left(1-\mathbb{E}_{|h_{k,C}^i|^2}\left\{\exp\left(-sP_{\max}|h_{k,C}^i|^2 r^{-\alpha}\right)\right\}\right)\mathrm{d}r\right) \tag{3.19}$$

$$\overset{(b)}{=}\exp\left(-\int_0^\infty 2\lambda\pi r\left(1-\int_0^\infty \exp(-sP_{\max}|h_{k,C}^i|^2 r^{-\alpha})\mu\exp(-\mu|h_{k,C}^i|^2)\,\mathrm{d}(|h_{k,C}^i|^2)\right)\mathrm{d}r\right) \tag{3.20}$$

$$=\exp\left(-\int_0^\infty 2\lambda\pi r\left(1-\mu\int_0^\infty \exp(-(sP_{\max}r^{-\alpha}+\mu)|h_{k,C}^i|^2)\,\mathrm{d}(|h_{k,C}^i|^2)\right)\mathrm{d}r\right) \tag{3.21}$$

$$=\exp\left(-\int_0^\infty 2\lambda\pi r\left(1-\frac{\mu}{sP_{\max}r^{-\alpha}+\mu}\right)\mathrm{d}r\right) \tag{3.22}$$

$$=\exp\left(-\int_0^\infty \lambda\pi\frac{1}{1+at^{\frac{\alpha}{2}}}\,\mathrm{d}t\right)\qquad \text{where } a=\frac{\mu}{sP_{\max}},\ t=r^2 \tag{3.23}$$

$$\overset{(c)}{=}\exp\left(-\frac{2\lambda\pi^2 a^{-2/\alpha}\csc(2\pi/\alpha)}{\alpha}\right),\qquad \text{when } \alpha>2 \tag{3.24}$$

■

where step (a) is from the probability generating functional of the SPPP [99], step (b) is derived by $|h_{k,C}^i|^2\sim\exp(1/\mu)$ and step (c) is the integration result of the previous equation.

The maximum transmit power of D2D communication should be limited to guarantee the QoS of CC UEs. The SIR requirement of the CC UE using the n^{th} subchannel is denoted as Γ_C^n. It is safe to assume $\Gamma_C^n\le\Gamma_C,\forall n=1,\cdots,N_C$, and without loss of generality, we use Γ_C as the SIR requirement for CC UE in the following discussions. The QoS requirement for each CC UL UE is that the probability of meeting the SIR requirement for a CC UL UE assigned with subchannel n needs to be kept above ρ_c. Thus when D2D communications reuse subchannel n, its transmit power should satisfy

$$\Pr(\gamma_C^n(P_{\max}^n)>\Gamma_C)\ge\rho_C, \tag{3.25}$$

With this QoS requirement for CC UL UEs, we have the following proposition

Proposition 3.3.2. *$P^n_{\max}$ is*

$$P^n_{\max} = \min\left\{P_{\max}, \frac{P^n_C}{\Gamma_C}\left(\frac{d_{D,C}}{d_C}\right)^{\alpha}\left[\frac{1}{\rho_C}\exp\left(-\frac{2\lambda\pi^2}{\alpha}\left(\frac{\Gamma_C P_{\max}}{P^n_C d_C^{-\alpha}}\right)^{\frac{2}{\alpha}}\csc\left(\frac{2\pi}{\alpha}\right)\right)-1\right]\right\} \tag{3.26}$$

where P^n_C is defined in (3.2) *and $d_{D,C}$ is the distance between the D2D transmitter and the BS.*

Proof. From (3.25), we know the $P^n_{\max}$ should satisfy

$$\Pr\left(\gamma^n_C(P^n_{\max}) > \Gamma_C\right) = \rho_C. \tag{3.27}$$

Thus we have

$$\Pr\left(\frac{g^n_C P^n_C}{\sum\limits_{k\in\mathscr{I}^n_C} g^n_{k,C}P_{\max} + g^n_{D,C}P^n_{\max}} > \Gamma_C\right) \tag{3.28}$$

$$= \Pr\left\{|h^n_C|^2 > \frac{\Gamma_C}{P^n_C d_C^{-\alpha}}\left(\sum_{k\in\mathscr{I}^n_C}|h^n_{k,C}|^2 P_{\max}(d^n_{k,C})^{-\alpha} + |h^n_{D,C}|^2 P^n_{\max} d^{-\alpha}_{D,C}\right)\right\} \tag{3.29}$$

$$\overset{(a)}{=} \mathbb{E}\left\{\exp\left[-\frac{\mu\Gamma_C}{P^n_C d_C^{-\alpha}}\left(P_{\max}\sum_{k\in\mathscr{I}^n_C}|h^n_{k,C}|^2(d^n_{k,C})^{-\alpha} + P^n_{\max}|h^n_{D,C}|^2 d^{-\alpha}_{D,C}\right)\right]\right\} \tag{3.30}$$

$$\overset{(b)}{=} \mathbb{E}_I\left\{\exp\left(-s\sum_{k\in\mathscr{I}^i_C}P_{\max}|h^i_{k,C}|^2(d^i_{k,C})^{-\alpha}\right)\right\}\mathbb{E}_{|h_{D,C}|^2}\left\{\exp\left(-sP^n_{\max}|h_{D,C}|^2 d^{-\alpha}_{D,C}\right)\right\} \tag{3.31}$$

$$\overset{(c)}{=} \exp\left(-\frac{2\lambda\pi^2 a^{-2/\alpha}\csc(2\pi/\alpha)}{\alpha}\right)\int_0^{\infty}\mu\exp\left[-(sP^n_{\max}d^{-\alpha}_{D,C}+\mu)|h^n_{D,C}|^2\right]\mathrm{d}(|h^n_{D,C}|^2) \tag{3.32}$$

$$= \exp\left(-\frac{2\lambda\pi^2 a^{-2/\alpha}\csc(2\pi/\alpha)}{\alpha}\right)\frac{\mu}{sP^n_{\max}d^{-\alpha}_{D,C}+\mu} \tag{3.33}$$

$$= \exp\left[-\frac{2\lambda\pi^2}{\alpha}\left(\frac{P^n_C d_C^{-\alpha}}{\Gamma_C P_{\max}}\right)^{-\frac{2}{\alpha}}\csc\left(\frac{2\pi}{\alpha}\right)\right]\frac{\mu}{sP^n_{\max}d^{-\alpha}_{D,C}+\mu} \tag{3.34}$$

where step (a) is derived from $|h^n_C|^2 \sim \exp(1/\mu)$, step (b) we have $s = \frac{\mu\Gamma_C}{P^n_C d_C^{-\alpha}}$, $\mathbb{E}_I$ is the expectation of the inter-cell interference I and $\mathbb{E}_{|h^n_{D,C}|^2}$ is the expectation of $|h^n_{D,C}|^2$, and step

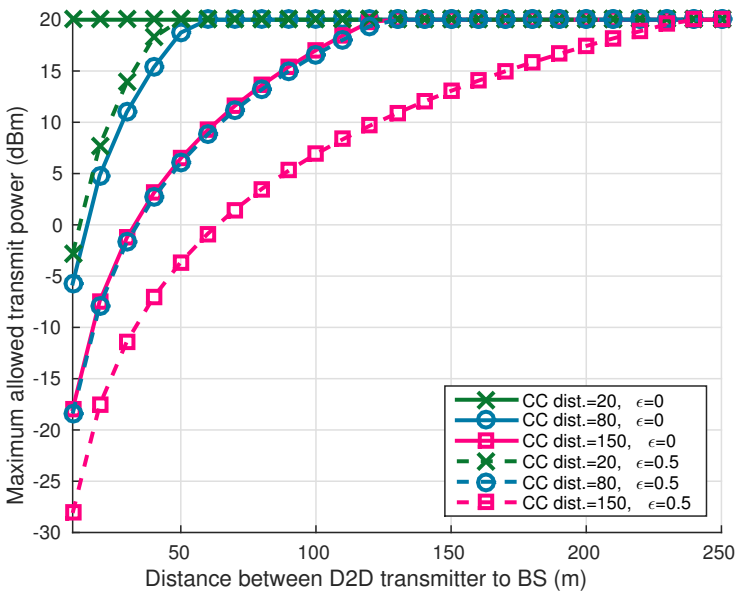

Fig. 3.2 Maximum allowed D2D transmit power versus the distance between D2D transmitter and the BS. "CC dist" is the distance (in metre) of the CC UL UE, which allocated subchannel is reused by the D2D, to the BS. ε is the power control parameter of CC UL UE defined in (3.2).

(c) is derived from the lemma 3.3.1, $a = \frac{\mu}{sP_{\max}}$ and $\alpha > 2$. Thus for $P^n_{\max}$ we have

$$P^n_{\max} = \frac{P^n_C}{\Gamma_C}\left(\frac{d_{D,C}}{d_C}\right)^{\alpha}\left[\frac{1}{\rho_C}\exp\left(-\frac{2\lambda\pi^2}{\alpha}\left(\frac{\Gamma_C P_{\max}}{P^n_C d_C^{-\alpha}}\right)^{\frac{2}{\alpha}}\csc\left(\frac{2\pi}{\alpha}\right)\right)-1\right] \tag{3.35}$$

■

Fig. 3.2 shows the maximum allowed transmit power $P^n_{\max}$ of D2D communications reusing the n$^{\text{th}}$ subchannel versus the D2D transmitter's distance to the BS, where $P_{\max} =$ 20dBm, $\rho_C = 0.8$ and $\Gamma_C = 0$dB. In Fig. 3.2, "CC dist." denotes the distance between the BS and the CC UE transmitting in subchannel n, and ε is the power control parameter in (3.2). In can be seen that $P^n_{\max}$ of D2D communications increases when the D2D transmitter is farther away from the central BS. For a given ε, $P^n_{\max}$ for D2D communications reaches $P_{\max}$ more quickly for a smaller "CC dist.", and $P^n_{\max}$ at a specific location is larger for a smaller "CC dist." for any ε. Furthermore, we have the following corollary.

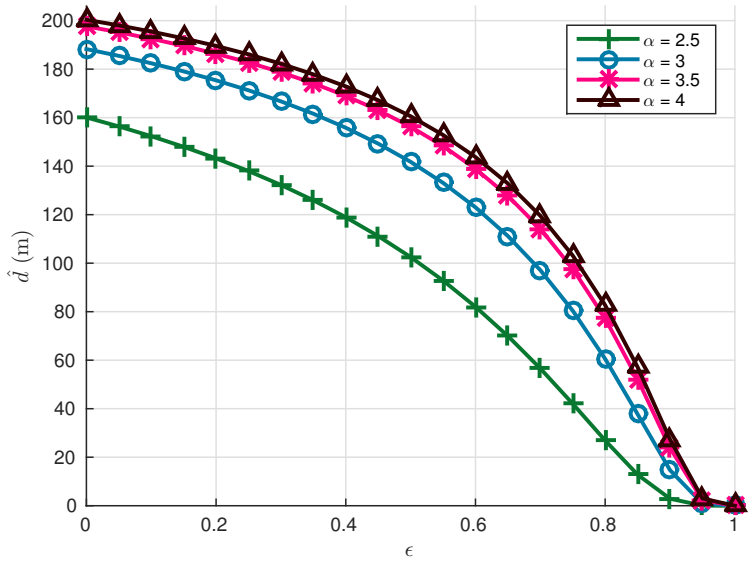

Fig. 3.3 The reusable distance $\hat{d}$ for D2D communications versus ε.

Corollary 3.3.3. *D2D communications can only reuse the subchannels allocated to CC UEs with distance d_C^i to the BS satisfying*

$$d_c^i \leq \hat{d} = \left[\frac{\bar{p}}{\Gamma_C P_{\max}} \left(\frac{-\alpha \ln \rho_C}{2\lambda \pi^2 \csc(2\pi/\alpha)} \right)^{\alpha/2} \right]^{\frac{1}{\alpha(1-\varepsilon)}}. \tag{3.36}$$

We denote $\hat{d}$ as the reusable distance for D2D communications.

Proof. For a D2D transmitter, it can transmit data only if its maximum allowed transmit power is larger then 0. From Proposition 1 and (3.2), we have

$$\exp\left(-\frac{2\lambda\pi^2}{\alpha} \left(\frac{\Gamma_C P_{\max}}{P_C^n d_C^{-\alpha}} \right)^{\frac{2}{\alpha}} \csc\left(\frac{2\pi}{\alpha} \right) \right) - 1 \geq 0 \tag{3.37}$$

■

Corollary 3.3.3 indicates that D2D communications are actually limited to reuse a part of subchannels that are allocated to the UL CC UEs in the cell center area. Fig. 3.3 shows the reusable distance $\hat{d}$ versus ε in different path loss environments. The reusable distance $\hat{d}$ decreases quickly as ε increases. In addition, we note that ε should not be larger than 0.9 otherwise there is no subchannel D2D can reuse. For any specific ε, the reusable distance increases as α becomes larger. This is because the D2D and CC UL links are more isolated

from each other in a larger path loss environment. Furthermore, D2D should never reuse the subchannels that are allocated to CC UL UEs with distance to the BS larger than 200m for α ranging from 2.5 to 4.5. This limitation decreases to 150m when $\alpha = 2.5$. In the following, we assume that D2D communications only reuse the subchannels that are allocated to the UL CC UEs within the area defined in Corollary 3.3.3.

We then discuss the maximum transmission distance of D2D communications. The SIR requirement of D2D communications in any subchannel is denoted as Γ_D. The QoS requirement for D2D communications reusing subchannel n is that the SIR requirement is met with a probability ρ_D. Thus we have the following definition.

Definition 3.3.1. *The maximum transmission distance of D2D communications at subchannel n is defined as*

$$R_D^{n,*} = \sup\left\{ R_D^n \middle| \Pr\left(\frac{|h_D|^2 (R_D^n)^{-\alpha} P_{\max}^n}{\sum_{k \in \mathscr{I}_C^i} g_{k,C}^i P_{\max} + g_{D,C}^i P_{\max}^n} > \Gamma_D \right) \right\} = \rho_D. \tag{3.38}$$

Based on Definition 3.3.1, the transmission radius for D2D communications is defined as the maximum transmission distance of D2D communications in any subchannel.

Definition 3.3.2. *The transmission radius of the D2D communications is defined as*

$$R_D = \max R_D^{n,*}, \forall n = 1, \cdots, N \tag{3.39}$$

Proposition 3.3.4. *$R_D^{n,*}$ is the solution of following equation*

$$\exp\left[\frac{2\lambda\pi^2}{\alpha} \left(\frac{P_{\max}^n}{\Gamma_D P_{\max}} \right)^{-\frac{2}{\alpha}} \csc\left(\frac{2\pi}{\alpha} \right) (R_D^{n,*})^2 \right] (\Gamma_D P_C^n (d_{C,D}^n)^{-\alpha} (R_D^{n,*})^{\alpha} + P_{\max}^n) = \frac{P_{\max}^n}{\rho_D}. \tag{3.40}$$

where $d_{C,D}^n = \sqrt{(r_C \cos\theta_C - R_D^{n,*} \cos\theta_D - r_D \cos\theta_D)^2 + (r_C \sin\theta_C - R_D^{n,*} \sin\theta_R - r_D \sin\theta_D)^2}$.

Proof. Similar to the computation in the proof of Proposition 3.3.2, we have,

$$\begin{aligned} &\Pr\left(\frac{|h_D|^2 (R_D^n)^{-\alpha} P_{\max}^n}{\sum_{k \in \mathscr{I}_C^i} g_{k,C}^i P_{\max} + g_{C,D}^i P_{\max}^n} > \Gamma_D \right) \\ &= \exp\left[-\frac{2\lambda\pi^2}{\alpha} \left(\frac{P_{\max}^n (R_D^n)^{-\alpha}}{\Gamma_D P_{\max}} \right)^{-\frac{2}{\alpha}} \csc\left(\frac{2\pi}{\alpha} \right) \right] \frac{\mu}{s P_C^n (d_{C,D}^n)^{-\alpha} + \mu}. \end{aligned} \tag{3.41}$$

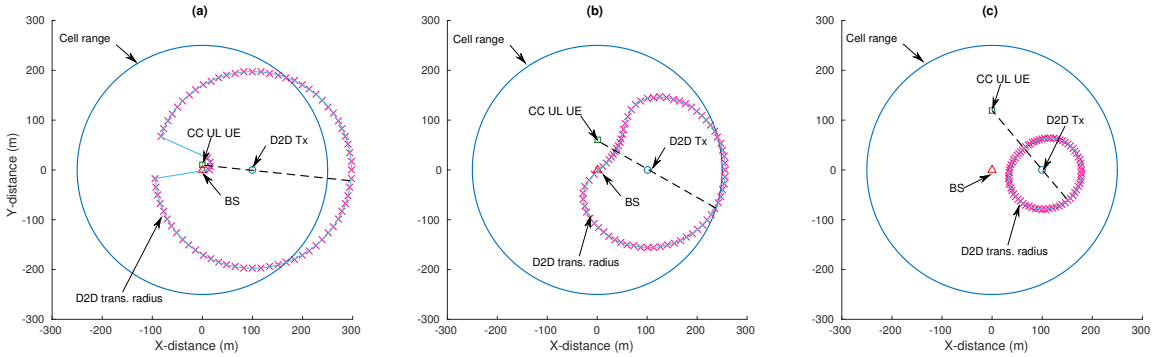

Fig. 3.4 Illustrations of the D2D transmission area depending on where the subchannel-sharing CC UL UE locates.

where $s = \mu\Gamma_D/P^n_{\max}(R^n_D)^{-\alpha}$. From (3.41), we know the left-side probability decreases with R^n_D. Thus we have $R^{n,*}_D$ is the solution of the following equation

$$\exp\left[-\frac{2\lambda\pi^2}{\alpha}\left(\frac{P^n_{\max}(R^n_D)^{-\alpha}}{\Gamma_D P_{\max}}\right)^{-\frac{2}{\alpha}}\csc\left(\frac{2\pi}{\alpha}\right)\right]\frac{P^n_{\max}}{\Gamma_D P^n_C(d^n_{C,D})^{-\alpha}(R^n_D)^{\alpha}+P^n_{\max}} = \rho_D \quad (3.42)$$

$$\exp\left[\frac{2\lambda\pi^2}{\alpha}\left(\frac{P^n_{\max}}{\Gamma_D P_{\max}}\right)^{-\frac{2}{\alpha}}\csc\left(\frac{2\pi}{\alpha}\right)(R^{n,*}_D)^2\right](\Gamma_D P^n_C(d^n_{C,D})^{-\alpha}(R^{n,*}_D)^{\alpha}+P^n_{\max}) = \frac{P^n_{\max}}{\rho_D}. \quad (3.43)$$

■

With Proposition 3.3.4, we illustrate the shape of the transmission area of D2D communications reusing different subchannels in Fig. 3.4, where the distance between the D2D transmitter (D2D Tx) and the BS is 100m, and the "CC UL UE" represents the CC UL UE whose subchannel is reused by D2D communications. We find three different and representative shapes of the D2D transmission area depending on where the subchannel-sharing CC UL UE locates. A common characteristic of the shapes is that, they are all axially symmetric with respect to the straight line connecting CC UL UE and D2D Tx.

As we can see from Fig. 3.4, the maximum transmission distance of D2D communications changes when the transmission direction changes. In Fig. 3.5, we use the box plot to demonstrate the range of the maximum D2D transmission distance versus the D2D transmitter's distance to the central BS, for two different values of ε and for three different locations of CC UL UE with respect to the central BS. For each box, the bottom, the band inside and the top of the box indicate the first quartile, the median and the third quartile of the set of maximum D2D transmission distances for a certain D2D transmitter location, a certain

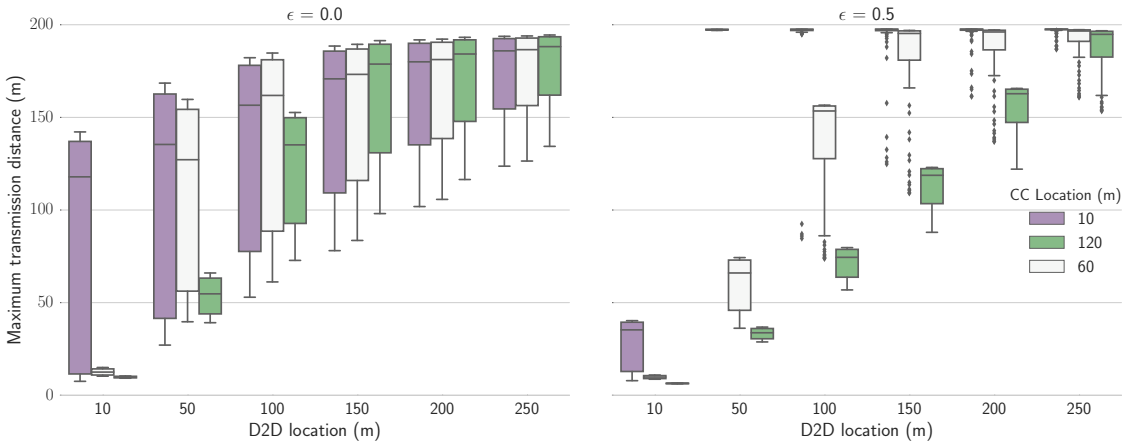

Fig. 3.5 Maximum D2D transmission distance versus the D2D transmitter's distance from the BS

CC UL UE location and a certain ε. From Fig. 3.5, we can see that the maximum D2D transmission distance increases when the D2D transmitter becomes farther from the BS. A large dispersion of the maximum D2D transmission distance corresponds to a shape of the D2D transmission area in Fig. 3.4(a). When the dispersion decreases, the shape of the D2D transmission area gradually changes from Fig. 3.4(a) to Fig. 3.4(b) and then to Fig. 3.4(c). D2D communications that reuse the subchannel allocated to a CC UL UE located closer to the BS can have a longer maximum transmission distance. For example, for $\varepsilon = 0$, the median of the maximum D2D transmission distance is about 120m when the D2D link reuses a subchannel that is allocated to a CC UL UE with the distance $10m$ to the BS, the median decreases to about 10m when it shares a subchannel with a CC UL UE that is 60m or 120m away from the BS.

We have the following corollary for the transmission radius R_D of D2D communications.

Corollary 3.3.5. *From Proposition 3.3.4, we have*

$$R_D \leq \sqrt{\frac{-\alpha \ln \rho_D}{2\lambda\pi^2(\Gamma_D)^{2/\alpha}\csc(2\pi/\alpha)}} \tag{3.44}$$

Proof. From (3.41), we know the left-side probability increases with $P^n_{\max}$ and decreases with P^n_C. Thus the upper bound $\hat{R}$ of all $R^{n,*}_D$ is the solution of the following equation:

$$\exp\left[-\frac{2\lambda\pi^2}{\alpha}(\Gamma_D)^{\frac{2}{\alpha}}\csc\left(\frac{2\pi}{\alpha}\right)\hat{R}^2\right] = \rho_D \tag{3.45}$$

Thus we have,

$$R_D < \hat{R}^2 = \sqrt{\frac{-\alpha \ln \rho_D}{2\lambda \pi^2 (\Gamma_D)^{2/\alpha} \csc(2\pi/\alpha)}} \tag{3.46}$$

■

We note that if D2D communications reuse the subchannels not allocated to any CC UL UE, R_D can reach the upper bound defined in Corollary 3.3.5. For $\Gamma_D = -8$dB, $\rho_D = 0.8$ and $\alpha = 3.5$, R_D is about 197m.

3.4 Optimal Radio Resource Management for D2D Communications

In this section, we present the solutions to the optimisation problems *OPT1* and *OPT2* defined in Section 3.2.2 based on the constraints found in Section 3.3. The D2D pair utilises the reusable subchannels (defined in Corollary 3.3.3) with the transmit power constraint $P^n_{\max}$ for each subchannel (defined in Proposition 3.3.2) and its transmission distance is within $R^{n,*}_D$ (defined in Proposition 3.3.4).

Denote $\mathscr{N}_C = \{1, \cdots, N_A\}$ as the set of N_A reusable subchannels for D2D communications (as defined in Corollary 3.3.3). Denote T^*_D as

$$T^*_D = -\sum \chi^n_D \log_2 \left(1 + \frac{P^n_D g^n_D}{I_D + I^n_C}\right). \tag{3.47}$$

To optimise the optimal RRM for D2D communications, we make two assumptions: 1) the channel states (i.e., fading coefficient h in (3.1)) are known to the BS [37], [100]; and 2) the UL inter-cell interference can be efficiently kept below a level I_D, i.e., $\sum_{l \in \mathscr{I}^n_D} g^n_{l,D} P^n_{l,D} \leq I_D, \forall n \in \mathscr{N}_C$ **inter-cell-interference** Under these two assumptions and denoting $I^n_C = g^n_{C,D} P^n_C$, we transform *OPT1* and *OPT2* into *OPT1** and *OPT2**, respectively, as follows.

$$OPT1^*: \arg\min_{\boldsymbol{P}_D, \boldsymbol{\chi}_D} T^*_D \tag{3.48}$$

$$\text{subject to (3.11), (3.12) and (3.26).} \tag{3.49}$$

and,

$$OPT2^*: \ \arg\min_{\boldsymbol{P}_D, \boldsymbol{\chi}_D} \frac{T_D^*}{(1+\beta)\boldsymbol{\chi}_D' \boldsymbol{P}_D} \tag{3.50}$$

$$\text{subject to (3.11), (3.12), (3.14) and (3.26).} \tag{3.51}$$

Both $OPT1^*$ and $OPT2^*$ are mixed integer nonlinear programming (MINLP) problems, which are NP-hard and difficult to solve [54]. In the following, we will transform them into continuous nonlinear programming (NLP) problems and solve them using the method of Lagrange multipliers.

3.4.1 Optimal Radio Resource Management for Throughput

It is easy to prove that T_n in (3.6) is a convex function. We relax the integer constraint of $\chi_n, \forall n \in \mathcal{N}_C$ and transform $OPT1^*$ into a convex NLP problem *NLP1* as follows.

$$NLP1: \ \mathbf{OPT1}^* \tag{3.52}$$

$$0 \le \chi_n \le 1, \quad \forall n = 1, \cdots, N_C \tag{3.53}$$

Introducing a Lagrange multiplier λ_1 for the inequality constraint in (3.11) and the Lagrange multipliers $\boldsymbol{\lambda}_2, \boldsymbol{\lambda}_3, \boldsymbol{\upsilon}_1, \boldsymbol{\upsilon}_2 \in \mathbb{R}^{N_A}$ for the inequality constraints in (3.12) and (3.53) respectively, we obtain the Karush-Kuhn-Tucker (KKT) conditions [101]:

$$-\log_2\left(1+\frac{P_D^n g_D^n}{I_D+I_C^n}\right)+\lambda_1 P_D^n+\upsilon_1^n-\upsilon_2^n=0, \qquad \forall n \in \mathcal{N}_C \tag{3.54}$$

$$-\frac{\chi_n}{\ln 2}\frac{g_D^n}{P_D^n g_D^n+I_D+I_C^n}+\lambda_1\chi_n+\lambda_2^n-\lambda_3^n=0, \qquad \forall n \in \mathcal{N}_C \tag{3.55}$$

$$\lambda_1\left(\sum_{n=1}^{N_A}\chi_n P_D^n - P_{\max}\right)=0 \tag{3.56}$$

$$\lambda_2^n(P_D^n-P_{\max}^n)=0, \quad \lambda_3^n P_D^n=0, \quad \upsilon_1^n(\chi_n-1)=0, \quad \upsilon_2^n\chi_n=0, \qquad \forall n \in \mathcal{N}_C \tag{3.57}$$

Based on (3.11) and (3.56), if $\sum_{n=1}^{N_A} P_{\max}^n \le P_{\max}$, the solution to *NLP1* is given by

$$\begin{cases} \chi_n = 1 \\ P_D^n = P_{\max}^n \end{cases}, \quad \forall n \in \mathcal{N}_C. \tag{3.58}$$

If $\sum_{n=1}^{N_A} P_{\max}^n > P_{\max}$, then from (3.56) we have $\lambda_1 = 0$. Furthermore, if $\chi_n = 0$, then $P_D^n = 0$. This is because if a subchannel is not used by to the D2D communications (i.e., $\chi_n = 0$), then no transmit power should be assigned to that sub-channel (i.e., $P_D^n = 0$).

If $\sum_{n=1}^{N_A} P_{\max}^n > P_{\max}$ and $\chi_n \neq 0$, then from (3.11), (3.54) and (3.57) we have:

$$\sum_{n=1}^{N_A} \chi_n P_D^n = P_{\max} \tag{3.59}$$

$$\chi_n \left(-\log_2 \left(1 + \frac{P_D^n g_D^n}{I_D + I_C^n} \right) + \lambda_1 P_D^n + \upsilon_1^n \right) = 0 \tag{3.60}$$

$$\left(-\frac{\chi_n}{\ln 2} \frac{g_D^n}{P_D^n g_D^n + I_D + I_C^n} + \lambda_1 \chi_n + \lambda_2^n \right) P_D^n = 0 \tag{3.61}$$

If $0 < P_D^n < P_{\max}^n$, from (3.57) we have

$$\lambda_2^n = 0. \tag{3.62}$$

Substitute (3.62) into (3.61) ad solving for P_D^n, we have

$$P_D^n = \frac{g_D^n}{\lambda_1 \ln 2} - I_C^n - I_D \triangleq P_D^{n\dagger} \tag{3.63}$$

If $P_D^{n\dagger} < 0$ or $P_D^{n\dagger} > P_{\max}^n$, it violates the power constraint (3.11), thus we conclude that the solution P_D^{n*} to P_D^n is

$$P_D^{n*} = \min\{P_{\max}^n, \max\{0, P_D^{n\dagger}\}\} \tag{3.64}$$

and

$$\chi_n = \begin{cases} 1, & \text{if } P_D^{n*} > 0 \\ 0, & \text{otherwise.} \end{cases} \tag{3.65}$$

Substituting (3.64) into (3.59) we have

$$\sum_{n=1}^{N_A} P_D^{n*} = P_{\max}. \tag{3.66}$$

We note that the left-hand side of (3.66) is a non-continuous function. The well-known Brent-Dekker algorithm [85] can be utilised to solve (3.66) for λ_1^*, and thus P_D^{n*}.

It can be proven that the solution to *NLP1* is the solution to *OPT1** with Theorem 3.4.1.

Theorem 3.4.1. *Let* $\boldsymbol{\chi}$ *be the integer variables in a MINLP optimisation problem* MINLP-OPT *and optimisation problem* NLP-OPT *be the relaxed nonlinear problem of* MINLP-OPT.

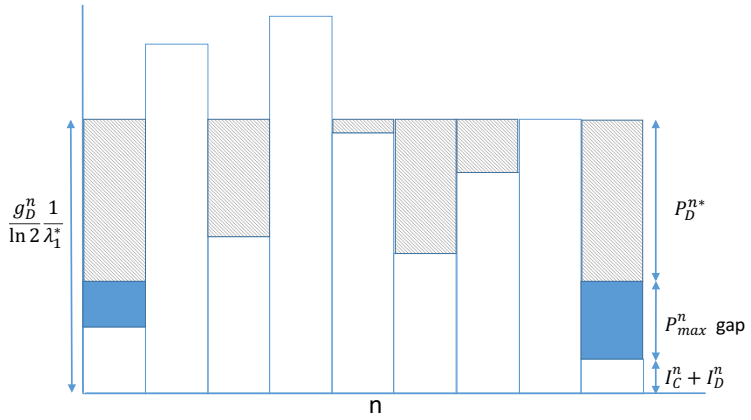

Fig. 3.6 Gap/Waterfilling type power control

If $\boldsymbol{\chi}^*$ *in the solution* $\boldsymbol{x}^*$ *of* NLP-OPT *are all integer, then the solution* $\boldsymbol{x}^*$ *is the optimal solution for the original MINLP problem* MINLP-OPT.

Proof. The branch-and-bound algorithm can be utilised to solve the MINLP problem [54]. The *NLP-OPT* problem is actually the relaxed problem to be solved in the first round of the branch-and-bound algorithm. It is proved in [54] that if the solution of this relaxed problem fulfils the strict integer constraints, the branch-and-bound algorithm terminates and the solution for *NLP-OPT* is the optimal solution for the original MINLP problem. ■

Fig. 3.6 illustrates the optimal power control scheme, which we refer to as *gap/waterfilling*. In Fig. 3.6, the top of the white area in the n$^{\text{th}}$ column is given by $I_C^n + I_D$ and is denoted as the ground level. Water is filled into each column on top of the white area up to the level of $g_D^n/(\lambda_1^* \ln 2)$ (the grey areas as in Fig. 3.6 denote the filled water). The depth of the grey area in the n$^{\text{th}}$ column is then the transmit power in subchannel n. If the difference between $g_D^n/(\lambda_1^* \ln 2)$ and $I_c^n + I_D$ is larger than $P_{\max}^n$, then a gap (the blue areas in Fig. 3.6) is filled between the water and the ground in order to maintain the depth of water as $P_{\max}^n$. The total amount of water is controlled by (3.66).

3.4.2 Optimal Radio Resource Management for Energy Efficiency

Similar to *OPT1**, *OPT2** can be transformed into a convex NLP problem as follows.

$$\textit{NLP2}\text{: } \textbf{OPT2}^* \tag{3.67}$$

$$0 \leq \chi_n \leq 1, \quad \forall n \in \mathcal{N}_C \tag{3.68}$$

1: **function** RRM_ENERGY_EFFICIENCY(δ)
2: $k \leftarrow 1, \quad \xi_k \leftarrow 0.$
3: **repeat**
4: Solve $\boldsymbol{\chi}_D^k, \boldsymbol{P}_D^k \leftarrow \arg\max_{\boldsymbol{\chi}_D, \boldsymbol{P}_D} F(\xi^k; \boldsymbol{\chi}_D, \boldsymbol{P}_D)$ ▷ Step (a)
5: $k \leftarrow k+1$ ▷ Update k for next iteration
6: $\xi^k \leftarrow T_D^*(\boldsymbol{\chi}_D^k, \boldsymbol{P}_D^k)/((\boldsymbol{\chi}_D^k)'\boldsymbol{P}_D^k + P_0)$ ▷ Update ξ^k for next iteration [102].
7: **until** $\pi(\xi^k) \leq \delta$
8: **return** $\boldsymbol{\chi}_D^k, \boldsymbol{P}_D^k$ as $\boldsymbol{\chi}_j^*, \boldsymbol{P}_D^*$
9: **end function**

Fig. 3.7 Algorithm to solve the *NLP2* problem.

In *NLP2*, T_D^* and $\boldsymbol{\chi}_D'\boldsymbol{P}_D$ are concave and convex function, respectively. Thus we can utilise the algorithm proposed in [102] to solve the problem. The algorithm is based on the following theorem

Theorem 3.4.2. *Denote* $F(\xi; \boldsymbol{\chi}_D, \boldsymbol{P}_D) = \max(T_D^* - \xi(\boldsymbol{\chi}_D\boldsymbol{P}_D + P_{\text{circ}}))$. *Let*

$$\pi(\xi) = \max F(\xi; \boldsymbol{\chi}_D, \boldsymbol{P}_D), \tag{3.69}$$

and let

$$\boldsymbol{\chi_D}(\xi), \boldsymbol{P}_D(\xi) = \arg\max_{\boldsymbol{\chi}_D, \boldsymbol{P}_D} F(\xi; \boldsymbol{\chi}_D, \boldsymbol{P}_D). \tag{3.70}$$

We have

1. $\pi(\xi)$ *is convex for any* $\xi \geq 0$.
2. *If there exists* $\xi^* \geq 0$ *for which* $\pi(\xi^*) = 0$, *then* $\boldsymbol{\chi}^*, \boldsymbol{P}_D^* \equiv \boldsymbol{\chi_D}(\xi^*), \boldsymbol{P}_D(\xi^*)$ *is the optimal solution of NLP2.*

Proof. See [102]. ■

The overall algorithm to solve *NLP2* is depicted in Fig. 3.7 [102]. In the algorithm, δ is a threshold which is utilised to determine whether $\pi(\xi_k)$ is close to 0. ξ_k is initialised as 0 (Line 2). In each iteration, we solve $\pi(\xi_k)$ (Line 4, Step (a)) and check whether $\pi(\xi_k) \leq \delta$ (Line 7). If so, the algorithm terminates and returns the final $\boldsymbol{\chi}_D^k, \boldsymbol{P}_D^k$ as $\boldsymbol{\chi}_D^*, \boldsymbol{P}_D^*$ (Line 8). Otherwise, the new ξ_k for the next iteration is calculated as $T_D^*(\boldsymbol{\chi}_D^k, \boldsymbol{P}_D^k)/((\boldsymbol{\chi}_D^k)'\boldsymbol{P}_D^k + P_0)$ [102] (Line 6). The convergence of the algorithm is proved in [102].

Now we give the solution of Step (a) (see in Fig. 3.7) in the proposed algorithm. For any ξ^k, it can be proved that $F(\xi^k; \boldsymbol{\chi}_D, \boldsymbol{P}_D)$ is a convex function in terms of $\boldsymbol{\chi}_D$ and $\boldsymbol{P}_D$. Introducing Lagrange multipliers $\lambda_1 \in \mathbb{R}^1$, $\boldsymbol{\lambda}_2\boldsymbol{\lambda}_3 \in \mathbb{R}^{N_A}$, $\boldsymbol{\mu}_1, \boldsymbol{\mu}_2 \in \mathbb{R}^{N_A}$ and $\upsilon \in \mathbb{R}^1$

for (3.11), (3.12), (3.68) and (3.14), respectively, we have the KKT conditions are for $\pi(\xi_k)$ given as followings

$$-(\upsilon+1)\log_2\left(1+\frac{g_D^n P_D^n}{I_D+I_C^n}\right)+\xi_k P_D^n+\lambda_1 P_D^n-\mu_1^n+\mu_2^n=0, \qquad \forall n\in\mathscr{N}_C \quad (3.71)$$

$$-(\chi_n+\upsilon)\frac{1}{\ln 2}\frac{g_D^n}{g_D^n P_D^n+I_D+I_C^n}+(\xi_k+\lambda_1)\chi_n+\lambda_2^n-\lambda_3^n=0, \qquad \forall n\in\mathscr{N}_C \quad (3.72)$$

$$\lambda_1\left(\sum_{n=1}^{N_A}\chi_n P_D^n-P_{\max}\right)=0 \quad (3.73)$$

$$\upsilon\left(\Phi_D-\sum_{n=1}^{N_A}\chi_n\log_2\left(1+\frac{g_D^n P_D^n}{I_D+I_C^n}\right)\right) \quad (3.74)$$

$$\lambda_2(P_D^n-P_{\max}^n)=0, \quad \lambda_3 P_D^n=0, \quad \mu_1\chi_n=0, \quad \mu_2(\chi_n-1)=0, \qquad \forall n\in\mathscr{N}_C \quad (3.75)$$

Following the discussions in Section 3.4.1, we have

$$P_D^{n\dagger}(\xi_k)=\min\left\{P_{\max}^n,\max\left\{0,\frac{1}{g_D^n}\left(\frac{(1+\upsilon)g_D^n}{\xi_k\ln 2}-I_C^n-I_D\right)\right\}\right\}, \qquad \forall n\in\mathscr{N}_C \quad (3.76)$$

Substituting $P_D^{n\dagger}(\xi_k)$ into (3.74) and solve the equation with Brent-Dekker algorithm [85] we can achieve $P_D^{n*}(\xi_k)$. Note that it can be interpreted as *gap/waterfilling* introduced in Section 3.4.1. The solution for $\chi_n^*(\xi_k)$ is

$$\chi_n^*(\xi_k)=\begin{cases}1, & \text{if } P_D^n>0\\ 0, & \text{otherwise}\end{cases}, \qquad \forall n\in\mathscr{N}_C. \quad (3.77)$$

Note that, with Theorem 3.4.1, the solution to *NLP2* is the solution to *OPT2*.

3.5 Performance Analysis of D2D Communications

In this section, we present the performance analysis of D2D communications from a geometrical perspective using numerical simulations. The simulated network contains one macro cell with its BS located at $(0,0)$ and inter-cell UL CC UEs distributed following an SPPP distribution with density $2.8\times10^{-6}/\text{m}^2$. We evaluate the performance of the macro-cell, where $N_C=10$ CC UL UEs and one D2D transmitter D_T are uniformly distributed in it. The D2D receiver is uniformly distributed in a circle centred at the D_T with a specific radius (called D2D radius and is given in Table 4.1). We adopt the Urban Micro (UMi) channel

Table 3.1 Simulation Parameters

Parameter	**Value**
Cell radius	250m
D2D radius	$10, 30, 50, 100$m
SIR threshold (β)	0dB
Number of CC UL UEs (N_C)	10
Circuit Power	0.25W [98]
Uplink bandwidth	10MHz
Pathloss exponent (α)	2.5, 3.5, 4.5
Maximum transmit power ($p_{\max}$)	20dBm
Multipath fading	Rayleigh distribution with the scale parameter of 0.5
Log-normal shadowing	Standard deviation of 4dB

model and the path loss model in [82, Table B.1.2.1–1]. Other major simulation parameters are summarised in Table 4.1.

3.5.1 Throughput

We apply the RRM schemes proposed in Section 3.4.1 to D2D communications. Fig. 3.8 demonstrates the throughput performance of D2D communications. The four sub-figures in Fig. 3.8 demonstrate the throughput of D2D communications with transmission radius as $10, 30, 50$ and 100m respectively. In each sub-figure, we plot the throughput of D2D communications versus its transmitter's location with different α and ε (i.e., the power control parameter for CC UEs) combinations. We note that, the throughput of D2D communications follow a common trend in terms of its transmitter's location in any environment (i.e., different α, ε and the transmission radius). We can divide the cell area into three zones in terms of the optimal throughput of D2D communications.

Dead zone (0–30m). This is the inner area of a cell. In this zone, the throughput of D2D communications is very low. When D2D communications have a long transmission distance (e.g., the transmission distance is 50m and 100m), the throughput is almost 0 bps (see (c) and (d) in Fig. 3.8). We call this a *dead zone* of D2D communications, as D2D can barely transmit data in this zone.

Developing zone (30–150m). This is the middle area of a cell. The throughput of D2D communications increases quickly and the D2D communications start to be available in this zone. Thus we call it the *developing zone* of D2D communications. With different power control schemes for CC UL UEs (i.e., different ε), the trends are slightly different. For $\varepsilon = 0$, the *developing zone* can be further divided into two zones: 1) *fast developing zone* (30–70m), in which the throughput of D2D UEs increases very quick; and 2) *static developing zone*

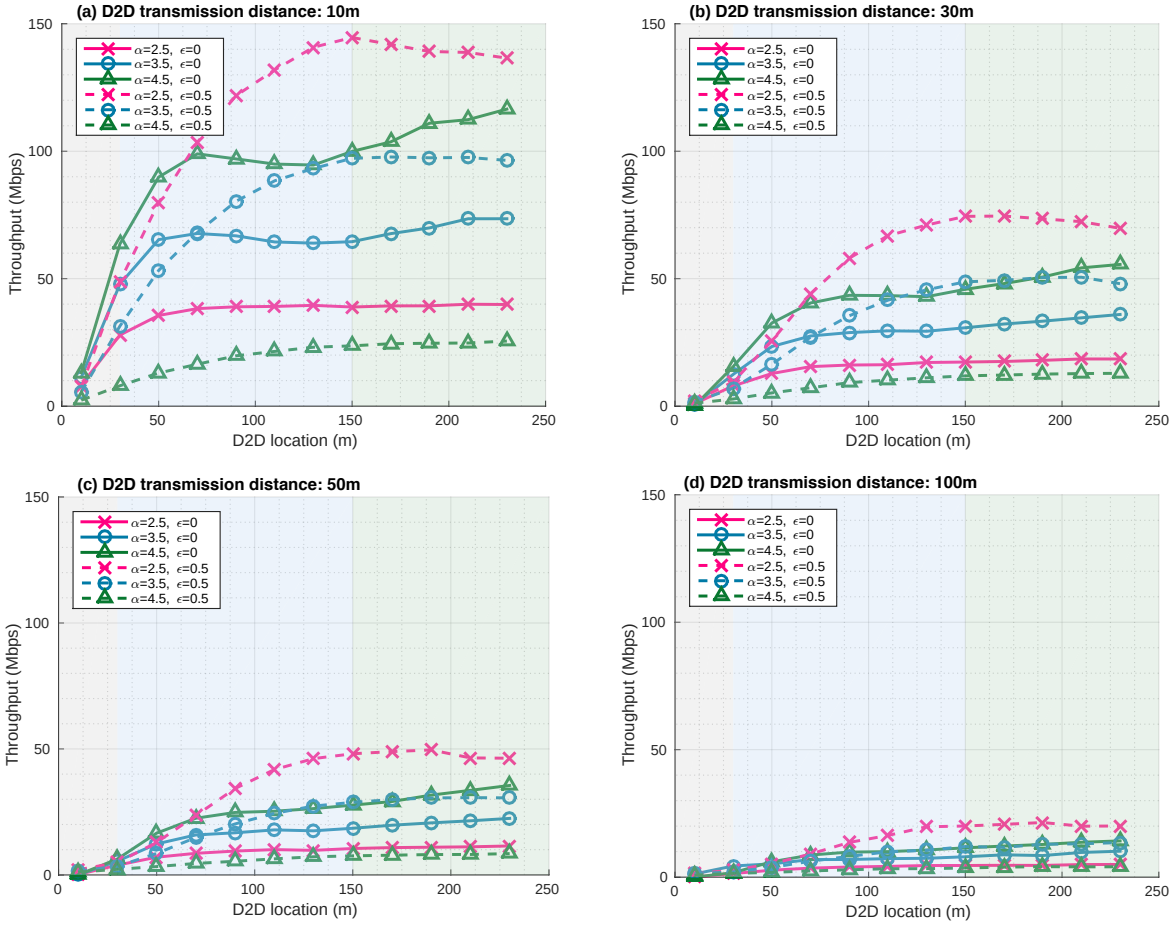

Fig. 3.8 Throughput performance of D2D communications in terms of its transmitter's location. The (a), (b), (c) and (d) show the throughput of D2D communications with transmission radius as $10, 30, 50$ and 100m respectively.

(70–150m), in which the throughput of D2D communications almost remains the same (see the solid lines in Fig. 3.8). For $\varepsilon = 0.5$, the throughput of D2D communications continually increases in this zone (see the dash lines in Fig. 3.8).

Developed zone (150–250m). This is the outer area of a cell. The throughput of D2D communications almost remains its maximum value in this zone, thus we call it *developed zone* of D2D communications. We can see from Fig. 3.8 that for $\varepsilon = 0$, the throughput of D2D communications increases slightly in this zone and reaches its maximum when the D2D transmitter locating at 230m (solid lines in Fig. 3.8). We note that for $\varepsilon = 0$, D2D can reuse most of the subchannels allocated to the CC UL UEs with the distance to the BS less than 150m (see Fig. 3.3) at the power level $P_{\max}$ when its transmitter located in both this zone and the developing zone (see Fig. 3.2). Thus when D2D transmitter is located in the developed zone, where is far from its intra-interfered CC UL UEs, the throughput

of D2D communications increase. On the other hand, for $\varepsilon = 0.5$ the throughput of D2D communications decreases slightly in this zone (see dash lines in Fig. 3.8). This is mainly because for $\varepsilon = 0.5$, the reusable subchannels for D2D communications are limited in this zone (see Fig. 3.3).

We then consider how the transmission distance, path loss exponent α and power control scheme for CC UL UE (i.e., ε in (3.2)) may affect the throughput of D2D communications. Comparing the throughput of D2D communications with different transmission distance, it can be concluded that the throughput of D2D communications with shorter transmission distance (see (a) in 3.8, transmission distance is 10m) significantly outperforms the one of D2D communications with longer transmission distance (see (d) in Fig. 3.8, transmission distance is 100m). We also find that, for $\varepsilon = 0$, the D2D communications achieve a higher throughput in larger path loss environment; on the contrary, for $\varepsilon = 0.5$, the throughput of D2D communications decreases with the increase of path loss exponent. This is because for $\varepsilon = 0$, the transmit power constraint for D2D communications at each subchannel is $P_{\max}$ in most of cases (see[(3.26), Proposition 1] and Fig. 3.2), a more isolated environment (i.e., larger α) can reduce the mutual interference between CC and D2D communications and thus improve the throughput of D2D communications. On the other hand, for $\varepsilon = 0.5$, the situation is more complicated. Define $G(d;\alpha_1,\alpha_2) = P^n_{\max}(d;\alpha_1) - P^n_{\max}(d;\alpha_2)$, where $P^n_{\max}(d;\alpha_k)$ is the $P^n_{\max}$ defined in (3.26) (Proposition 1) with $d_{D,C} = d$, $\alpha = \alpha_k$ and we assume $\alpha_1 < \alpha_2$. It is easy to prove that $G(d;\alpha_1,\alpha_2)$ is a convex function and there exists $d^\dagger$, which $G(d;\alpha_1,\alpha_2) > 0, d \in (0,d^\dagger)$. Thus for $d \in (0,d^\dagger)$, P^n_{max} is larger, which leads to a better throughput of D2D, in a smaller path loss environment. For $d \in (d^\dagger, r)$, the $P^n_{\max}$ is close to $P_{\max}$ with the α range considered in this work (i.e., $2.5 \leq \alpha \leq 4.5$). In this case, the difference in maximum transmit power constraint shows little impact on the throughput performance. The smaller path loss exponent may lead to a larger received power and thus the D2D receiver may have a better SIR. For these reasons, the optimal throughput of D2D communications decreases with the path loss exponent when $\varepsilon = 0.5$. Finally we note that, for any given D2D transmission distance in our simulations, the D2D achieves its best throughput performance when $\alpha = 2.5$ and $\varepsilon = 0.5$. This is because the transmit power of CC UL UEs is more restricted for $\varepsilon = 0.5$ and thus the mutual interference is less severe.

3.5.2 Energy Efficiency

We then evaluate the energy efficiency of D2D communications. Fig. 3.9 shows the overall energy efficiency of D2D communications with different transmission distance in a cell. In each sub-figure, we demonstrate the energy efficiency of D2D communications with different circuit power. We consider 0.25W as the typical circuit power of an UE [98], and we consider

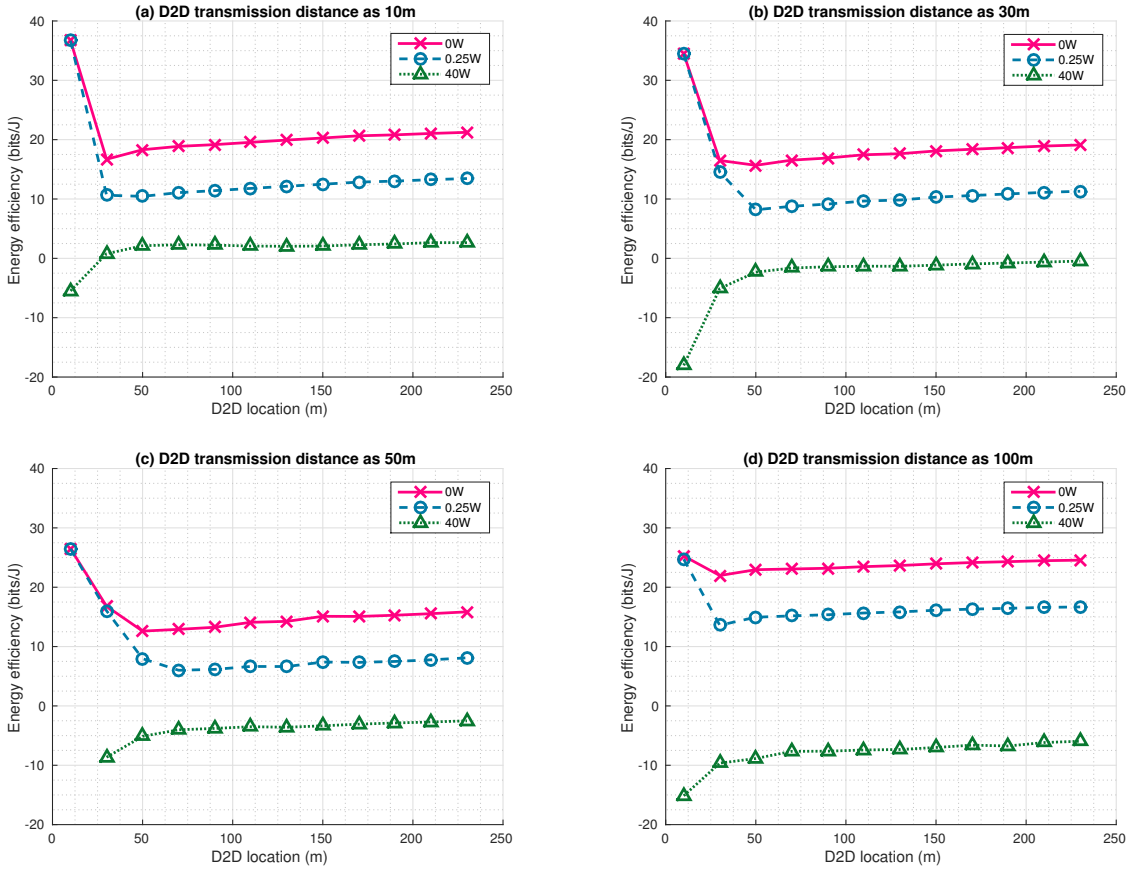

Fig. 3.9 Energy efficiency (in dB) of D2D communications in terms of its transmitter's location. The (a), (b), (c) and (d) show the energy efficiency of D2D communications with transmission distance as $10, 30, 50$ and 100m respectively.

two other circuit powers 0W and 40W, which represent a very low circuit power and a very high circuit power (a circuit power that is $>$ 100x of the maximum total transmit power), respectively. We can see from Fig. 3.9 that, the energy efficiency of D2D communications increases as its transmitter locates far away from the central BS in developing and developed zones (30–150m in the cell) for any circuit power. For the dead zone (0–30m), we can conclude that for D2D UE with low to typical circuit power (i.e., 0W and 0.25W), its energy efficiency decreases as the distance its transmitter to the BS increases. However, the energy efficiency of the D2D UEs with high circuit power (i.e., 40W in Fig. 3.9) increases with distance. We note that, the energy efficiency follows a similar trend of the throughput of D2D communications with high circuit power, as its power consumption is dominated by the high circuit power. It can be concluded from Fig. 3.9, for the D2D UEs with low to typical circuit power, they achieve the best energy efficiency at the centre of the cell, while for the

D2D UEs with high circuit power, they have best energy efficiency performance when the D2D transmitters located at the edge of the cell.

Finally, comparing the four sub-figures in Fig. 3.9, we note that the energy efficiency of D2D communication decreases when its transmission distance increases when the D2D transmitter locates in the dead zone (0–30m). In the developing and the developed zones (30–250m), for the D2D UE with low to typical circuit power, its energy efficiency decreases with the transmission distance increasing from 10m to 50m, but reaches its maximum when the transmission distance is 100m; for the D2D UE with high circuit power, its energy efficiency always decreases with the increase of D2D transmission distance.

3.5.3 Trade-off in D2D Communications

As we can see from aforementioned discussions, for D2D UEs with low to typical circuit power, there exists a trade-off between energy efficiency and throughput. Within a dead zone (0–30m), D2D communications would have a very low throughput, but with a high energy efficiency. Then in the developing zone and developed zone (30–250m), the throughput of D2D communications significantly improve while energy efficiency decrease to a relatively low range (about 10 dB). Furthermore, the D2D communications with the transmission distance of 100m, it has the lowest throughput but the highest energy efficiency comparing to the ones of D2D communications with transmission distance from 10m to 50m, when the circuit power of a D2D UE ranges from low to the typical level.

3.6 Conclusion

In this work, we present a geometrical perspective analysis for D2D communications. We present how the maximum allowed transmit power, the subchannel D2D can reuse, and the transmission distance of D2D communications relate to the location of the D2D transmitter in a cell. We show that the D2D should never reuse a subchannel which is allocated to a CC UL UE with a distance to the BS larger than 200m in the cell with a cell radius set as 250m. Furthermore we find that the transmission radius (defined in Definition 3.3.2) of D2D is about 197m. Then we present the optimal RRM for D2D communications based on our analytical framework. Our proposed RRM has low complexity and can be easily interpreted as *gap/waterfilling*. With our proposed RRM, we conclude that the throughput and the energy efficiency of D2D communications have a significant correlation with its transmitter's location. We find that the cell can be divided into three zones (i.e., dead zone (0–30m), developing zone (30–150m) and developed zone (150–250m)) according to the

throughput of D2D communications. Furthermore, we show there exists a trade-off between throughput and energy efficiency of D2D communications in our works. We believe these works will provide some meaningful insights in the analysis of D2D communications in a cell and inspire future works in the design of D2D communications.

Finally we note that, the future works may include: 1) analysis of multiple D2D pairs in a cell. We can solve a bin packaging problem based on our analytical framework to achieve the upper bound of throughput of D2D communications following the concepts in [103]; 2) a sector-partitioned cell (i.e., the BS is equipped with directional antenna) can be included in the analytical framework; and 3) analysis of mode selection problem (i.e., UEs choose CC communications or D2D communications) in a geometrical perspective.

Chapter 4

Iunius: Combining D2D and P2P system

4.1 Introduction

In the previous chapters, we focus on the fundamental optimisation problems in D2D communications. However, D2D communications can not directly benefit users without a proper application protocol. Few research works considering a proper application protocol for D2D communications. And to our best knowledge, it is lack of published works considering joint application and physical layers optimisation for D2D communications. Nevertheless, we believe these are important for D2D communications that can be actually deployed and leveraged by massive users. Thus we develop Iunius: a peer-to-peer (P2P) system based on multi-hop D2D communications.

A peer-to-peer (P2P) system enables two or more clients communicate with each other without the help from a dedicated server. Although some P2P systems (e.g., BitTorrent) require a central server to facilitate one client to find other clients, the server is not involved in actual data transmissions [104]. Conventional P2P systems usually focus on the design of application layer mechanisms without incorporating the underlaying network or physical layer characteristics [104], [105]. In [106], the authors proposed a context-aware proximity-based P2P (CA-P2P) protocol, which considers the context of physical layer transmission. However, some critical information in the application layer (e.g., how data files are stored in the P2P system) is missing in CA-P2P.

The infrastructureless nature of D2D communications makes it easy to integrate into the conventional P2P systems. The wireless P2P systems proposed in [107]–[109] are based on WiFi-direct, with which efficient interference management is not available. FlashlinQ [24], [25] is a prototype P2P system based on D2D communications without considering an optimised RRM for D2D communications and an efficient P2P protocol for the system. A multicast P2P streaming application based on D2D communications was proposed in [110],

where the authors focused on the node selection problem for P2P multicast considering the characteristics of D2D communications. However, many critical details, including the P2P protocol, RRM scheme and multi-hop routing algorithm are still missing in the above works. In [111], the authors proposed a D2D assisted video transmission system including an optimised physical layer and an application layer model, but they only considered one single-hop D2D pair. A power control scheme for multi-hop D2D communications to maximise the throughput of D2D links without affecting the performance of conventional cellular (CC) UEs was proposed in [37], where a distributed routing protocol was used for multi-hop route discovery. However, the fully distributed routing protocol restricts the route discovery efficiency and the coverage area over which power control can be optimised. Moreover, there is a lack of optimised RRM for multi-hop D2D communications.

In addition, it has been observed that there are often some popular and frequently requested files in a local area network during a period of time. Studies show that the top 10% most popular videos in YouTube attract nearly 80% of total views [112]. Given that the widely used smart personal devices (e.g., smart phones, tablets and laptops) are equipped with storage capabilities for file caching, in this paper, we devise a D2D–based P2P system, called Iunius to facilitate the local caching and transmissions of files among UEs in a cellular network, where D2D communications utilise the UL radio resources. The ultimate goals are to significantly offload data traffic from the cellular BSs and core networks, and to reduce the overall system energy consumption.

The Iunius system optimises D2D communications for P2P local file sharing, improves user experience, and offloads traffic from the BSs. The Iunius system features: 1) a wireless P2P protocol based on Bittorrent protocol in the application layer; 2) a simple centralised routing mechanism for multi-hop D2D communications; 3) an interference cancellation technique for conventional cellular (CC) uplink communications; and 4) a radio resource management scheme to mitigate the interference between CC and D2D communications that share the cellular uplink radio resources while maximising the throughput of D2D communications.

The remainder of this chapter is organised as follows. In Section 4.2, we introduce the network model and the Iunius system. Section 4.3 presents the application layer P2P protocol. In Section 4.4, we present the BS assisted GPSR scheme, interference cancellation technique for CC UL, and RRM for multi-hop D2D communications. In Section 4.5, we evaluate the performance of Iunius through simulations. Finally, conclusions and possible future extensions are given in Section 4.6.

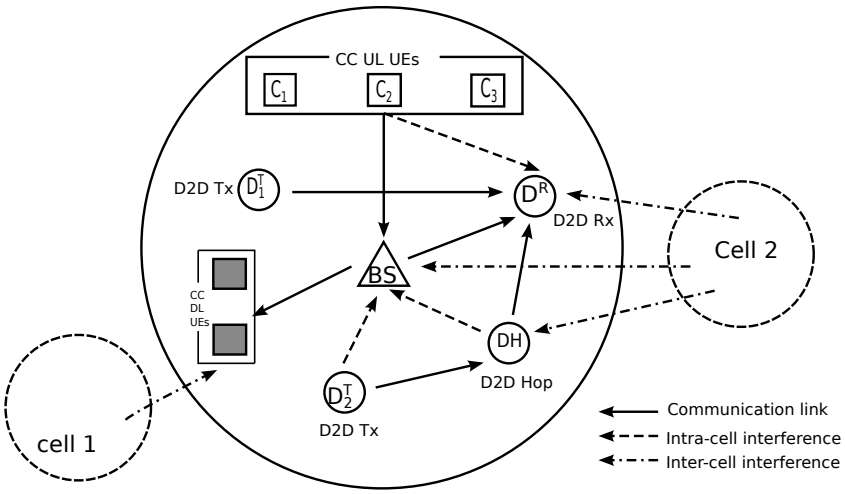

Fig. 4.1 System model of P2P framework, where $N_C^U = 3$ CC UL UEs and $N_D^T = 2$ D2D links share the UL resources, $N_C^D = 2$ CC DL UEs utilise the DL resources. The intra-cell interference includes the interference from D2D transmitters to the BS and the interference from the CC UEs to the D2D receivers. We also consider the inter-cell interference in our system model.

4.2 Iunius System and Network Architecture

4.2.1 Network Model

In this work, we consider a frequency division duplex (FDD) cellular system consisting of multiple cells, as depicted in Fig. 4.1. A BS equipped with an omni-directional antenna is deployed at the center of each cell. For BS assisted D2D communications, we assume that the inter-cell interference plus noise power can be estimated at the D2D receivers and the BSs [29]. The UL and DL channels each have a bandwidth of B, which is divided into K orthogonal subchannels. D2D communications may fully reuse the UL radio resources. A signal-to-interference-plus-noise ratio (SINR) of Γ_D is required for a reliable link to be established between a D2D transmitter and a D2D receiver.

There are three types of UEs: 1) N_C^D DL CC UEs; 2) N_C^U UL CC UEs; and 3) n D2D UEs in the coverage area of a BS. The CC UL and DL UEs are uniformly distributed in the network [37] and communicate with their serving BS directly. A pair of D2D UEs communicate with each other in an ad-hoc fashion over a single or multiple hops, bypassing the BS. We consider one D2D destination receiver d_R, which requires data from the set $\mathscr{D}_T = \{d_1^T, \cdots, d_{N_D}^T\}$ of N_D D2D sources. If there is no direct link available between a D2D source and the D2D destination, relays can be selected from the set $\mathscr{D}_H = \{d_1^H, \cdots, d_{N_H}^H\}$ of N_H idle D2D UEs (by the algorithm to be described in Section 4.4.1). The D2D relays are

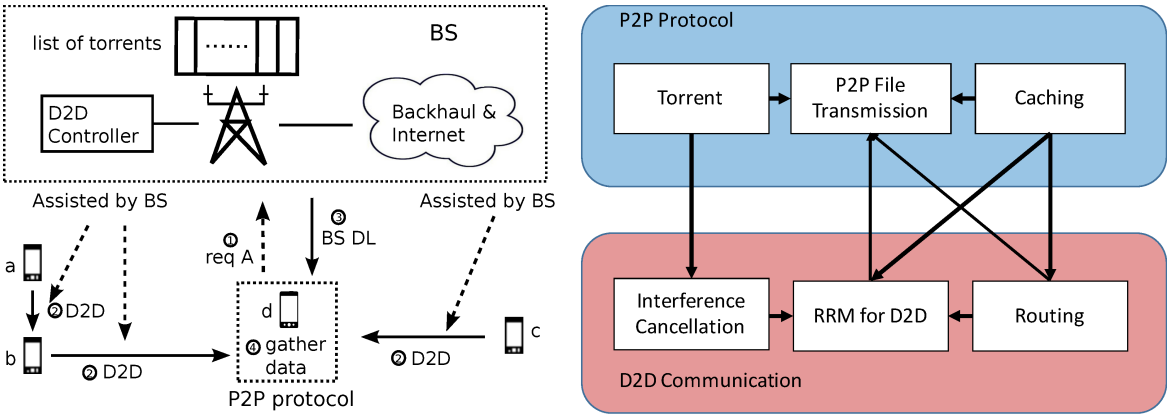

Fig. 4.2 Iunius system model. The left part shows how Iunius works. a, b, c, d are four Iunius subscribers. d requests file A through P2P protocol. a and c are required by BS to transmit parts of file A to d via BS assisted D2D communications. b acts as the relay in the multi-hop D2D communications. Finally d gathers data from all links through P2P protocol. The right part shows how the core components in Iunius are interrelated to each other.

decode-and-forward half-duplex (DF–HD) relays [113]. Accordingly, the set of all D2D UEs is given by $\mathscr{D} = \mathscr{D}_T \cup \mathscr{D}_H \cup \{d_R\}$ with the total number of D2D UEs $n = N_D + N_H + 1$. If the file or data requested by the D2D destination is not fully cached by the D2D sources, then the BS will transmit the rest of data through the CC DL.

The channel model consists of distance dependent path loss, fading and shadowing. Accordingly the channel gain g of a link is given by

$$g = \kappa d^{-\alpha} \|h\|^2 \zeta, \tag{4.1}$$

where κ is a constant determined by the environment [82], d is the distance between the transmitter and the receiver, α is the path loss distance exponent, h is the Rayleigh fading coefficient, and ζ denotes the log-normal shadowing.

4.2.2 Iunius System

Fig. 4.2 shows the Iunius system architecture, which consists of a spatially distributed cache system to provide local file caching services. Iunius subscribers, i.e., the UEs participating in the Iunius system, would cache a list of pre-selected files. Each of these files can be fully or partially cached in Iunius. How each file is divided into chunks and stored at different subscribers is described by a *torrent*. Each BS maintains a list of torrents and has full knowledge of the data stored in each Iunius subscriber associated with it. As we

can see in Fig. 4.2, a subscriber can receive a locally cached file through the following four sub-routines:

1. **Request**: A Iunius subscriber requests a file through the P2P protocol from the BS.
2. **D2D**: The BS then requests proper Iunius subscribers to transfer the data to the requesting subscriber via BS assisted D2D communications, where the BS chooses the route from the D2D source to the D2D destination.
3. **BS DL**: For any partially, locally cached file or any failed end-to-end transmission, the BS transmits the remaining parts of the file to the requesting subscriber.
4. **Data gathering**: The requesting subscriber gathers the data from multiple D2D sources and the BS DL through the P2P protocol.

Note that Iunius subscribers would act as CC UEs when they either do not request any locally cached files or are not involved in D2D communications as sources or relays.

As shown in Fig. 4.2, the Iunius system consists of two major parts: an application layer P2P protocol and physical layer D2D communications. The components in Iunius are interrelated to each other as shown in Fig. 4.2. The torrent files (see Section 4.3.1) and the local caching (see Section 4.3.2 support the P2P file transmissions in application layer. The proposed context-aware P2P protocol enables the interference cancellation in Iunius (see Section 4.4.2). Then we propose an optimised RRM scheme (see Section 4.4.3) for D2D communications, considering the caching, routing and interference cancellation factors, and thereby better supporting the P2P file sharing.

4.3 P2P Protocol

In this section, we demonstrate our P2P protocol design from three key aspects: *torrent*, *spatially distributed caching system*, and *P2P file transmission*. The BS maintains and updates a list $\mathscr{F}$ of pre-selected files for the Iunius system. Each file in $\mathscr{F}$ is split into *chunks*, which are cached by a group of Iunius subscribers. The chunking and location information of a file is stored in a torrent. When a Iunius subscriber d_R requests a file $F(\in \mathscr{F})$ via the P2P protocol, the *P2P file transmission* would be set up by the system.

4.3.1 Torrent

The BS maintains a list $\mathscr{T}$ of torrents, each containing the following information:

- Identifier: Each torrent has a unique identifier and represents exactly one file [104].
- Application layer information: We adopt BitTorrent protocol [104] for the application layer P2P protocol, including both *metainfo* and *tracker* information of BitTorrent protocol. In addition, we add the location information of the peers, i.e., Iunius subscribers, to the *peer* part of BitTorrent protocol. Thus each Iunius subscriber is required to periodically report its location, which can be obtained by the Global Positioning System (GPS) that is available in most contemporary mobile devices.
- Cache information: 1) the identifier and content of each chunk; and 2) which Iunius subscriber each chunk is cached to.
- Context information: We adopt CA-P2P protocol [106] for the transmission of a chunk.

4.3.2 Spatially Distributed Caching System

In the spatially distributed caching system, when a Iunius subscriber d_R receives data through the P2P protocol, it automatically caches the received data if it has available storage space. If it is out of storage space, then it will report to the BS. The BS will decide what data should be cached in d_R and return a series of instructions which would be executed by d_R to update its cache. The communications between the BS and d_R utilise the CC UL and DL links and the BS takes the following steps to make caching decisions:

Step 1 Initialize four lists: the **CURRENT** list contains the identifiers of the chunks already cached at d_R according to $\mathscr{T}$; the **ADD** list holds the identifiers of the newly received chunks at d_R; the **ALL** list consists of both **CURRENT** and **ADD** lists; and the **REMOVE** list is initialised as an empty list.

Step 2 Remove redundancy: remove all the identifiers of chunks that are already cached by other subscribers within a distance p to d_R from the lists **CURRENT**, **ADD** and **ALL**, and put the chunk identifiers removed from **CURRENT** into the list **REMOVE**.

Step 3 Check storage availability: if all the chunks corresponding to **ALL** can be fully cached into d_R, the BS sends the (**ADD**, **REMOVE**) lists to d_R and d_R caches all the chunks of **ADD** and removes all the chunks of **REMOVE**. The BS updates $\mathscr{T}$ and terminates the decision process. Otherwise, move on to Step 4.

Step 4 Classify the priority of chunks in **ALL**: among all chunks in the list **ALL**, the ones that have not been cached by any other subscribers are given the highest priority and with their identifiers put in the list **NEW**. The remaining chunks in **ALL** are classified

into different **POPULARITY** groups according to the popularity of their relevant files. The popularity of a file can be defined according to the frequency or the most recent time of being requested. The priorities of the **POPULARITY** groups are ranked in descending order of their popularity.

Step 5 Remove the lowest priority chunks: remove the identifiers of chunks of the lowest priority group from the lists **CURRENT**, **ADD** and **ALL**, and put the chunk identifiers removed from **CURRENT** into the list **REMOVE**. Go back to Step 3.

The above BS decision process achieves four goals: 1) *Spatially distributed caching with redundancy avoidance*: Step 3 enables every subscriber to cache the data they receive via the P2P protocol, and Step 2 eliminates the redundancy of a chunk being cached in several Iunius subscribers. 2) *Caching fairness*: the chunks that haven't been cached by any subscribers are given the highest priority, and would first be locally cached when there is storage available (Steps 4 and 5). 3) Removal of *Least Recently Used (LRU) chunks* [114]: Step 5 removes the chunks belonging to the LRU files from the spatially distributed caching system first. 4) *Efficiency*: It requires only two messages to be exchanged between the BS and the Iunius subscriber d_R to accomplish the whole BS decision process, i.e., d_R uploads the **ADD** list to the BS and the BS sends back the (**ADD**, **REMOVE**) lists after the decision has been made. Moreover, each list contains only the identifiers of chunks and thus leads to a small size of each message. Therefore, the proposed mechanism ensures that only necessary information is exchanged between the BS and an Iunius subscriber and that the communication overhead is kept at minimum.

4.3.3 P2P File Transmission

Each Iunius subscriber maintains a list of torrent identifiers. When subscriber d_R requests the file $F(\in \mathscr{F})$ through the P2P protocol, the BS chooses a group of subscribers $\mathscr{D}_T$ as source nodes to send chunks of F to d_R via D2D transmissions based on the following rules.

- Uniqueness: A chunk is transmitted by at most one subscriber in the group $\mathscr{D}_T$.
- Proximity: The BS first chooses the subscribers in the neighbourhood of the requesting subscriber d_R to transmit chunks of F to it. The neighbourhood of a subscriber is defined as the area in which a direct link between the subscriber and any other subscribers can be established following the mechanism to be presented in Section 4.4.
- Isolation: If some chunks of F are not cached in the neighbourhood of d_R, then the BS chooses the subscribers outside the neighbourhood of d_R. Since the chunks

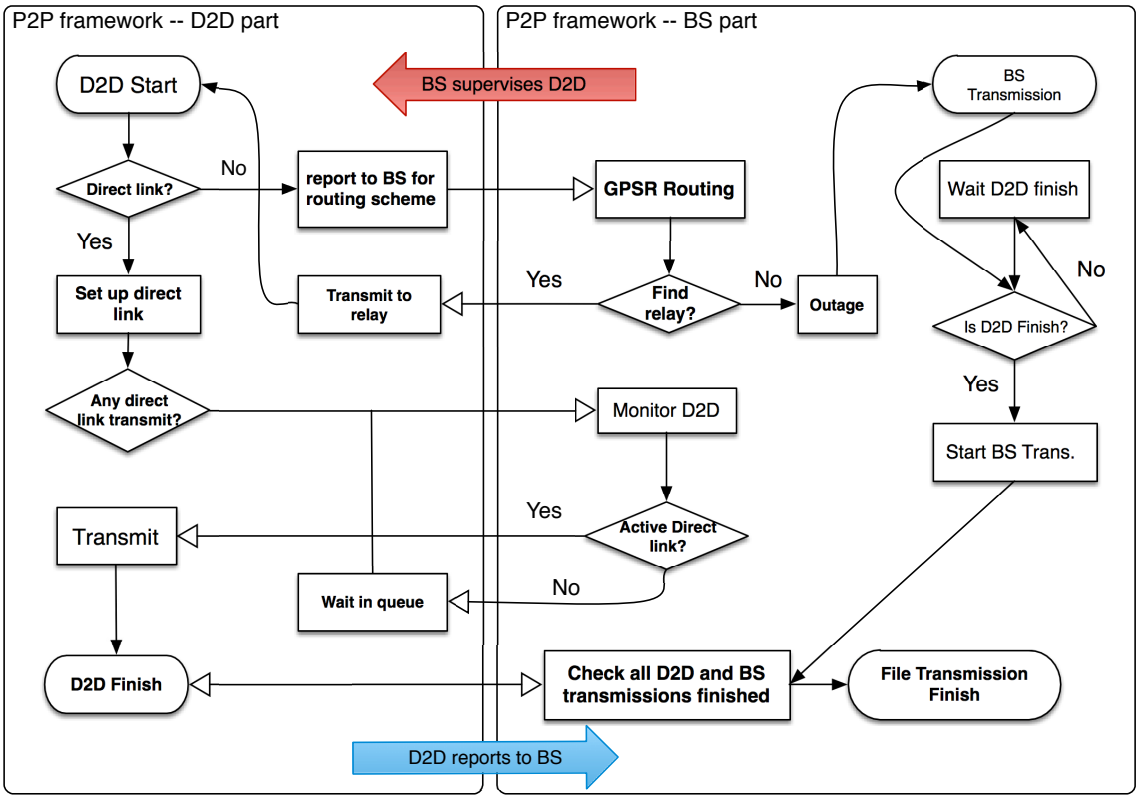

Fig. 4.3 P2P framework flow chart. It shows the process of BS assisted D2D communications carrying out the proposed P2P protocol. The BS supervises the D2D transmissions and D2D pairs report to the BS of their state changes. BS also transmits all the chunks that cannot be transmitted by D2D communications to the receiver. The lines with solid arrows indicate the process within D2D part/BS part, and the lines with blank arrows denote the communications between D2D and the BS.

cached by subscribers outside the neighbourhood of d_R would require multi-hop D2D transmissions to reach d_R, the selected subscribers are preferred to be far apart from each other so that they can transmit data simultaneously to different relays without causing significant interference.

- Greediness: Subscribers would be chosen into the group $\mathscr{D}_T$ until: 1) no more subscribers can fulfil the *proximity* or *isolation* condition; or 2) no more subscribers have cached any chunks of F that have not been cached in $\mathscr{D}_T$.

The overall P2P file transmission mechanism is described by the flow chart in Fig. 4.3. We now devise a physical layer D2D communication scheme to handle the application layer P2P data transmission. At first, each D2D source in the selected group $\mathscr{D}_T$ checks whether it can set up a reliable direct link (i.e., SINR $> \Gamma_D$) to the D2D destination. The infrastructure proposed in [106] and the method proposed in [30] can be used for two D2D

UEs to know the link quality between them. When a direct link is not available, the BS assists the two D2D UEs to find a D2D relay utilising the GPSR algorithm (to be presented in Section 4.4.1). Outage might occur in two situations: 1) GPSR algorithm fails to find an idle Iunius subscriber as relay; or 2) the SINR at the selected relay is less than Γ_D. If outage occurs, the D2D transmitter reports outage to the BS, and the BS will transmit the corresponding data to the D2D destination via CC DL. These operations will repeat until all requested locally-cached chunks are received by the requesting subscriber d_R. The framework in [106] is used to update the BS on the transmission states of D2D communications in a real-time manner (see Section 4.3.1). Thus, the BS can determine whether or not there exists any active direct D2D link, or identify a relay device for the D2D device to set up a new direct D2D link.

As required for DF-HD relay, there is only one active D2D link allowed at a time slot t for each multi-hop D2D route. In addition, there is only one active direct link to d_R allowed during a time slot t. If there are more than one direct links to d_R waiting for transmission, the BS chooses the direct link with the best link quality to be active while withholding the others. The transmissions from different D2D transmitters to different relays would conduct simultaneously. The *isolation* characteristics of the D2D sources in $\mathscr{D}_T$, the GPSR algorithm (proposed in Section 4.4.1) and the RRM scheme (presented in Section 4.4.3) ensure that there will be no significant mutual interference between the concurrent D2D transmissions. Each active D2D link would utilise all the reliable UL subchannels. Finally, the BS would transfer any requested data that are not locally cached by the subscribers in $\mathscr{D}_T$ to d_R.

4.4 D2D Communications Support P2P

In support of the D2D based P2P transmissions, in this section we develop a routing scheme and a joint resource allocation and power control scheme to maximize the throughput of D2D communications while maintaining the QoS of UL CC communications. Furthermore, we prove that in the Iunius system the interference from D2D communications to CC UL communications is negligible.

4.4.1 Greedy Perimeter Stateless Routing for D2D

For cases when there is no reliable direct link between a D2D source and the destination, we propose a multi-hop D2D routing scheme based on the GPSR algorithm [115]. In GPSR-like routing protocols, there are two kinds of package forwarding modes: greedy mode and perimeter mode, which are used to forward packets alternately. A packet is first forwarded

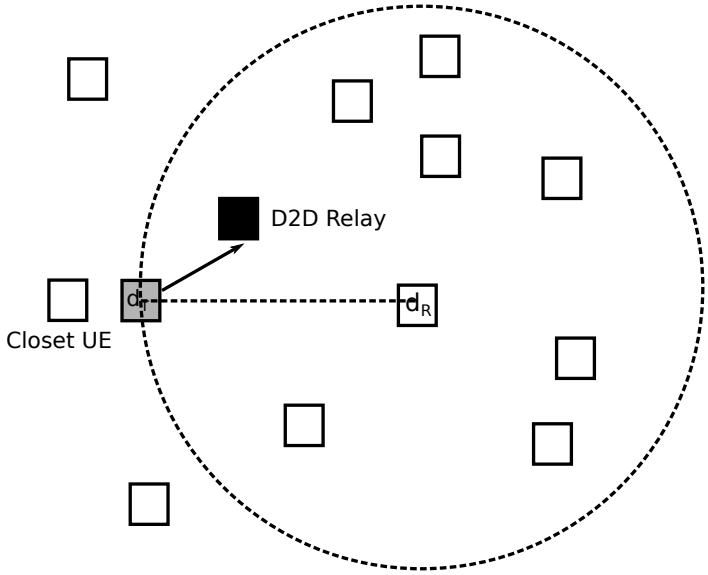

Fig. 4.4 GPSR algorithm. d_T is the D2D transmitter and d_R is the target D2D receiver. The idle subscriber in black is chosen as the relay. The closest idle subscriber to the transmitter is not chosen as it is not in the circle area.

greedily to the destination according to the geo–locations of relays until the packet reaches a relay with no neighbour closer to the destination than itself (i.e., a concave node), then the packet is forwarded using the perimeter mode until the packet reaches a node closer to the destination than the concave node (i.e., a progress node) [115]. In our proposed routing algorithm, both geolocations and channel conditions of relays are considered in the greedy mode, and in perimeter mode (i.e., a concave node is identified), the concave node reports the status to the BS and the BS would send the related packet to the D2D destination. This can improve the routing efficiency and reduce the outage probability of multi-hop D2D communications. The proposed D2D routing algorithm is summarised as follows:

- *greedy mode*: The D2D source is first set as the transmitter d_T. An idle Iunius subscriber fulfilling the following two conditions will be selected as a relay for the D2D communication between transmitter d_T and the file requesting destination d_R: 1) it locates within the circle centred at d_R with a radius of the distance between d_T and d_R (see Fig. 4.4); and 2) it is the closest idle Iunius subscriber to d_T in the circle (see Fig. 4.4). The closest idle subscriber to d_T is selected in order to guarantee the least outage probability of D2D communications for each hop and reduce the energy consumption of each D2D transmitter along the multi-hop D2D route. If such a relay is selected, then the selected relay is set as d_T and the above relay selection repeats

until either no qualifying relay can be found or a complete route is formed from the D2D source to the destination d_R.

- *perimeter mode*: if for a given d_T, the greedy mode fails to find a relay, then that d_T reports to the BS. The BS stops the D2D transmission and forwards the corresponding data to d_R.

4.4.2 Interference Cancellation for CC UL

Without loss of generality, we assume that the set $\mathscr{C}_i$ of subchannels are allocated to CC UE i, where $i = 1, \cdots, N_C^U$, $\bigcup_{i=1}^{N_C^U} \mathscr{C}_i = \{1, \cdots, K\}$, and $\mathscr{C}_i \cap \mathscr{C}_j = \emptyset$ for any $i \neq j$. Since the data to be transmitted and the modulation and coding scheme of the D2D transmissions are known by the BS (see *context info* in Section 4.3.1), we have the following proposition for CC UE i.

Proposition 4.4.1. *The UL channel capacity T_i^c of CC UE i at subchannel c is given by*

$$T_i^c = \frac{B}{K} \log_2 \left(1 + \frac{g_i^c P_i^c}{\sum_{m \in \mathscr{C}} I_i^m + N_0} \right), \tag{4.2}$$

where $c \in \mathscr{C}_i$, $\mathscr{C}$ is the set of cells in the neighbourhood, g_i^c, P_i^c and I_i^m are the channel gain (as defined in (4.1)*), the transmit power and the received power of the interference from cell m at subchannel c in the UL of CC UE i, respectively, and N_0 is the additive white Gaussian noise (AWGN) power.*

Proof. We model the UL channel between CC UE i and the BS as a channel with state. We denote the output at BS as $Y \sim f(y)$, the signal from CC UE i and the inter-cell interference as input $X \sim f(x)$, and the signal from the interfering D2D link as the state $S \sim f(s)$. The channel can be expressed as

$$Y = X + S + N \tag{4.3}$$

where $N \sim N(0, \sigma^2)$ denotes the Gaussian noise. We assume X, S, N are independent. As discussed in Section 4.2, the channel state information is available at the decoder. Thus S is fully acknowledged at the BS and is independent to both X and N. In this case, S can be deducted from the received signal and the information about X obtained from Y is [116]

$$I(X;Y) = I(X;X+S+N) = I(X;X+N) = H(X+N) - H(N), \tag{4.4}$$

where $H(\cdot)$ is the entropy of a signal. According to the theory in [116], and considering the channel capacity in *bit/s*, we have

$$T_i^c = \max_{f(x)} I(X;Y) = \max_{f(x)} H(X+N) - H(N) = \frac{B}{K}\log_2\left(1+\frac{g_i^c P_i^c}{Q_i^c + N_0}\right) \tag{4.5}$$

■

Proposition 4.4.1 indicates that the interference from D2D communications to CC UL communications is cancelled in the Iunius system. As a result, the UL SINR of a CC UE and its throughput are not affected by D2D transmissions.

4.4.3 Radio Resource Management Scheme for D2D

In this subsection, we propose a RRM scheme to maximize the total throughput of D2D links subject to QoS requirements of UL CC UEs.

First, to support the proposed P2P protocol (see Section 4.3.3), which assumes the mutual interference between any two simultaneously active D2D links is negligible, we define the maximum allow transmit power $P_{\max}^{d_a^j,k}$ for D2D communications at subchannel k as

$$P_{\max}^{d_a^j,k} = \min\left\{P_{\max}^C, \frac{P_\delta}{G_{d_a^j,k}}\right\}, \tag{4.6}$$

where P_δ is a very low power level that is negligible by any D2D receiver, $G_{d_a^j,k}$ is the largest channel gain in subchannel k of all the interfering links from d_a^j to the receivers of other active D2D links, and $G_{d_a^j,k}$ can be estimated using the method in [37]. Thus $P_{\max}^{d_a^j,k}$ is the maximum D2D transmit power that d_a^j can utilise without generating significant interference to other concurrent D2D transmissions. We use the statistical estimate of $G_{d_a^j,k}$, i.e., $\overline{G_{d_a^j,k}} = \mathbb{E}[G_{d_a^j,k}]$, as discussed in [37]. Accordingly, the maximum transmit power for d_a^j at the k^{th} subchannel is given by $P_{\max}^{d_a^j,k} = \min\{P_{\max}^C, P_\delta/\overline{G_{d_a^j,k}}\}$.

Consider the D2D source $d_j^T (\in \mathscr{D}_T)$, which requires n_j hops $\mathscr{H}_j = \{h_1^j, \cdots, h_{n_j}^j\}$ to reach the D2D destination. At time slot t, T_a^j is the data rate of the current hop $h_a^j \in \mathscr{H}_j$, in which the D2D transmitter is d_a^j. We have

$$T_a^j = \frac{B}{K}\sum_{k=1}^{K} \chi_{d_a^j}^k \log_2(1+\gamma_{d_a^j}^k). \tag{4.7}$$

where $\gamma^k_{d_a^j}$ is the receiver SINR of the hop h_a^j and is given by

$$\gamma^k_{d_a^j} = \frac{g^k_{d_a^j} P^k_{d_a^j}}{g^k_{i,d_a^j} P^k_i + Q^k_{d_a^j} + N_0} \tag{4.8}$$

where $g^k_{d_a^j}$ and g^k_{i,d_a^j} are the channel gains (as defined in (4.1)) of the D2D link and the interfering link from CC UE i (which is transmitting at subchannel k) to the D2D receiver, respectively, $P^k_{d_a^j}$ and P^k_i are the transmit power of the D2D transmitter d_a^j and the CC UE i at the k^{th} subchannel, respectively, $Q^k_{d_a^j}$ is the inter-cell interference power received by the D2D receiver at subchannel k, and the subchannel assignment indicator $\chi^k_{d_a^j}$ is defined as

$$\chi^k_{d_a^j} = \begin{cases} 1, & \text{if subchannel } k \text{ is allocated to } d_a^j, \\ 0, & \text{otherwise.} \end{cases} \tag{4.9}$$

At time slot t the D2D transmitters of all active D2D links form a group $\mathscr{D}_A^t$. The total throughput T_D^t of all active D2D links at time t is given by

$$T_D^t = \sum_{d_a^j \in \mathscr{D}_A^t} T_a^j. \tag{4.10}$$

We propose to maximise the total throughput of all active D2D links via joint resource allocation and power control as follows.

$$\text{OPT1: } \arg\max_{\boldsymbol{P}_C, \boldsymbol{P}_D, \boldsymbol{\chi}_D} T_D^t \tag{4.11}$$

subject to

$$\sum_{c \in \mathscr{C}_i} T_i^c \geq \Phi_i, \qquad i = 1, \cdots, N_C^U, \tag{4.12}$$

$$0 \leq P_i^c \leq P_{\max}^C, \quad i = 1, \cdots, N_C^U, \tag{4.13}$$

$$0 \leq P^k_{d_a^j} \leq P^{d_a^j,k}_{\max}, \quad \forall d_a^j \in \mathscr{D}_A^t, k = 1, \cdots, K, \tag{4.14}$$

$$\gamma^k_{d_a^j} > \Gamma_D, \quad \forall d_a^j \in \mathscr{D}_A^t, k = 1, \cdots, K, \tag{4.15}$$

$$\chi^k_{d_a^j} = \{0, 1\}, \quad \forall d_a^j \in \mathscr{D}_A^t, k = 1, \cdots, K. \tag{4.16}$$

where the K-by-N_C^U matrix $\boldsymbol{P}_C$, the K-by-$|\mathscr{D}_A^t|$ matrix $\boldsymbol{P}_D$ and the K-by-$|\mathscr{D}_A^t|$ matrix $\boldsymbol{\chi}_D$ contain transmit power for CC UL UEs, transmit power and subchannel assignment indicators for active D2D transmitters, respectively; if the k^{th} subchannel is not used by CC UE i, then

the $(k,i)^{\text{th}}$ element of $\boldsymbol{P}_C$ is 0; T_i^c is given in (4.2), Φ_i is the minimum required UL data rate of CC UE i, $P_{\max}^C$ is the maximum transmit power per subchannel for a CC UE, and $P_{\max}^{d_a^j,k}$ is the maximum D2D transmit power allowed in the k^{th} subchannel for the active D2D transmitter d_a^j. Constraint (4.12) guarantees the UL data rate requirements for CC UEs, where the data rate of CC UE i is the sum data rate of all subchannels allocated to it.

To solve the joint optimisation problem in (4.11) directly would be difficult. From Proposition 1, we know that the D2D transmit power $\boldsymbol{P}_D$ will not affect the throughput of CC UEs. Following (4.6), the mutual interference between coexisting D2D links is negligible. Thus, for any given feasible $\boldsymbol{P}_C$, the objective function in (4.11) is monotonically increasing with $P_{d_a^j}^k$. Therefore, the total throughput of all active D2D links is maximized by each D2D transmitter transmitting in all UL subchannels with the maximum allowed D2D transmit power, i.e., the optimal D2D transmit power and subchannel allocations are given by

$$\begin{cases} P_{d_a^j}^{k,*} = P_{\max}^{d_a^j,k} \\ \chi_{d_a^j}^{k,*} = 1 \end{cases}, \quad d_a^j \in \mathscr{D}_A^t, k = 1,\cdots,K. \tag{4.17}$$

4.4.4 Power Control for CC UL UEs

Following (4.17), the optimisation problem (4.11) can be simplified as

$$\text{OPT2:} \quad \arg\min_{\boldsymbol{P}_C} -\frac{B}{K} \sum_{d_a^j \in \mathscr{D}_A^t} \sum_{k=1}^{K} \log_2 \left(1 + \frac{g_{d_a^j}^k P_{\max}^{d_a^j,k}}{g_{i,d_a^j}^k P_i^k + Q_{d_a^j}^k + N_0} \right) \tag{4.18}$$

subject to

$$-\sum_{c \in \mathscr{C}_i} T_i^c \leq -\Phi_i, \qquad i = 1,\cdots,N_C^U \tag{4.19}$$

$$0 \leq P_i^c \leq P_{\max}^C, \qquad \forall c \in \mathscr{C}_i, i = 1,\cdots,N_C^U \tag{4.20}$$

It can be proven that the objective function in (4.18) is concave and the non-linear constraints (4.19) are convex. Hence, *OPT2* can be considered as a *global separable concave minimisation* problem [117], [118], and the widely used algorithm of [117] can be adopted to solve *OPT2*. Note that this is an *NP-hard* problem and the optimal solution can not be achieved in linear computational time. In the following we propose a reduced-complexity sub-optimal solution for *OPT2*.

We first discuss the necessary and sufficient conditions for *OPT2* to have a feasible solution. As the data rate T_i^c of CC UE i at the c^{th} subchannel is monotonically increasing

with the transmit power P_i^c, the total data rate $\sum_{c\in\mathscr{C}_i} T_i^c$ of CC UE i reaches its maximum value when $P_i^c = P_{\max}^C, \forall c \in \mathscr{C}_i$. We then have the following conclusion.

Lemma 4.4.2. *The necessary and sufficient condition for OPT2 is*

$$\Phi_i \le \Phi_i^\dagger = \frac{B}{K} \sum_{c\in\mathscr{C}_i} \log_2\left(1 + \frac{g_i^c P_{\max}^C}{Q_i^c + N_0}\right). \tag{4.21}$$

Proof. The sufficiency can be proven by combining Proposition 1, (4.2) and (4.19). For an arbitrary $\Phi_i \le \Phi_i^\dagger$, the solution x_0^i to the following equation exists [85], and apparently it satisfies (4.19).

$$\prod_{c\in\mathscr{C}_i}\left(1 + \frac{g_i^c x_0^i}{Q_i^c + N_0}\right) = 2^{K\Phi_i/B}. \tag{4.22}$$

As T_i^c is monotonically increasing with P_i^c, we have $x_0^i \le P_{\max}^i$. Thus x_0^i is a feasible solution of (4.18). The necessity is proven. ■

Hereafter, we assume that Φ_i fulfils Lemma 4.4.2. Denote $f(\boldsymbol{P}_C)$ as the objective function in (4.18) and $\boldsymbol{P}_i$ as the $|\mathscr{C}_i|$-by-1 vector of transmit power allocated to the subchannels utilised by the CC UE i . As each subchannel is assigned to at most one CC UE in each cellular cell, $\boldsymbol{P}_i, \forall i = 1, ..., N_C^U$, are a sequence of disjoint sets. According to the definition of the sets $\mathscr{C}_i$ in Section 4.4.2, we have $f(\boldsymbol{P}_C) = \sum_{i=1}^{N_C^U} f_i(\boldsymbol{P}_i)$, where

$$f_i(\boldsymbol{P}_i) = -\frac{B}{K} \sum_{c\in\mathscr{C}_i} \sum_{d_a^j\in\mathscr{D}_A^t} \log_2\left(1 + \frac{g_{d_a^j}^c P_{\max}^{d_a^j,c}}{g_{i,d_a^j}^c P_i^c + Q_{d_a^j}^c + N_0}\right). \tag{4.23}$$

Thus, minimising the objective function $f(\boldsymbol{P}_C)$ is equivalent to minimising each $f_i(\boldsymbol{P}_i)$. Accordingly, *OPT2* is transformed into *OPT3* as follows,

$$\text{OPT3:} \quad \arg\min_{\boldsymbol{P}_i} f_i(\boldsymbol{P}_i), \qquad \forall i = 1, \cdots, N_C^U \tag{4.24}$$

subject to

$$-\sum_{c\in\mathscr{C}_i} T_i^c \le -\Phi_i, \qquad i = 1, \cdots, N_C^U, \tag{4.25}$$

$$0 \le P_i^k \le P_{\max}^C, \qquad \forall k \in \mathscr{C}_i, i = 1, \cdots, N_C^U. \tag{4.26}$$

We then construct an algorithm to solve each subproblem of *OPT3*. Denote

$$f_i^c(P_i^c) = -\sum_{d_a^j \in \mathscr{D}_A^t} \log_2 \left(1 + \frac{g_{d_a^j}^c P_{\max}^{d_a^j,c}}{g_{i,d_a^j}^c P_i^c + Q_{d_a^j}^c + N_0}\right), \tag{4.27}$$

then $f_i(\boldsymbol{P}_i) = -B/K \sum_{c \in \mathscr{C}_i} f_i^c(P_i^c)$. It can be shown that $f_i^c(P_i^c)$, $c \in \mathscr{C}_i$, are concave functions. This indicates that each subproblem of *OPT3* can be transformed into a *global separable concave minimisation* problem [117].

Definition 4.4.1. *A rectangular domain is defined as* $\mathscr{R} = \{x_i | l_i \leq x_i \leq h_i, i = 1, \cdots, n\}$.

Definition 4.4.2. *A set* $\tilde{\mathscr{R}}$ *is a compact convex set iff*

- *It is a compact set.*
- *For every* $x_1, x_2 \in \tilde{\mathscr{R}}$ *and* $0 < \lambda < 1$, $\lambda \in \mathbb{R}$, *the point* $\lambda x_1 + (1-\lambda)x_2 \in \tilde{\mathscr{R}}$.

Definition 4.4.3. *For a continuous function* $f(x)$ *defined on a compact convex set* $\tilde{\mathscr{R}}$, *a function* $\hbar(x)$ *is its convex envelope iff*

- $\hbar$ *is a convex function on* $\tilde{\mathscr{R}}$.
- $\hbar(x) \leq f(x)$ *for every* $x \in \tilde{\mathscr{R}}$
- *If* $h(x)$ *is a convex function defined on* $\tilde{\mathscr{R}}$ *such that* $h(x) \leq f(x)$ *for all* $x \in \tilde{\mathscr{R}}$, *then* $\hbar(x) \leq h(x)$ *for all* $x \in \tilde{\mathscr{R}}$.

Theorem 4.4.1. *The convex envelope* $\hbar(x)$ *for a separable concave function* $f(x) = \sum f_i(x_i)$, $i = 1, \cdots, s$, *defined on a set* $\tilde{\mathscr{R}} \cap \mathscr{R}$, *where* $\tilde{\mathscr{R}}$ *is a compact convex set and* $\mathscr{R} = \{x_i | l_i \leq x_i \leq h_i, i = 1, \cdots, n\}$ *is a rectangular domain, is given by*

$$\hbar(x) = \sum_{i=1}^{s} (a_i x_i + b_i), \tag{4.28}$$

where a_i *and* b_i *are defined as*

$$a_i l_i + b_i = f_i(l_i), \qquad a_i h_i + b_i = f_i(h_i) \tag{4.29}$$

Proof. See [117], [118]. ■

Corollary 4.4.3. *For the optimisation problem defined in OPT3, denote $\hbar_{v,i}(\boldsymbol{P}_i)$ as the convex envelope of $f_i(\boldsymbol{P}_i)$ on any rectangular domain $\mathscr{R}_{v,i} = \{P_i^c | l_{v,i}^c \leq P_i^c \leq h_{v,i}^c, c \in \mathscr{C}_i\} \subseteq \mathscr{R}_{0,i}$, where $\mathscr{R}_{0,i}$ is the feasible rectangular domain of* (4.26)*, then we have*

$$\hbar_{v,i}(\boldsymbol{P}_i) = \sum_{c \in \mathscr{C}_i} (a_{v,i}^c P_i^c + b_{v,i}^c), \tag{4.30}$$

where $a_{v,i}^c$ and $b_{v,i}^c$ are given by

$$\begin{bmatrix} a_{v,i}^c \\ b_{v,i}^c \end{bmatrix} = \begin{bmatrix} l_{v,i}^c & 1 \\ h_{v,i}^c & 1 \end{bmatrix}^{-1} \begin{bmatrix} f_i^c(l_{v,i}^c) \\ f_i^c(h_{v,i}^c) \end{bmatrix} \tag{4.31}$$

Proof. We prove that the feasible domain of (4.25), $\tilde{\mathscr{R}}_i$, is a compact convex set. First, we have $\tilde{\mathscr{R}}_i \subset \mathscr{R}_{0,i}$, thus $\tilde{\mathscr{R}}_i$ is bounded and closed, i.e., $\tilde{\mathscr{R}}_i$ is a compact set. As aforementioned, T_i^c is monotonically increasing with P_i^c, thus $\tilde{\mathscr{R}}_i$ is also a convex set. According to Definition 4.4.1, $\tilde{\mathscr{R}}_i$ is a compact convex set.

Note that (4.31) is the solution of (4.29). Then with Theorem 4.4.1, we prove this corollary. ■

Following the above discussion, we propose a power control algorithm in Fig. 4.5 to solve *OPT3* based on the *branch-and-bound* algorithm [117]. In Fig. 4.5, we define two operators $\ominus$ and $\oplus$ (Lines 24–26) as removing a specific bound and adding a specific bound to a rectangular area, respectively. We use $\{\cdot\}$ to represent the "array" concept in programming, which is a set of unordered elements. The power control algorithm initialises the vector $\boldsymbol{R}$ with its only element given by $\mathscr{R}_{0,i}$ and the index of iteration q as 1.

In the q^{th} iteration, $\mathscr{R}_{0,i}$ is subdivided into s_q rectangular domains, which are put into the vector $\boldsymbol{R}$ (Lines 4–6). For each rectangle $\mathscr{R}_{v,i}$ (Line 6), the algorithm calculates the convex envelope function $\hbar_{v,i}((P)_i)$ defined in (4.30) and (4.31) (Lines 7–9,13) and the associated solution $\boldsymbol{P}_C^v$ of the convex optimisation problem defined as follows (Lines 14,15).

$$\begin{aligned} &\text{OPT4:} && \arg\min_{\boldsymbol{P}_i} \hbar_{v,i}(\boldsymbol{P}_i) \\ &\text{subject to} && \boldsymbol{P}_i \in \tilde{\mathscr{R}}_i \cap \mathscr{R}_{v,i} \end{aligned} \tag{4.32}$$

We notice that the intersection of $\tilde{\mathscr{R}}_i$ and $\mathscr{R}_{v,i}$ might be empty. In this case, we remove the rectangle $\mathscr{R}_{v,i}$ from $\boldsymbol{R}$ and continue the calculation for the next rectangle (Line 10–11). We choose the solution P_C^t of *OPT4* on the rectangle domain $\mathscr{R}_{t,i}$, which has the smallest objective function value (Line 19). Let $\boldsymbol{P}_q^*$ denote P_C^t (Line 20). The algorithm terminates when $f(\boldsymbol{P}_q^*) = \hbar_{q,i}(\boldsymbol{P}_q^*)$ (Line 27), and the solution $\boldsymbol{P}_q^*$ is returned (Line 28). Otherwise,

1: **function** CCPOWERCONTROL($\boldsymbol{P}^C_{\max}$, $\tilde{\mathscr{R}}_i$, $\mathscr{R}_{0,i}$, $\mathscr{C}_i$, i)
2: **Initialise** $q \leftarrow 1$; $\boldsymbol{R} \leftarrow \{\mathscr{R}_{0,i}\}$;
3: **repeat**
4: $\boldsymbol{P} \leftarrow \{\}$; $s_q \leftarrow \text{LEN}(\boldsymbol{R})$;
5: **for all** $v = 1, \cdots, s_q$ **do**
6: $\mathscr{R}_{v,i} \leftarrow \boldsymbol{R}[v]$;
7: **for all** $k \in \mathscr{C}_i$ **do**
8: $(a^c_{v,i}, b^c_{v,i}) \leftarrow$ (4.31) with $\mathscr{R}_{v,i}$;
9: **end for**
10: **if** $\tilde{\mathscr{R}}_i \cap \mathscr{R}_{v,i} = \emptyset$ **then**
11: $\boldsymbol{P}^v_C \leftarrow \emptyset$; $\boldsymbol{R} \leftarrow \boldsymbol{R} \ominus \mathscr{R}_i$;
12: **else**
13: $\hbar_{v,i}(\cdot) \leftarrow$ (4.30) with $(a^c_{v,i}, b^c_{v,i})$;
14: $\boldsymbol{P}^v_C \leftarrow$ solve (4.32) with $\hbar_{v,i}(\cdot)$, $\mathscr{R}_{v,i}$ and $\tilde{\mathscr{R}}_i$;
15: $\boldsymbol{P} \leftarrow \boldsymbol{P} \oplus \boldsymbol{P}^v_C$;
16: **end if**
17: **end for**
18: $s_q \leftarrow \text{LEN}(\boldsymbol{R})$;
19: $t \leftarrow \arg\min_v \hbar_{v,i}(\boldsymbol{P}^v_C), \forall v = 1, \cdots, s_q$;
20: $\boldsymbol{P}^*_q \leftarrow \boldsymbol{P}[t]$; $\quad \hbar_{q,i}(\cdot) \leftarrow \sum_{c \in \mathscr{C}_i} \hbar^c_{t,i}(\cdot)$;
21: $r \leftarrow \arg\max_c \left(f_c(\boldsymbol{P}^*_q[c]) - \hbar^c_{t,i}(\boldsymbol{P}^*_q[c])\right), \forall c \in \mathscr{C}_i$;
22: $P^{*,r}_q \leftarrow \boldsymbol{P}^*_q[r]$;
23: $\mathscr{R}^l_q \leftarrow \mathscr{R}_{t,i} \ominus \{P^r_i | l^r_{t,i} \le P^r_i \le h^r_{t,i}\} \oplus \{P^r_i | l^r_{t,i} \le P^r_i \le P^{*,r}_q\}$;
24: $\mathscr{R}^u_q \leftarrow \mathscr{R}_{t,i} \ominus \{P^r_i | l^r_{t,i} \le P^r_i \le h^r_{t,i}\} \oplus \{P^r_i | P^{*,r}_q \le P^v_C \le h^v_t\}$;
25: $\boldsymbol{R} \leftarrow \boldsymbol{R} \ominus \mathscr{R}_{t,i} \oplus \mathscr{R}^l_q \oplus \mathscr{R}^u_q$
26: $q \leftarrow q + 1$
27: **until** $f(\boldsymbol{P}^*_q) = \hbar_{q,i}(\boldsymbol{P}^*_q)$
28: **return** $\boldsymbol{P}^*_q$ as the solution to the i^{th} subproblem;
29: **end function**

Fig. 4.5 Power control algorithm.

the weak branching rule is applied to divide the rectangle $\mathscr{R}_{t,i}$ into two sub-rectangles as follows [118]: we first find the point r in $\boldsymbol{P}^*_q$, which maximises the difference between $f_c(\boldsymbol{P}^*_q[c])$ and $\hbar^c_{t,i}(\boldsymbol{P}^*_q[c])$, $\forall c \in \mathscr{C}_i$; we then divide $\mathscr{R}_{t,i}$ into two rectangles at the point $\boldsymbol{P}^*_q[r]$ (Lines 21–24). These two new rectangles replace the original $\mathscr{R}_{t,i}$ in $\boldsymbol{R}$ (Line 25). The above process repeats until the termination rule is fulfilled.

According to [119], any limit point generated by the proposed algorithm is a solution to a subproblem of *OPT3*. Therefore, we can relax the termination rule for the proposed algorithm as: when the iteration index q reaches a pre-determined maximum value, the algorithm terminates and returns the solution $\boldsymbol{P}^*_q$.

Finally we discuss a sub-optimal solution specifically tailored for current LTE/LTE-A systems, which use SC-FDMA in the UL. SC-FDMA requires an equal power allocation in all subchannels assigned to a UE to achieve a low peak-to-average power ratio. Thus the sub-optimal solution to *OPT2* can be obtained by solving the following equations for P_i^*,

$$\prod_{c\in\mathscr{C}_i}\left(1+\frac{g_i^c P_i^*}{Q_i^c+N_0}\right)=2^{K\Phi_i/B},\quad i=1,\cdots,N_C^U. \tag{4.33}$$

Each equation in (4.33) is a polynomial of P_i^*. Thus it has a radical–expression solution when the highest order of the equation is less then five [85]. Otherwise, it can be solved using *Newton-Raphson* method numerically [85]. The matrix $\boldsymbol{P}_C$ can be initialised as an all-zero matrix. It is worth noticing that the rate of convergence of *Newton-Raphson* method is high and several methods have been proposed to further improve the convergence rate [85].

In summary, the power control for the CC UL UEs and the RRM for the D2D communications can be performed as follows:

- Each D2D link is assigned with all available UL subchannels.
- Each D2D transmitter utilises the maximum allowed transmit power defined in (4.6) to ensure no significant mutual interference between D2D links.
- The transmit power of a CC UE follows the optimal power control algorithm presented in Fig. 4.5 or the sub-optimal solution defined in (4.33) for SC-FDMA UL in LTE/LTE-A systems.

4.5 Simulation Results

We perform Monte–Carlo simulation to evaluate the performance of Iunius. The simulation model consists of 19 hexagonal cells and each cell has 3 sectors as described in [82]. We use the channel model in Table B.1.2.1–1 (Urban Micro) in [82]. The remain important simulation parameters are summarised in Table 4.1. The data rate threshold Φ_i, $\forall i=1,\cdots,N_C^U$ is randomly generated under the restriction defined in (4.21) (Lemma 1).

Fig. 4.6 plots the central cell where the Iunius system is deployed and evaluated. We randomly choose a position in the central cell as the location of the Iunius receiver. The Iunius subscribers are uniformly distributed in the central cell. The Iunius transmitters are chosen by rules described in the proposed P2P protocol. In Fig. 4.6, the circular area around the Iunius receiver is its neighbourhood area. In addition, the CC UL UEs and the CC

Table 4.1 Simulation Parameters

Parameter	**Value**
Inter-site distance	500m
AWGN power density (N_0)	-120 dBm/Hz
Bandwidth	10 MHz
Frequency	2.3 GHz
Number of Subchannels	50
Pathloss exponent (α)	$2, 2.5, 3, 3.5, 4, 4.5$
Distance threshold (δ_d)	20m
Negligible power level (P_{δ_D})	-60 dBm
Number of CC UL UEs (N_C^U)	5
Number of CC DL UES (N_C^D)	10
SINR threshold (Γ_D)	8.75 dB
Maximum transmit power $P_{\max}^C$	23 dBm
Multipath fading (Rayleigh distribution)	Scale parameter 0.5
Shadowing (Log-normal)	Standard deviation of 4 dB

DL UEs are generated following a spatial uniform distribution. Although we focus on the performance of the central cell, all the effects of neighbouring cells are included.

4.5.1 Outage Probability and Average Number of Hops

We first evaluate the outage probability and the average number of hops of the muliti-hop D2D transmissions in the Iunius system. The outage probability is the probability of an outage event (as defined in Section 4.3.3) occurring. These two metrics show the performance of the P2P protocol and the GPSR algorithm.

Assuming that the Iunius subscribers are uniformly distributed in the cellular network with a spatial density ρ (the number of Iunius subscribers per square kilometre), we show in Fig. 4.7 the outage probability of D2D transmissions versus the Iunius subscriber density ρ. We can see that for all path loss exponents considered the outage probability of D2D transmissions decreases as ρ increases. This is because with a higher density of Iunius subscribers, it is more likely for the proposed P2P protocol and GPSR algorithm to find relays and the average transmission distance of each hop becomes shorter, thus reducing the outage probability. For each considered α, when ρ gets larger than 1000, the outage probability falls below 0.1. This indicates that in high population density areas, such as city centres, our proposed P2P protocol and GPSR algorithm can efficiently find routes from D2D transmitters to the D2D destination, and thus can efficiently support the end-to-end data transmissions in the Iunius system.

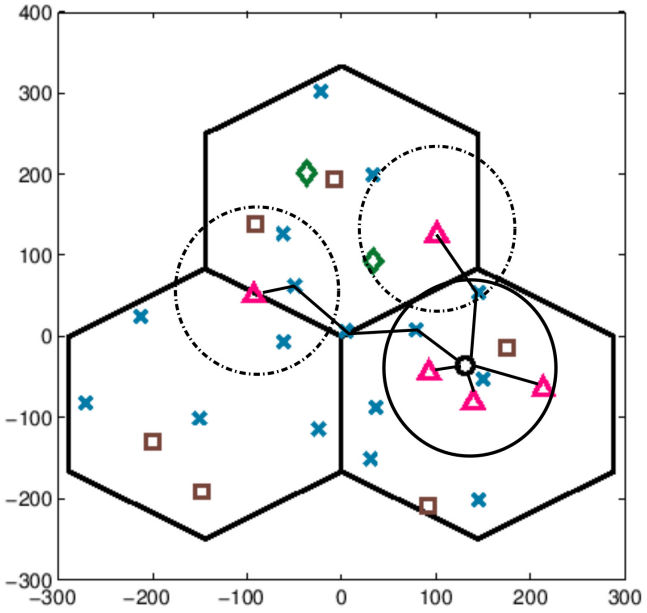

Fig. 4.6 Simulation model. The figure shows the central cell while the 18 outer cells are omitted for simplicity. The chosen D2D transmitters (triangle shape) follow the *proximity* and *isolation* rules described in Section 4.3.3. The red triangle, black circle, blue cross, green diamond and brown square represent the Iunius transmitters, Iunius receiver, idle Iunius subscribers, CC UL UEs and CC DL UEs, respectively.

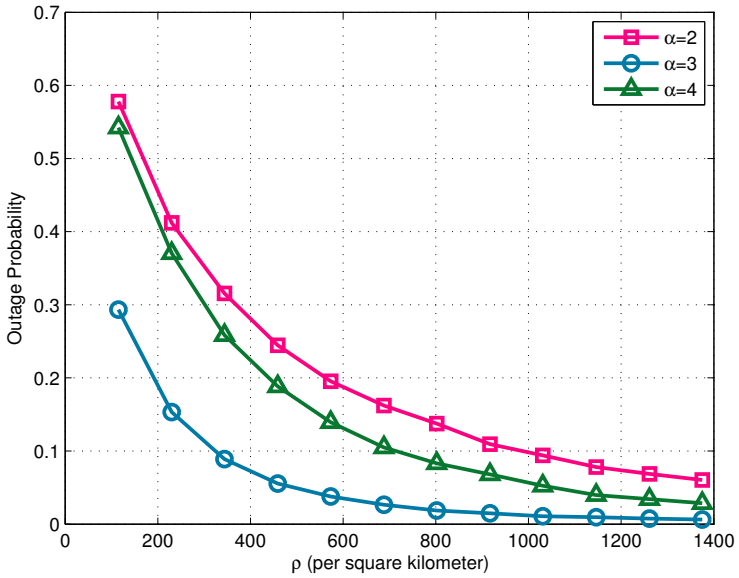

Fig. 4.7 Simulated outage probability of D2D transmissions.

Fig. 4.8 illustrates the average number of hops for D2D communications in the Iunius system versus the subscriber density ρ. We can see that for each considered α, the average number of hops for D2D communications increases with ρ, while the rate of increase slows down at higher values of ρ. We note that for $\alpha = 3$ even with a very high density of Iunius subscribers ($\rho = 1400$), the average number of D2D hops is below 5. This ensures that the BS assisted D2D communications in the Iunius system would not overwhelm the BS.

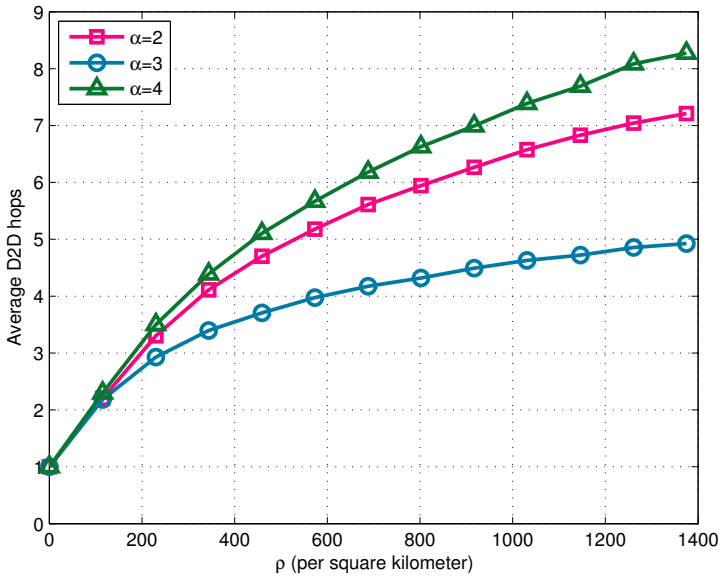

Fig. 4.8 The average number of hops of D2D communications in the Iunius system versus the density of Iunius subscribers.

From both Fig. 4.7 and Fig. 4.8 we note that, for a given ρ, the Iunius system achieves the lowest outage probability and requires the lowest average number of D2D hops in the moderate path loss environment ($\alpha = 3$). According to (4.6) and (4.17) in Section 4.4.3, all the D2D communications utilise their maximum allowed transmit power $P_{\max}^{d_a^j,k}$. In a small path loss environment (e.g., $\alpha = 2$), the D2D communications are restricted to a small $P_{\max}^{d_a^j,k}$ ($P_{\max}^{d_a^j,k} \leq P_\delta / G_{d_a^j,k}$) and might suffer from severe interference from CC UL UEs, thus it has a larger outage probability and shorter transmission distance leading to more hops compared to those in the moderate path loss environment. On the other hand, in a large path loss environment ($\alpha = 4$), the transmit power of D2D transmitters would not be significantly larger than that in the moderate path loss environment (as $P_{\max}^{d_a^j,k} \leq P_{\max}^{C}$) while the D2D UEs are more isolated from each other, thus both the outage probability and the average number of hops are larger than those for $\alpha = 3$.

4.5.2 Throughput

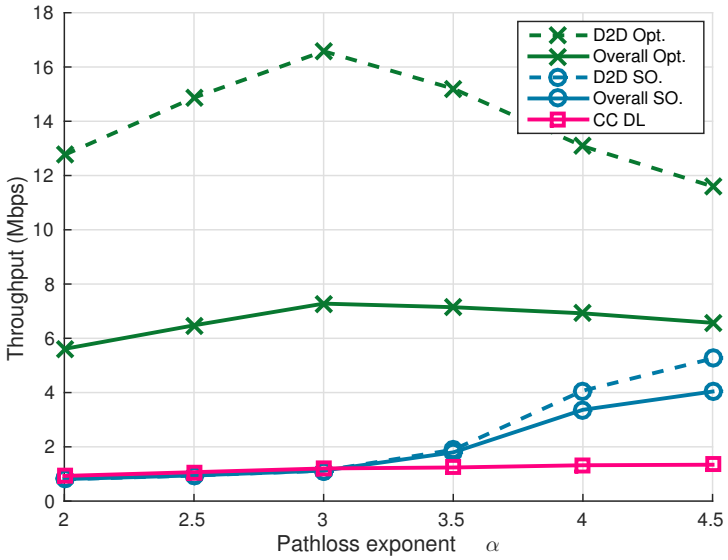

Fig. 4.9 Throughput of D2D communications, the overall Iunius system, and CC DL versus path loss exponents (with file sharing ratio 90%).

Fig. 4.9 plots the throughput of D2D communications T_{DL}, the overall throughput of the Iunius system T_{Iunius} and the throughput of CC DL transmissions T_{D2D} versus the path loss exponent α, where performance corresponding to both the proposed optimal RRM and sub-optimal RRM schemes is included, $\rho = 700$, and 90% of the requested file has been evenly cached by the randomly chosen D2D transmitters. The overall throughput of the Iunius system is calculated as

$$T_{\mathrm{Iunius}} = \frac{1}{0.1 * (1 + \Pr(\text{outage}))/T_{\mathrm{DL}} + 0.9 * (1 - \Pr(\text{outage}))/T_{\mathrm{D2D}}}, \tag{4.34}$$

where $\Pr(\text{outage})$ is the outage probability of D2D communications which is evaluated in Fig. 4.7. We note that, T_{Iunius} is the average throughput which the Iunius system can achieve. It can be seen that the D2D communications with the optimal RRM scheme achieves a much high throughput than that with the suboptimal RRM scheme in all path loss environments, so does the overall throughput of the Iunius system. In accordance with the results in Fig. 4.7 and Fig. 4.8, the throughput of the D2D communications with optimal RRM reaches its maximum (almost 17 Mbps) at $\alpha = 3$. As we can see from *OPT2* defined in (4.18) and its constraint (4.19), with the optimal RRM scheme and $\rho = 700$, the throughput of D2D communications scales with the transmit power $P_{\max}^{d_a^j,k}$ in (4.6), which

increases with α in small and moderate path loss environments but is capped by $P^{C}_{\max}$ in a high path loss environment where D2D UEs are isolated from each other, leading to the decrease of D2D throughput. With the sub-optimal RRM, the D2D throughput increases with α. This is because the power control for CC UL UEs defined in (4.33) does not prevent the interference from CC UL UEs to the D2D communications and in a larger path loss environment the D2D communications are more isolated from the CC UL communications, i.e., suffer less interference from CC UL UEs. The overall throughput of the Iunius system with the optimal RRM is much higher than that of CC DL in all path loss environments, and the overall throughput with the suboptimal RRM is increasingly higher than the CC DL throughput at higher values of α. This shows that the Iunius system significantly outperforms the CC system in terms of DL throughput.

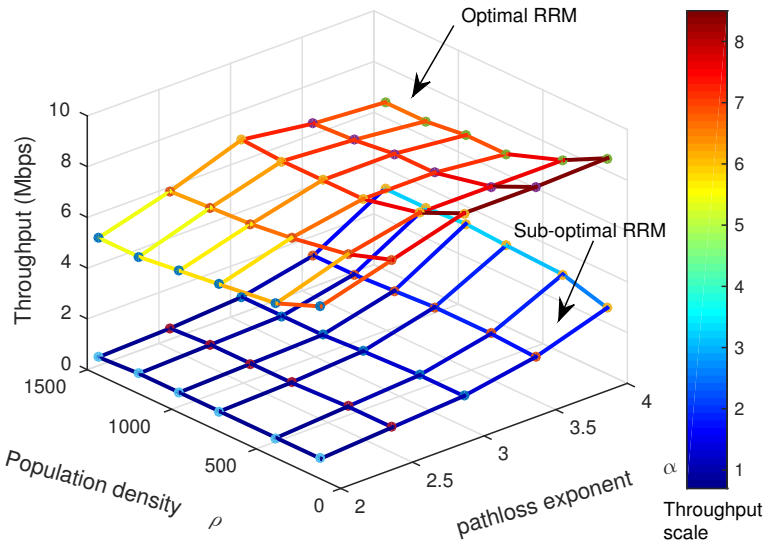

Fig. 4.10 Iunius system throughput performance for different Iunius subcribers density ρ and path loss exponent α. Different colors represent different throughputs of the Iunius system.

Fig. 4.10 compares the overall throughput of the Iunius system deploying the optimal and sub-optimal RRM schemes. For each considered pair of ρ and α, the throughput achieved by the optimal RRM is much higher than that of the suboptimal RRM, with the gap between them decreasing with both ρ and α. For the optimal RRM scheme, we can see that for a given α the throughput of the Iunius system decreases with ρ, indicating that a high density of Iunius subscribers does not help to improve the performance of Iunius system deploying optimal RRM. This is mainly because with a higher ρ, more hops might be taken from the D2D source to the destination (see Fig. 4.8), thereby reducing the throughput. For a low density of Iunius subscribers ($\rho < 500$), the throughput increases with α. This is

because with a lower ρ, the D2D transmissions have a longer average distance per hop and become more vulnerable to the interference from CC UL UEs, thus preferring a more isolated transmission environment (i.e., larger α). For the sub-optimal RRM scheme, we observe that the throughput always increases with α for a given ρ. In small and moderate path loss environments ($2 \leq \alpha \leq 3$), the throughput almost remains constant for different ρ. While in a high path loss environment ($\alpha = 4$), the throughput increases with ρ. This shows that the sub-optimal RRM scheme is more applicable in a high path loss environment with a high Iunius subscriber density.

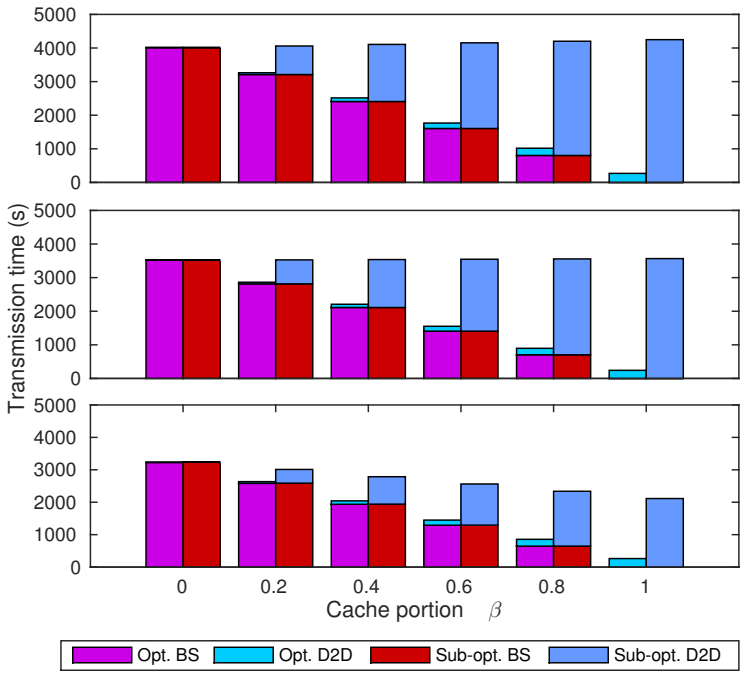

Fig. 4.11 Transmission times in the Iunius system. From top to bottom, α is $2,3,4$, respectively.

Fig. 4.11 illustrates the time consumptions of BS transmissions and D2D transmissions in the Iunius system deploying the optimal or sub-optimal RRM scheme versus the portion of file being locally cached in Iunius, which is denoted by the local cache portion β, for $\rho = 700$, $\alpha = 2,3,4$. We can see that for given β and α, the total time consumption with the optimal RRM scheme is much less than that with the suboptimal scheme, and the difference between the two schemes increases with β for a given α. For a given β, the total time consumption, time for D2D transmissions, and time for BS transmissions all decrease with α for both the optimal and suboptimal RRM schemes. For any $\beta < 1$, the time for BS transmissions always dominates the time consumption with the optimal RRM scheme. This is mainly

due to the high throughput that D2D communications can achieve with the optimal RRM scheme. On the contrary, with the sub-optimal RRM scheme, when $\beta > 0.6$ the time for D2D transmissions becomes dominant in the Iunius system. We note that, the total transmission time of the Iunius system will never exceed the time required by the CC DL solely ($\beta = 0$) to transmit the same amount of data for any given β and α. Thus, the Iunius system can efficiently offload traffic from the cellular BSs.

4.5.3 Energy Saving

In the Iunius system, the total energy consumption of a multi-hop D2D route is determined by two parts: the number of hops from D2D source to its associated destination and the energy consumption for each hop, which is discussed in Section 4.4.

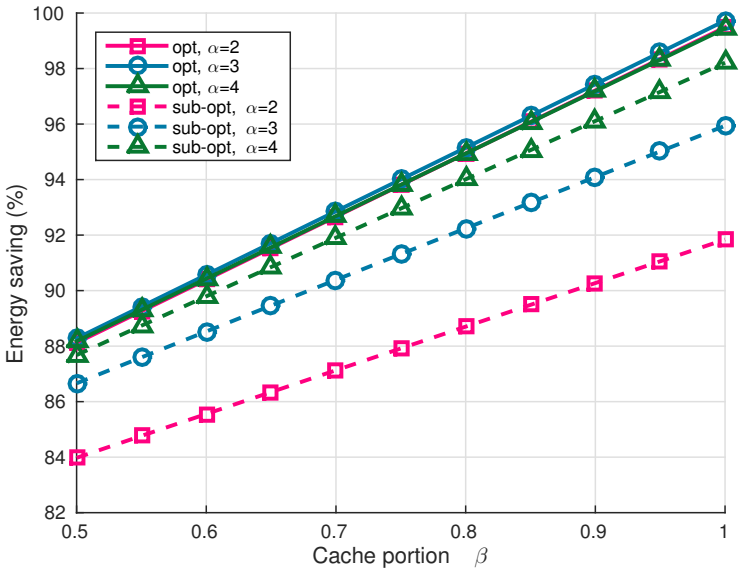

Fig. 4.12 Energy saving of the Iunius system as compared to the CC system for transmitting the same amount of data.

We quantify the energy saving of the Iunius system compared to the CC transmission versus the local cache portion β under the same setting as for Fig. 4.7 and Fig. 4.8. The normalised energy saving is defined as

$$E_{\text{save}} = \frac{E_{\text{BS}} - E_{\text{Iunius}}}{E_{\text{BS}}} \times 100\% = \frac{E_{\text{BS}} - (\sum_{n=1}^{n_j} E_{\text{hop}}^{n} + E'_{\text{BS}})}{E_{\text{BS}}} \times 100\%, \tag{4.35}$$

where E_{BS} is the total energy consumed by the CC DL to transmit a data file of 4 Gbits at the data rate of 1 Mbps, E_{Iunius} is the total energy consumed by the Iunius system to

deliver the same file at the same data rate, E^n_{hop} is the energy consumed by each D2D hop, n_j is the average number of D2D hops, and E'_{BS} is the energy consumed by the BS for transmitting the part of the file not locally cached in Iunius. We can see that with the same β and α, the optimal RRM scheme achieves a higher energy saving than the suboptimal RRM scheme. For a given α, the energy saving of the Iunius system increases with β for both the optimal and suboptimal RRM schemes. With the optimal RRM scheme, for any given β, there is no significant difference in energy saving in different path loss environments. With the sub-optimal RRM scheme, that for a given β the energy saving increases with α, and when $\alpha = 4$ it achieves a similar energy saving as the optimal RRM. This is because the sub-optimal RRM scheme achieves a higher data rate for larger α (as shown in Fig. 4.10), leading to a higher energy saving per hop. This surpasses the negative effect of a large number of D2D hops in a high path loss environment to energy saving.

4.5.4 Computational Complexity

The superior performance of the proposed optimal RRM scheme over the sub-optimal RRM scheme is achieved at the cost of a very high computational complexity and the theoretical upper bound of such complexity is difficult to be derived [118], [119]. In our simulations, the optimal RRM scheme has to solve more than 1000 convex optimisation problems defined in (4.32), while the sub-optimal RRM scheme can solve the problem in (4.33) within 20 loops.

4.6 Conclusion

In this paper we have proposed a novel peer-to-peer system based on D2D communications, called Iunius. The proposed P2P protocol combines the conventional application-layer P2P protocol and the routing and scheduling schemes in lower layers. An interference cancellation technique for the CC UL, a GPSR based routing algorithm for multi-hop D2D communications, and a semi-distributed RRM scheme for both CC UL and D2D communications have been proposed for D2D communications to support the proposed P2P protocol.

Simulation results have shown that the Iunius system significantly improves the network performance in terms of throughput, BS traffic offload and energy saving. The P2P protocol and the GPSR algorithm can efficiently find a route from the D2D source to the destination while keeping the outage probability low. With the proposed interference cancellation technique, the Iunius system also guarantees the QoS of CC UL UEs.

To further improve the performance of the Iunius system, more cooperation between D2D links and other QoS requirements (such as error rate) for CC UEs could be considered. Mode selection between the proposed D2D-based P2P communications and the conventional directly downloading for the BS is another important research topic. Advanced network coding and cooperative communication techniques, can be applied to further enhance the system throughput and reduce the transmission delay. A more sophisticated local caching mechanism in conjunction with multi-hop routing for the Iunius system could also be an interesting topic of future work.

Chapter 5

Incorporate D2D Communications with LTE-unlicensed

5.1 Introduction

In Chapter 2 and Chapter 3, we see optimal RRM can improve the performance of D2D communications, and in Chapter 4 we see a joint application protocol and physical transmission can further exploit the capability of D2D. We note that, all of these works are based on the current mechanism of D2D communications. In this chapter, we want to develop new features for D2D communications. That is, we develop mechanism combining D2D with LTE-unlicensed, and thus allowing D2D to operate in the unlicensed bands with protective fairness measures for Wi-Fi transmissions.

LTE-Unlicensed (LTE-U), also known as License-Assisted Access, has attracted significant research and development attention. LTE-U extends LTE transmissions into the unlicensed ISM bands while adhering to unlicensed spectrum requirements [120]. By utilizing the considerable amount of unlicensed spectrum available around the globe, low power transmissions can avoid cross-tier interference. LTE-U has been included in 3GPP Release 13 standardization along with carrier aggregation [121].

In this chapter, we demonstrate how the combination of state-of-the-art base station (BS) assisted D2D [32] and LTE-U can significantly improve the Quality of Service (QoS) of both conventional cellular (CC) and D2D UEs. We show in Section II that without the flexibility of extending to and dynamically selecting the unlicensed ISM bands, CC QoS targets will constrain D2D operations to specific regions of a cell's coverage area. In Sections III and IV, we discuss the routing path selection and radio resource management (RRM) schemes to enable the combination of multi-hop D2D and LTE-U, respectively. The simulation results

in Section V show that by allowing D2D to operate in the unlicensed bands with protective measures for Wi-Fi and LTE-U CC transmissions, D2D is able to operate across the LTE network and in doing so, efficiently scale the overall network capacity whilst minimizing cross-tier and cross-technology interference. We review both centralized and distributed algorithms that enable multihop D2D path selection and RRM. We also show that, compared to other direct communication technologies operating on unlicensed bands (e.g., Wi-Fi Direct, Bluetooth, etc.), LTE-U D2D communications exhibit advantages in terms of efficient peer discovery and link establishment [32], and flexible RRM.

5.2 D2D and LTE-U System Overview

In future HetNets, D2D communications are expected to coexist with Small-Cell (SC) networks. The SC network can comprise small BSs operating in licensed cellular spectrum, as well as access points (APs) operating in unlicensed bands. In addition, D2D is likely to feature as a temporary network tier that utilizes the spectrum in an ad-hoc fashion. In the coverage area of a macro-BS, a single D2D link will reuse the spectrum occupied by a CC link. Thus, two types of interference exist: (1) intra-cell cross-tier interference between the D2D link and the CC link, and (2) inter-cell interference between the D2D links in coverage areas of different BSs. More complex analysis may consider how multiple separate D2D links utilize the same band and cause intra-cell D2D interference.

5.2.1 D2D and CC Performance Trade-off

Due to the mobilities of devices and the complex interference effects, traditional static radio planning can prove to be difficult to apply, while statistical methods have recently been proven to yield useful insights [122]–[124]. In a recent study on multi-hop D2D [124], where BSs, CC UEs, and D2D UEs all conform to spatial Poisson Point Processes (PPPs) of different densities, it was found that statistically D2D sharing the uplink (UL) band performs much better than D2D sharing the downlink (DL) band in terms of outage probability. However, D2D sharing the UL band leads to higher interference to CC transmissions. Therefore, there is a trade-off between D2D and CC communication performance while considering whether to use the UL or DL band for D2D communications. Letting D2D transmissions utilise the DL band will favor CC reliability over D2D reliability, whereas letting D2D transmissions utilise the UL band will favor D2D reliability over CC reliability.

The performance trade-off between D2D and CC communication performances also has implications on the geometric zones where D2D communications should use the UL or

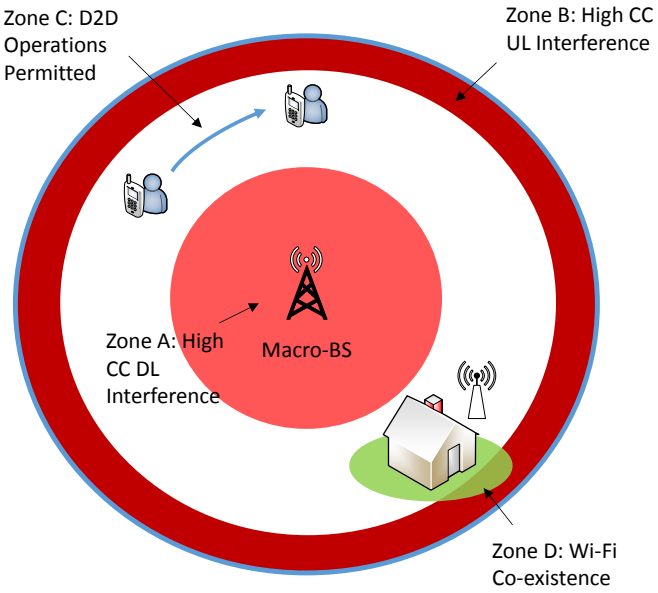

Fig. 5.1 D2D operation are restricted to certain parts of a macro-BS's coverage area due to cross-tier interference with CC transmissions.

DL band. As shown in Fig. 5.1, the centre of the BS's coverage area (*Zone A*) is generally off-limits to D2D transmissions using the cellular DL band due to the high DL interference from the nearby macro-BS. The macro-BS's cell edge (*Zone B*) is generally off-limits to D2D transmissions using the cellular UL band due to the high UL interference from cell-edge CC UEs transmitting at high power levels. Hence, if only the cellular DL or UL bands can be used, reliable D2D communications would be kept away from the cell-centre or the cell-edge respectively, and only operate in *Zone C*.

5.2.2 D2D Integration with LTE-U

The mutual interference and aforementioned limitations of D2D communications utilising licensed band would be more significant in higher cellular traffic areas (e.g., city centre during office hours), where would also be the hotspots of D2D communications. Targeting these problems, we propose an architecture to allow D2D communications to use LTE-U. As we will show later, LTE-U opens up the possibility for D2D to operate anywhere in the macro-BS's coverage area except for the regions where other unlicensed-band radio-access technologies (RATs) are in use (e.g., the Wi-Fi hotspot in *Zone D*). In order to communicate in the unlicensed band, there are two major coexistence requirements: (1) low transmit power levels (typically 200mW to 1W), and (2) interference avoidance through Clear Channel Assessment (CCA) or Listen Before Talk (LBT).

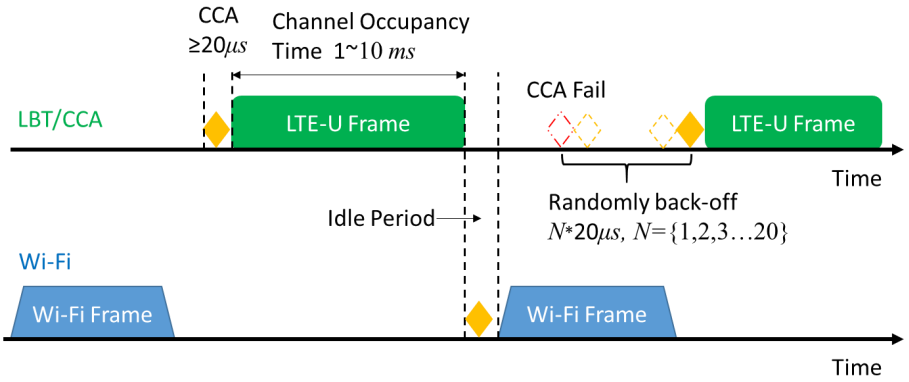

Fig. 5.2 Listen-Before-Talk (LBT) for LTE-U.

An LTE-U D2D UE needs to periodically perform spectrum sensing to check for the presence of other occupants in the channel before transmission (LBT). This is achieved by first detecting the energy level of the channel for a designed duration (normally 20μs). If the energy level in the channel is below the CCA energy threshold, the UE transmits for a Channel Occupancy Time (COT) (normally 1-10ms). If the energy level is over the CCA energy threshold, the D2D UE waits for a random period, before it performs another CCA. After the COT has elapsed, if the UE wants to continue transmitting, it has to repeat the CCA process[1]. This entire process is illustrated in Fig. 5.2. In fact, LTE-U enabled multi-hop D2D will no longer be restricted to the previously mentioned operation zones as long as the unlicensed spectrum regulations are fulfilled [120]. This would significantly expand the D2D operational areas.

5.3 Multi-hop Routing Algorithms

Conventional wireless multi-hop communications have been studied for ad-hoc networks, where distributed or centralized tabular-based routing methods are used to extend communication range via relay nodes. D2D multi-hop routing is different from conventional multi-hop routing in that: 1) D2D communications are assisted and/or controlled by the LTE network; 2) the mutual interference between D2D and CC transmissions needs to be considered in D2D multi-hop routing. Hence, multi-hop routing algorithms need to be revisited for D2D communications. In this section, we first review multi-hop routing schemes for D2D communications and then propose a routing algorithm for LTE-U enabled multi-hop D2D.

[1]3GPP Release 13 Technical Report R1-152182 (2015): Response LS on Clarification of LBT Categories.

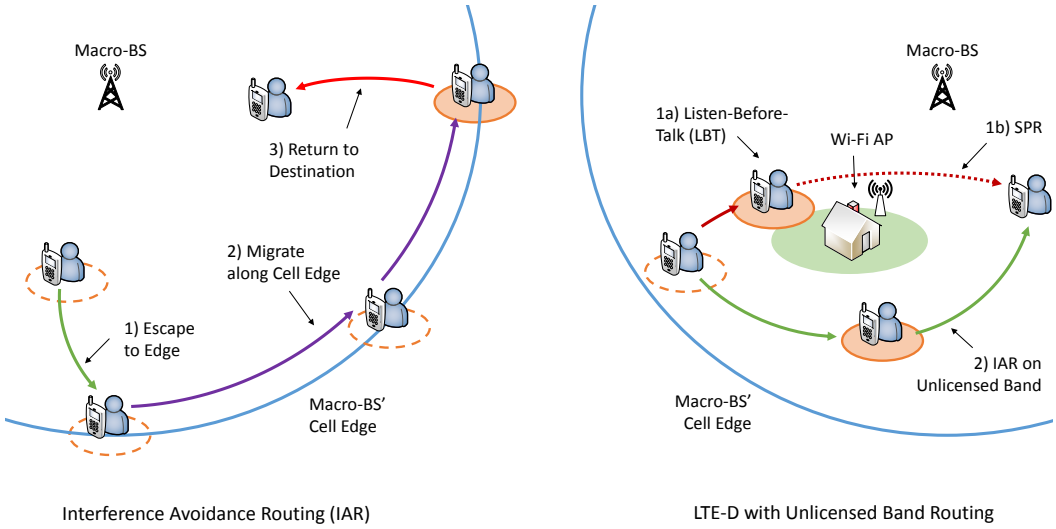

Fig. 5.3 Interference-Avoidance-Routing and Unlicensed LBT Routing for Multi-hop D2D.

5.3.1 Routing Algorithms for D2D

In order to limit the mutual interference between D2D and CC transmissions, a popular approach is to introduce and optimise an exclusion zone, wherein only D2D transmissions are allowed on a given frequency band. The exclusion zone is usually defined as a geometric area centred at the receiving D2D UE. The size of an exclusion zone is defined such that up to a certain number of CC and D2D UEs can transmit simultaneously in the macro-BS coverage area without causing failed reception at the central D2D UE [125]. By controlling the size and location of the exclusion zone through D2D transmit power control, exclusion-zone based D2D relay selection can ensure low outage probabilities for both D2D and CC UEs. In [79], the exclusion zone is defined in terms of the interference-to-signal ratio at the D2D receiver in a system consisting of one BS, one D2D pair, and multiple CC UEs. More specifically, the exclusion zone is defined as a δ_D-interference limited area (ILA), in which CC UEs could generate an accumulated interference level no larger than $\delta_D P_{D,R}$ to the D2D receiver, where δ_D is the the interference-to-signal ratio threshold and $P_{D,R}$ is the received power at the D2D receiver.

In [126], the authors proposed a framework to build up a global network graph representation for the transmission states of all UEs and a graph-based optimal routing algorithm for two types of multi-hop D2D communications: connected transmission, and opportunistic transmission. However, due to the fast changing nature of wireless channels, it is infeasible to build up and maintain a large-scale network graph for all UEs.

Shortest-Path-Routing (SPR)

The commonly used greedy path selection algorithm is called shortest-path-routing (SPR) [124], [127]. SPR seeks to minimize the total multi-hop distance or the number of hops, in order to improve the multi-hop D2D transmission reliability. In SPR, each D2D UE knows its own location and that of the final destination UE [124], which is similar to the greedy algorithm in [128]. This is achieved by the BS relaying the destination location information to the active relay UE in order to update the SPR path selection in the presence of mobility. Each UE that holds the message will first identify the UEs that it can reliably transmit to, and then transmit to the one that is closest to the destination UE. The SPR algorithm for a generic D2D source and destination pair is as follows:

1. The transmitting UE identifies the UEs that can decode its transmissions reliably within a coverage radius.

2. The transmitting UE identifies the UEs (from Step 1) that are closer to the destination than itself.

3. The transmitting UE transmits to the UE that is of the longest distance from itself among the UEs identified in Step 2), and this receiving UE becomes the transmitting UE in the next step.

4. Repeat Steps 1)-3) until the destination UE is reached.

Interference Avoidance Routing (IAR)

Whilst algorithms such as the SPR can yield a reasonable performance and minimize the delay, it may not always yield the best reliability performance. This is because when cross-tier interference between CC and D2D transmissions is considered, selecting the shortest path is not always the optimal strategy. The cross-tier interference is the lowest when the D2D transmissions occur at the macro-BS's coverage boundary (cell-edge). As previously shown in Fig. 5.1, a cell-edge routing path would reduce the D2D interference to CC transmissions in the UL band; and would reduce the CC interference to D2D transmissions using the DL band. The interference avoidance routing (IAR) algorithm tends to migrate along the cell-edge in order to trade-off a longer route for reduced interference. Such an IAR algorithm has 3 stages (as illustrated in Figure 5.3):

- *Stage 1 (Escape to Cell Edge):* D2D transmission from the source UE to the closest cell-edge UE.

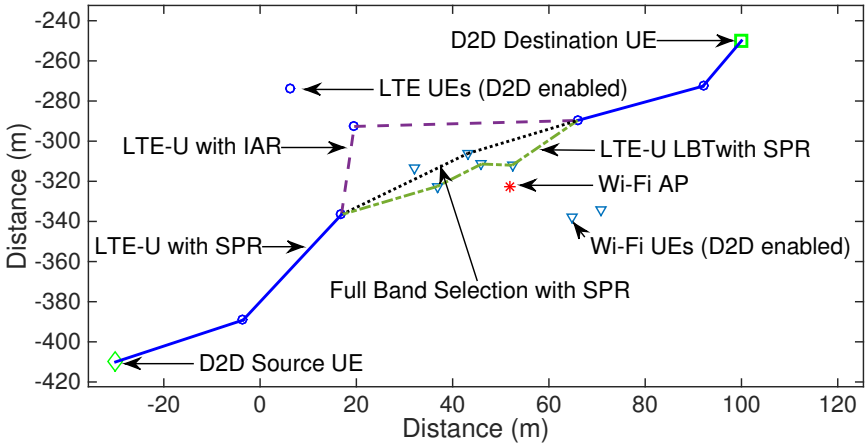

Fig. 5.4 Routing Paths for D2D (Unlicensed Band Enabled): 1) LTE-U with SPR using LBT contention, 2) LTE-U with IAR to avoid contention, and 3) Full Band Selection with SPR. A single path is shown for illustrative purposes.

- *Stage 2 (Migrate along Cell Edge):* D2D transmission from the cell-edge UE to a cell-edge UE closer to the destination.

- *Stage 3 (Return to Destination):* D2D transmission from the cell-edge UE closest to the destination to the destination UE.

In [127], a case study based on a single macro-BS and multiple D2D UEs in Ottawa city showed that the cross-tier interference can be effectively mitigated. In essence, the IAR algorithm will result in a trade-off between improving the performance of each hop and increasing the total number of hops. It was found that the IAR route is approximately 2.5-fold longer than the SPR route on average [127], but the advantage is that the mutual interference between D2D and CC UEs can be significantly reduced and the reliability performance of IAR is superior to that of SPR unless the distance between the source and destination D2D UEs is small. The results in [127] show that there is an intuitive trade-off in the outage probability performance between CC and D2D UEs. For a stringent CC outage constraint, D2D transmission is not permitted. As the CC outage constraint gets relaxed, the optimal D2D routing algorithm changes from IAR to SPR. Aside from the longer route and higher complexity of IAR as compared to SPR, IAR is sensitive to the selection between the UL and DL bands for D2D transmissions and the mutual interference between multiple D2D transmissions in proximity.

5.3.2 Routing Scheme for D2D with LTE-U

Base on the above discussion, we propose a routing algorithm for LTE-U enabled multi-hop D2D communications. D2D routing decisions are based on SPR wherever LTE-U transmission opportunities are available. The blue solid line in Fig. 5.4 shows an LTE-enabled multi-hop D2D route based on SPR. If the D2D UE does not get a chance to transmit in the unlicensed bands or the LTE-U transmission cannot fulfill the QoS requirement, then the D2D UE would choose one of the following strategies:

- *Wait for a CCA period:* the D2D UE holds the data transmission and performs LBT until there is an unlicensed channel available for transmission.

- *Perform a localized IAR:* the IAR is used for D2D transmissions to hop around the local Wi-Fi APs, thus avoiding contention with Wi-Fi transmissions. Unlike the macro-BSs, there is no clearly defined Wi-Fi cell-edge, and the localized IAR will rely on exchanging channel energy information between UEs and finding a UE that measures channel energy below the CCA energy threshold.

- *Switch to the licensed cellular band:* the D2D transmission uses the resource block (RB) allocation scheme in [60], where the UL band is viable when the D2D path is far from the nearest BS and the DL band is viable when the D2D path is far from the cell-edge.

The SPR and IAR algorithms (LTE-U enabled) are both distributed algorithms, where the routing decision lies entirely with the relay UE node that currently holds the data packets. Based on 3GPP recommendations [2]: the nearest BS acts as a centralized coordination unit that sends regular control commands to either continue D2D communications, or should it fail, establish CC communications. The BS also forwards location updates of the destination UE, so that each relay UE can make accurate route selection choices. In terms of UE velocity, our studies found that as long as it is below high speed train velocities, the speed of the multi-hop routing process is sufficiently fast to be responsive to UE movements.

[2] Study on architecture enhancements to support Proximity-based Services (ProSe), 3GPP TR 23.703 v12.0.0 (Release 12).

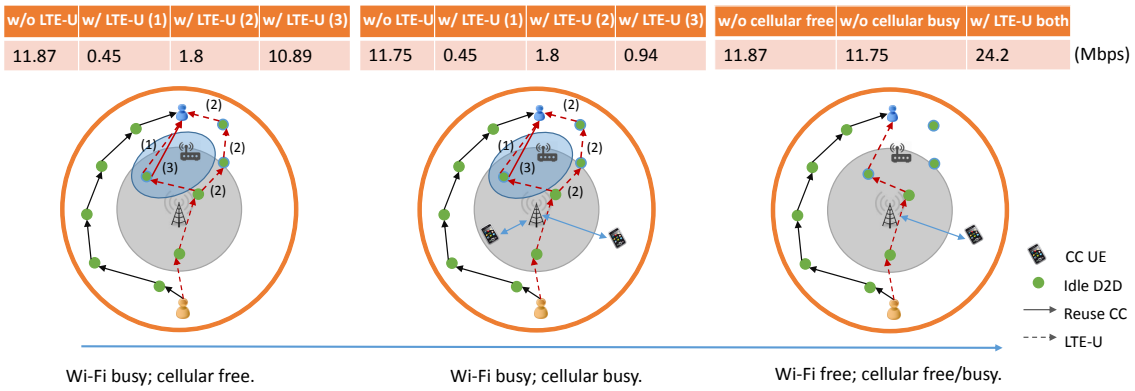

Fig. 5.5 Throughput performance in different scenarios. The black solid lines denote the D2D routes without LTE-U, the red lines represent the D2D routes with LTE-U enabled (a solid line denotes a D2D link utilising the cellular band, and a dashed line represents a D2D link using unlicensed band(s)), and the blue lines show the CC communications.

5.4 Radio Resource Management

5.4.1 Radio Resource Management for D2D

There exists a trade-off between the efficiency of RRM and the associated overhead (including control and computational overhead) to the cellular network [60]. In a network consisting of multiple concurrent multi-hop D2D links, such overhead might increase out of control and eventually overwhelm the whole network. In [123], the authors presented a theoretical upper bound of the total throughput of D2D communications without optimising RRM. They considered a single cell with the BS at the center of its disk coverage area, where one CC UE and multiple D2D UEs coexist. The CC UE and each D2D transmitter utilise a constant transmit power P_C and P_D, respectively. There is a data rate requirement R_D for each D2D pair. With these settings, the authors concluded that:

- D2D transmission is prevented when its distance to the BS is smaller than a guard distance G_B to protect the CC communications. G_B increases with P_D and decreases with P_C.

- There exists a guard distance G_D between D2D pairs to guarantee the data rate requirement R_D of D2D communications. G_D increases with R_D and slightly decreases with P_D.

- There exists a range of P_D that maximise the total throughput of all D2D pairs in the system. The total D2D throughput drops quickly when P_D goes beyond the optimal range.

Optimised RRM mechanisms have been proposed for multi-hop D2D communications. In [37], the distributed RRM mechanism for multi-hop D2D communications features reduced overhead. In [129], the authors proposed a network coding and caching mechanism for improving the throughput and decreasing transmission delays of multi-hop D2D. The two-stage semi-distributed RRM mechanism in [60] limits the overhead through:

1. RB allocation (long-term scheduling): the BS conducts a centralised RB allocation for both CC and D2D UEs periodically (e.g., several seconds).

2. Power control (short-term scheduling): after the RB allocation, each D2D UE decides the transmit power based on its own channel measurements.

Although this semi-distributed RRM mechanism was proposed for single-hop D2D communications, we can modify it to be used for multi-hop D2D communications: 1) in the first stage, RBs are allocated to all hops; and 2) in the second stage, each hop performs power control based on local channel measurement. In the following, we will illustrate how this algorithm can be adopted for LTE-U enabled D2D communications.

5.4.2 Joint Routing and Radio Resource Management for D2D with LTE-U

Following the analysis in [123], we note that the vacuum area for D2D communications (i.e., the disk area centered at the BS with radius G_B) can be filled up if D2D communications are allowed to utilise unlicensed bands (see the strategies in Section 5.3.2). Furthermore, the average G_D can be decreased by combining D2D and LTE-U, because the guard distance required between a D2D pair utilising licensed band and one using unlicensed band is small. Based on the RRM mechanism [60] and incorporating the routing algorithm proposed in Section 5.3.2, we propose the following joint routing and RRM mechanism for LTE-U enabled multi-hop D2D:
(1) **Stage one: location updating and channel allocation.** Each D2D transmitter would first try to use unlicensed bands and may fall back to the licensed band according to the strategies in Section 5.3.2. In that case, the BS would allocate cellular radio resource (e.g., resource blocks in LTE/LTE-A) to D2D communications [60] and update the location information of UEs periodically (see Section 5.3.2). This is a long-term scheduling considering long-term factors, such as traffic load and UE status, and decisions are made in a centralised manner.

(2) **Stage two: power control and routing.** Each UE decides its transmit power according to its channel state. If the D2D transmission utilises unlicensed bands, it may choose any transmit power $P_D \leq P_{\max}$, e.g., based on a water-filling algorithm for maximizing throughput [60]. D2D communications utilising the licensed band may follow the power control schemes discussed in [32], [37], [129]. The UE also choose its receiver according to the strategies proposed in Section 5.3.2. These are short-term scheduling decisions considering the time-varying wireless channel and are thus performed in a distributed manner.

5.5 Performance Analysis

In Fig. 5.5, we evaluate the throughput performance of LTE-U enabled D2D communications in different traffic load scenarios through simulations in a network consisting of one cellular BS and one Wi-Fi AP. For LTE-U enabled D2D communications, the transmission period t is set as 1ms. In the scenarios with 'Wi-Fi busy', we compare the three routing strategies for LTE-U enabled D2D: (1) wait for a CCA period, (2) LTE-U IAR, and (3) switch to the cellular band, as proposed in Section 5.3.2. D2D communications in the cellular band use the IAR algorithm and the RRM mechanism proposed in [37], which can be summarised as: a) the UL CC UE transmits at a power level that keeps its SINR at $a\Gamma_C$ when there is no D2D transmission, where Γ_C is the UL SINR requirement for CC UEs and $a > 1$ is a control parameter; and b) the D2D UE transmits at a power level that keeps the SINR of the interfered CC UE above Γ_C.

The throughput of D2D with or without LTE-U enabled is shown in the table above each scenario in Fig. 5.5. It can be seen that when Wi-Fi is in light usage, LTE-U can manifestly improve the throughput of D2D communications (by more than 100% to 24.2Mbps). However, when the traffic load of Wi-Fi is heavy, D2D communications should utilise the licensed cellular band with IAR. This is mainly because of the low probability of D2D accessing the unlicensed bands and the mutual interference between Wi-Fi and D2D transmissions in unlicensed bands due to spectrum sensing errors in the LBT process. If a multi-hop D2D route needs to go through a busy Wi-Fi hotspot, it is better to switch to the cellular band (i.e., strategy (3)).

5.6 Conclusions and Open Challenges

In this article, we have examined how two emerging cellular technologies can merge together and create synergies. Whilst D2D communications underlaying cellular networks can potentially improve the network capacity of a conventional LTE network, it lacks the full spatial flexibility due to cross-tier interference. Combining D2D with LTE-U, we have shown that D2D can operate across the full coverage area of a network and achieve improved network-wide capacity. We note that there are several challenges in combining D2D communications with LTE-U. In terms of performance versus fairness, it is obvious that a longer transmission period t for D2D communications utilising unlicensed bands can improve the throughput performance of D2D communications. As we can see from the results, in the *Wi-Fi busy* scenario, a longer t is critical to the throughput performance of LTE-U enabled D2D communications. However, a longer t might affect the performance of nearby Wi-Fi APs and users. Thus an efficient algorithm should be proposed for choosing an appropriate t.

A number of cross-RAT joint optimisation and coordination challenges remain when combining D2D with LTE-U. Routing and RRM are still the paramount challenges for the combination of D2D communications with LTE-U. A more capable algorithm, such as ant colony optimisation and graph theory [126], may be used to develop joint routing and RRM mechanism for LTE-U enabled D2D communications. In *Wi-Fi free* scenario, LTE-U enabled D2D communications can achieve a very high throughput due to the plenty of spectrum available and the possible use of maximum transmit power, where it would be valuable to discuss the trade-off between throughput and energy efficiency.

Chapter 6

Conclusions and Future Works

How can we improve the performance of D2D communications and make it more practical to the cellular users? This thesis presents three possible ways: 1) an optimised RRM for D2D communications; 2) joint optimisation of application protocol and physical transmission for D2D communications; and 3) combining D2D communications with other advanced wireless technologies.

Our works demonstrate that an optimised RRM for D2D communications can significantly improve the performance of D2D communications. However, such optimisation solutions are difficult to achieve in many cases. The joint power control and subchannel allocation RRM problem is a MINLP problem that is lack of low computational complexity mathematical solution (see Section 2.2, Section 2.3 and Section 4.4.4). However, in Chapter 3 we show that, if we consider location information in our RRM optimisation problem, it can be transformed into a convex problem and solved by Lagrangian multiplier algorithm.

We also successfully combine D2D communications with other technologies to build new applications and extend the capability of D2D communications. Iunius system proposed in Chapter 4 enables D2D communications for local file sharing. The results demonstrate that Iunius can manifestly improve the QoE of cellular users and offload local traffic from central BS. In Chapter 5, we show how to apply LTE-unlicensed into D2D communications. This can extend the transmission area and improve the throughput of D2D communications.

In this chapter, we first summarise the highlights of this thesis and the experiences we learn from the works we have done. Then we will list several potential research topics of the D2D communications which we think that are related to this thesis and are critical to the development of D2D.

6.1 Highlights in the Thesis

In this section, we summarise the highlights in this thesis and the experiences we have learned.

Branch-and-bound/branch-and-cut is efficient to solve MINLP problem in D2D communications. In our works, we always utilise branch-and-bound to solve the MINLP problem of joint power control and subchannel allocation problem for D2D communications. Even though branch-and-bound/branch-and-cut has not been theoretically proved the complexity boundary and in the worst case it is actually an exhausted search, it is quite efficient in our practices. We note that, the general branch-and-bound algorithm should be modified for specific RRM problem to improve its searching efficiency. In addition, as we can see in Chapter 3, taking auxiliary information (e.g., location information of D2D communications in Chapter 3) into consideration may help us to transform the MINLP RRM problem into a problem that has a low computational complexity solution.

Caching is important to D2D communications. In both Section 2.3 and Section 4.3, we see the importance of caching for D2D communications. First, for multi-hop D2D communications, caching can improve the performance of the system. In Section 2.3, we show that with caching capability at D2D UEs, the throughput of multi-hop D2D communications can improve $10\% - 20\%$ and the time for transmitting 1000Mbits data can be reduced 25% for NC-D2D. Then in Section 4.3, we see that the caching at D2D UEs is the foundation of the P2P application and thus the foundation of Iunius. We note that, caching capability is the foundation of building any kinds of local application service based on D2D communications.

Multi-hop D2D can be realised with proper RRM and advanced wireless technologies. Multi-hop D2D communications can significantly enhance the transmission range of D2D communications. However, there is doubt that whether multi-hop D2D is practical and efficient. In this thesis, we show that multi-hop D2D communications can be efficiently deployed with proper designed RRM and advanced wireless technologies. We demonstrate in Section 2.3 and Chapter 4 that, with an optimised RRM for multi-hop D2D communications, multi-hop D2D communications can enhance the QoS for D2D UEs with high energy efficiency. Furthermore, we show in Section 2.3 that NC can improve the throughput and reduce the delay of multi-hop D2D communications. And in Chapter 5, we demonstrate how LTE-unlicensed can significantly extend the transmission area of D2D by allowing D2D to take place in the centre area of the cellular, which is proved to be the dead zone for conventional D2D (see Chapter 3 and [79], [123]).

Joint application protocol and physical transmission optimisation is important for the development of D2D. It is obvious that D2D cannot benefit the cellular users without an application running on top of it. The application protocol and the D2D communications are

studied separately in the existing works. Our works suggest that, it is worth to doing a joint optimisation of application protocol and physical transmission for D2D communications. We develop the Iunius system, in which we do a cross-layer optimisation of P2P protocol and D2D communications (see Chapter 4). We develop the P2P protocol which supports interference cancellation in D2D communications. Then we develop a proper routing scheme and an optimised RRM scheme for multi-hop D2D communications which can better support the P2P file transmission. We see that, thanks to the joint optimisation of P2P protocol and D2D communications, the proposed Iunius system achieves a 100% improvement in system throughput and more than 80% improvement in energy efficiency comparing to the conventional file sharing methods.

6.2 Future Works

In this thesis, we study the optimised RRM for D2D communications in different scenarios, propose Iunius which is a cross-layer P2P system with D2D communications and applying LTE-U to D2D communications. We summarise some of the potential future topics that are based on this thesis as follows.

As we can see from Chapter 2 and Chapter 3, there remains many limitations in our current works of RRM for D2D communications. As it is one of the paramount challenges in D2D communications, it is worth further researches in following areas.

- **RRM for D2D underlaying heterogeneous network.** In our current works, we only consider D2D communications coexisting with macro-cell communications. The circumstances would be much more complex if D2D communications taking place in heterogeneous networks, especially coexisting with hyper-dense small cell communications. New RRM schemes are definitely necessary for such scenarios.

- **RRM for D2D in 5G network.** As we mentioned in Chapter 1, several advanced technologies have been proposed for next generation cellular communications. We should investigate how massive-MIMO, mmWave and other new technologies may affect D2D communications and thus propose related optimised RRM schemes.

- **RRM for moving D2D UEs.** We assume D2D UEs are static in our current works and it is a common assumption in existing works. We suggest to remove this assumption and propose new RRM schemes for the communications between moving D2D UEs.

We propose Iunius, a cross-layer P2P system with D2D communications in Chapter 4. As we discussed in Chapter 4, our works are still on early stage. Main areas of extensions are:

- **A distributed caching mechanism for Iunius.** In Chapter 4, we discuss an intuitive distributed caching mechanism for Iunius system. We note that, a more sophisticated design of the caching mechanism for Iunius system is critical to its performance. In addition, more advanced mathematical models, such as queue theory, are required to analyse the caching performance of the system.

- **Mechanisms for sequenced data transmission.** In our current works, we only consider non-sequenced data transmissions (such as file sharing) in Iunius system. In order to support more applications and services, we should design a proper P2P protocol and D2D transmission scheme for sequenced data transmissions. We should propose a RRM scheme which can guarantee that the data chunk with higher priority (i.e., data chuck is next to be needed) can be transmitted in advance. In addition, the P2P protocol should support the sequenced data transmission.

- **Interference cancellation/mitigation in Iunius.** We consider an ideal interference cancellation scheme with strong assumptions (e.g., the CSI of D2D communications is known by the BS) in our current works. To remove those assumptions, we should consider more practical interference cancellation schemes in the future. Some related works we believe that can be incorporated into Iunius system are listed as: [130]–[134].

- **Experimental Iunius system.** Finally, we hope to realise Iunius on top of the experimental D2D network. We believe Iunius system can actually improve the QoE of cellular users, introduce new services and opportunities for operators, and thus boost the whole industry.

Last but not least, we believe that by combining D2D communication with other latest technologies, it can have great potential in some emerging research areas, such as smart city and internet-of-thing (IoT).

- **Big data in D2D.** Social-aware D2D is a hot topic. We can combine social network data analysis with D2D communications. This can improve the system performance of D2D communications. In addition, such researches may also reveal interesting findings in sociology [135].

- **D2D with SDN.** Combining D2D with SDN would allow D2D communications having the capability to support new applications (e.g., fog computing) and business models [12]. The key challenge would be how to apply SDN to a network which topology changes quickly.

- **Business model in D2D.** Business model is the key point for a technology to gain business success. In [33], authors gave a simple discussion about the fee charges for D2D users. We believe a more detailed discussion of the business model for D2D communications based on game theory or other economic theories would be an interesting topic.

We hope that continued researches in D2D communications can improve the usability and performance of it, inspire other researches in wireless communications, and lead to novel products that can eventually benefit the economic development and our society.

References

[1] Y. Wu, S. Wang, W. Liu, W. Guo, and X. Chu, "Iunius: A cross-layer peer-to-peer system with device-to-device communications," *IEEE Transactions on Wireless Communications*, vol. 15, no. 10, pp. 7005–7017, Oct. 2016.

[2] Y. Wu, W. Guo, H. Yuan, L. Li, S. Wang, X. Chu, and J. Zhang, "Device-to-device meets LTE-unlicensed," *IEEE Communications Magazine*, vol. 54, no. 5, pp. 154–159, May 2016.

[3] Y. Wu, W. Liu, S. Wang, W. Guo, and X. Chu, "Network coding in device-to-device (D2D) communications underlaying cellular networks," *2015 IEEE International Conf. Commun. (ICC)*, pp. 2072–2077, Jun. 2015.

[4] Y. Wu, S. Wang, W. Guo, X. Chu, and J. Zhang, "Optimal resource management for device-to-device communications underlaying SC-FDMA systems," *2014 9th International Symposium on Communication Systems, Networks Digital Signal Processing (CSNDSP)*, pp. 569–574, Jul. 2014.

[5] S. Qiu, W. Guo, B. Li, Y. Wu, X. Chu, S. Wang, and Y. Y. Dong, "Long range and long duration underwater localization using molecular messaging," *IEEE Transactions on Molecular, Biological and Multi-Scale Communications*, vol. 1, no. 4, pp. 363–370, Dec. 2015.

[6] B. Yang, Y. Wu, X. Chu, and G. Song, "Seamless handover in software-defined satellite networking," *IEEE Communications Letters*, vol. 20, no. 9, pp. 1768–1771, Sep. 2016.

[7] S. Wang, W. Guo, Z. Zhou, Y. Wu, and X. Chu, "Outage probability for multi-hop d2d communications with shortest path routing," *IEEE Communications Letters*, vol. 19, no. 11, pp. 1997–2000, Nov. 2015.

[8] W. Guo, S. Wang, Y. Wu, J. Rigelsford, X. Chu, and T. O'Farrell, "Spectral- and energy-efficient antenna tilting in a hetnet using reinforcement learning," *Wireless Communications and Networking Conference (WCNC), 2013 IEEE*, pp. 767–772, Apr. 2013.

[9] B. Yang, G. Song, Y. Chen, Y. Zheng, and Y. Wu, "Qos-aware indiscriminate volume storage cloud," *Concurrency and Computation: Practice and Experience*, 2016.

[10] B. Yang, G. Song, Y. Zheng, and Y. Wu, "Qosc: A qos-aware storage cloud based on hdfs," *2015 International Symposium on Security and Privacy in Social Networks and Big Data (SocialSec)*, pp. 32–38, Nov. 2015.

[11] Y. Wu, W. Guo, H. Hu, X. Chu, and J. Zhang, "Location-based radio resource management for device-to-device communications," *IEEE Trans. Commun.*, Jul. 2016.

[12] Y. Wu, B. Yang, W. Guo, X. Chu, S. Wang, and H. Zhang, "A software-defined network protocol for device-to-device communications: Challenges, solutions and business model," *IEEE Network*, Jul. 2015.

[13] R. Tao, Y. Wu, B. Yang, X. Chu, and J. Zhang, "Small cell throughput optimization with in-band wireless backhaul," *IET Electronic Letters*, Jul. 2016.

[14] T. S. Rappaport, S. Sun, R. Mayzus, H. Zhao, Y. Azar, K. Wang, G. N. Wong, J. K. Schulz, M. Samimi, and F. Gutierrez, "Millimeter wave mobile communications for 5G cellular: It will work!" *IEEE Access*, vol. 1, pp. 335–349, 2013.

[15] I. Hwang, B. Song, and S. S. Soliman, "A holistic view on hyper-dense heterogeneous and small cell networks," *IEEE Communications Magazine*, vol. 51, no. 6, pp. 20–27, Jun. 2013.

[16] E. G. Larsson, O. Edfors, F. Tufvesson, and T. L. Marzetta, "Massive MIMO for next generation wireless systems," *IEEE Communications Magazine*, vol. 52, no. 2, pp. 186–195, Feb. 2014.

[17] F. M. Abinader, E. P. L. Almeida, F. S. Chaves, A. M. Cavalcante, R. D. Vieira, R. C. D. Paiva, A. M. Sobrinho, S. Choudhury, E. Tuomaala, K. Doppler, and V. A. Sousa, "Enabling the coexistence of LTE and Wi-Fi in unlicensed bands," *IEEE Communications Magazine*, vol. 52, no. 11, pp. 54–61, Nov. 2014.

[18] J. S. Lee, Y. W. Su, and C. C. Shen, "A comparative study of wireless protocols: Bluetooth, UWB, ZigBee, and Wi-Fi," in *33rd Annual Conference of the IEEE Industrial Electronics Society (IECON 2007)*, Nov. 2007, pp. 46–51.

[19] D. Camps-Mur, A. Garcia-Saavedra, and P. Serrano, "Device-to-device communications with Wi-Fi Direct: Overview and experimentation," *IEEE Wireless Communications*, vol. 20, no. 3, pp. 96–104, Jun. 2013.

[20] J. Khun-Jush, P. Schramm, G. Malmgren, and J. Torsner, "Hiperlan2: Broadband wireless communications at 5 GHz," *IEEE Communications Magazine*, vol. 40, no. 6, pp. 130–136, Jun. 2002.

[21] L. Pelusi, A. Passarella, and M. Conti, "Opportunistic networking: Data forwarding in disconnected mobile ad hoc networks," *IEEE Communications Magazine*, vol. 44, no. 11, pp. 134–141, Nov. 2006.

[22] S. Andreev, O. Galinina, A. Pyattaev, K. Johnsson, and Y. Koucheryavy, "Analyzing assisted offloading of cellular user sessions onto D2D links in unlicensed bands," *IEEE Journal on Selected Areas in Communications*, vol. 33, no. 1, pp. 67–80, Jan. 2015.

[23] K. Doppler, M. Rinne, C. Wijting, C. Ribeiro, and K. Hugl, "Device-to-device communication as an underlay to LTE-advanced networks," *IEEE Communications Magazine*, vol. 47, no. 12, pp. 42–49, 2009.

[24] M. Corson, R. Laroia, J. Li, V. Park, T. Richardson, and G. Tsirtsis, "Toward proximity-aware internetworking," *IEEE Wireless Communications*, vol. 17, no. 6, pp. 26–33, Dec. 2010.

[25] X. Wu, S. Tavildar, S. Shakkottai, T. Richardson, J. Li, R. Laroia, and A. Jovicic, "Flashlinq: A synchronous distributed scheduler for peer-to-peer ad hoc networks," *IEEE/ACM Trans. Netw.*, vol. 21, no. 4, pp. 1215–1228, Aug. 2013.

[26] S. Balraj, "LTE Direct overview," Qualcomm Research, Tech. Rep., 2012.

[27] 3GPP TSG, "Study on architecture enhancements to support proximity-based services (prose)," 3GPP Technical Report, 3GPP TR 23.703 v12.0.0, Feb. 2014.

[28] A. Asadi, Q. Wang, and V. Mancuso, "A survey on device-to-device communication in cellular networks," *IEEE Communications Surveys Tutorials*, vol. 16, no. 4, pp. 1801–1819, Fourthquarter 2014.

[29] G. Fodor, E. Dahlman, G. Mildh, S. Parkvall, N. Reider, G. Miklós, and Z. Turányi, "Design aspects of network assisted device-to-device communications," *IEEE Commun. Mag*, vol. 50, no. 3, pp. 170–177, 2012.

[30] L. Lei, Z. Zhong, C. Lin, and X. Shen, "Operator controlled device-to-device communications in LTE-advanced networks," *IEEE Wireless Commun. Mag.*, vol. 19, no. 3, pp. 96–104, Jun. 2012.

[31] L. Lei, Y. Kuang, X. Shen, C. Lin, and Z. Zhong, "Resource control in network assisted device-to-device communications: Solutions and challenges," *IEEE Communications Magazine*, vol. 52, no. 6, pp. 108–117, Jun. 2014.

[32] L. Wei, R. Hu, Y. Qian, and G. Wu, "Enable device-to-device communications underlaying cellular networks: Challenges and research aspects," *IEEE Commun. Mag.*, vol. 52, no. 6, pp. 90–96, Jun. 2014.

[33] M. N. Tehrani, M. Uysal, and H. Yanikomeroglu, "Device-to-device communication in 5G cellular networks: Challenges, solutions, and future directions," *IEEE Communications Magazine*, vol. 52, no. 5, pp. 86–92, May 2014.

[34] C.-H. Yu, K. Doppler, C. Ribeiro, and O. Tirkkonen, "Resource sharing optimization for device-to-device communication underlaying cellular networks," *IEEE Trans. Wireless Commun.*, vol. 10, no. 8, pp. 2752–2763, August, 2011.

[35] G. Yu, L. Xu, D. Feng, R. Yin, G. Y. Li, and Y. Jiang, "Joint mode selection and resource allocation for device-to-device communications," *IEEE Transactions on Communications*, vol. 62, no. 11, pp. 3814–3824, Nov. 2014.

[36] K. Zhu and E. Hossain, "Joint mode selection and spectrum partitioning for device-to-device communication: a dynamic stackelberg game," *IEEE Transactions on Wireless Communications*, vol. 14, no. 3, pp. 1406–1420, 2015.

[37] B. Kaufman, J. Lilleberg, and B. Aazhang, "Spectrum sharing scheme between cellular users and ad-hoc device-to-device users," *IEEE Trans. Wireless Commun.*, vol. 12, no. 3, pp. 1038–1049, Mar. 2013.

[38] K. W. Choi and Z. Han, "Device-to-device discovery for proximity-based service in LTE-advanced system," *IEEE Journal on Selected Areas in Communications*, vol. 33, no. 1, pp. 55–66, Jan. 2015.

[39] S. Vasudevan, K. Sivanesan, S. Kanugovi, and J. Zou, "Enabling data offload and proximity services using device to device communication over licensed cellular spectrum with infrastructure control," in *IEEE 78th Vehicular Technology Conference (VTC Fall)*, Sep. 2013, pp. 1–7.

[40] P. Phunchongharn, E. Hossain, and D. I. Kim, "Resource allocation for device-to-device communications underlaying LTE-advanced networks," *IEEE Wireless Communications*, vol. 20, no. 4, pp. 91–100, Aug. 2013.

[41] Y. Pei and Y. C. Liang, "Resource allocation for device-to-device communications overlaying two-way cellular networks," *IEEE Transactions on Wireless Communications*, vol. 12, no. 7, pp. 3611–3621, Jul. 2013.

[42] Y. Cao, T. Jiang, and C. Wang, "Cooperative device-to-device communications in cellular networks," *IEEE Wireless Communications*, vol. 22, no. 3, pp. 124–129, Jun. 2015.

[43] P. Pahlevani, M. Hundebøll, M. V. Pedersen, D. Lucani, H. Charaf, F. H. P. Fitzek, H. Bagheri, and M. Katz, "Novel concepts for device-to-device communication using network coding," *IEEE Communications Magazine*, vol. 52, no. 4, pp. 32–39, Apr. 2014.

[44] W. Xu, L. Liang, H. Zhang, S. Jin, J. C. F. Li, and M. Lei, "Performance enhanced transmission in device-to-device communications: Beamforming or interference cancellation?" In *IEEE Global Communications Conference (GLOBECOM)*, Dec. 2012, pp. 4296–4301.

[45] L. Yang, W. Zhang, and S. Jin, "Interference alignment in device-to-device LAN underlaying cellular networks," *IEEE Transactions on Wireless Communications*, vol. 14, no. 7, pp. 3715–3723, Jul. 2015.

[46] H. Min, W. Seo, J. Lee, S. Park, and D. Hong, "Reliability improvement using receive mode selection in the device-to-device uplink period underlaying cellular networks," *IEEE Transactions on Wireless Communications*, vol. 10, no. 2, pp. 413–418, Feb. 2011.

[47] W. Zhong, Y. Fang, S. Jin, K. K. Wong, S. Zhong, and Z. Qian, "Joint resource allocation for device-to-device communications underlaying uplink MIMO cellular networks," *IEEE Journal on Selected Areas in Communications*, vol. 33, no. 1, pp. 41–54, Jan. 2015.

[48] X. Shen, "Device-to-device communication in 5G cellular networks," *IEEE Network*, vol. 29, no. 2, pp. 2–3, Mar. 2015.

[49] A. Gupta and R. K. Jha, "A survey of 5G network: Architecture and emerging technologies," *IEEE Access*, vol. 3, pp. 1206–1232, 2015.

[50] J. Qiao, X. S. Shen, J. W. Mark, Q. Shen, Y. He, and L. Lei, "Enabling device-to-device communications in millimeter-wave 5G cellular networks," *IEEE Communications Magazine*, vol. 53, no. 1, pp. 209–215, Jan. 2015.

[51] A. T. Gamage, H. Liang, R. Zhang, and X. Shen, "Device-to-device communication underlaying converged heterogeneous networks," *IEEE Wireless Communications*, vol. 21, no. 6, pp. 98–107, Dec. 2014.

[52] M. Usman, A. A. Gebremariam, U. Raza, and F. Granelli, "A software-defined device-to-device communication architecture for public safety applications in 5G networks," *IEEE Access*, vol. 3, pp. 1649–1654, 2015.

[53] M. Abolhasan, J. Lipman, W. Ni, and B. Hagelstein, "Software-defined wireless networking: Centralized, distributed, or hybrid?" *IEEE Network*, vol. 29, no. 4, pp. 32–38, Jul. 2015.

[54] P. Belotti, C. Kirches, S. Leyffer, J. Linderoth, J. Luedtke, and A. Mahajan, "Mixed-integer nonlinear optimization," Mathematics and Computer Science Division, Argonne National Laboratory, Argonne, Illinois, U.S.A., Tech. Rep., Mar. 2012.

[55] C.-H. Yu, O. Tirkkonen, K. Doppler, and C. Ribeiro, "On the performance of device-to-device underlay communication with simple power control," in *IEEE 69th Vehicular Technology Conference*, 2009, pp. 1–5.

[56] P. Jänis, C.-H. Yu, K.Dopper, C. Ribeiro, C. Wijting, K. Hugl, O. Tirkkonen, and V. Koivunen, "Device-to-device communication underlaying cellular communication systems," *International Journal on Communications, Network and System Science*, 2009.

[57] P. Jänis, V. Koivunen, C. Ribeiro, J. Korhonen, K. Doppler, and K. Hugl, "Interference-aware resource allocation for device-to-device radio underlaying cellular networks," in *IEEE 69th Vehicular Technology Conference*, 2009, pp. 1–5.

[58] S. Xu, H. Wang, T. Chen, Q. Huang, and T. Peng, "Effective interference cancellation scheme for device-to-device communication underlaying cellular networks," in *IEEE 72nd Vehicular Technology Conference Fall (VTC 2010-Fall), 2010*, Sept. Pp. 1–5.

[59] D. Feng, L. Lu, Y. Yuan-Wu, G. Li, G. Feng, and S. Li, "Device-to-device communications underlaying cellular networks," *Communications, IEEE Transactions on*, vol. 61, no. 8, pp. 3541–3551, Aug. 2013.

[60] D. H. Lee, K. W. Choi, W. S. Jeon, and D. G. Jeong, "Two-stage semi-distributed resource management for device-to-device communication in cellular networks," *IEEE Trans. Wireless Commun.*, vol. 13, no. 4, pp. 1908–1920, Apr. 2014.

[61] Q. Ye, M. Al-Shalash, C. Caramanis, and J. G. Andrews, "Distributed resource allocation in device-to-device enhanced cellular networks," *IEEE Transactions on Communications*, vol. 63, no. 2, pp. 441–454, Feb. 2015.

[62] M. Sheng, Y. Li, X. Wang, J. Li, and Y. Shi, "Energy efficiency and delay tradeoff in device-to-device communications underlaying cellular networks," *IEEE Journal on Selected Areas in Communications*, vol. 34, no. 1, pp. 92–106, 2016.

[63] L. Wei, R. Q. Hu, Y. Qian, and G. Wu, "Energy efficiency and spectrum efficiency of multihop device-to-device communications underlaying cellular networks," *IEEE Transactions on Vehicular Technology*, vol. 65, no. 1, pp. 367–380, Jan. 2016.

[64] Y. Zhao, Y. Li, H. Zhang, N. Ge, and J. Lu, "Fundamental tradeoffs on energy-aware D2D communication underlaying cellular networks: a dynamic graph approach," *IEEE Journal on Selected Areas in Communications*, vol. 8716, no. c, pp. 1–1, 2016.

[65] X. Xu, Y. Zhang, Z. Sun, Y. Hong, and X. Tao, "Analytical modeling of mode selection for moving D2D enabled cellular networks," *IEEE Communications Letters*, vol. 20, no. 6, pp. 1–1, 2016.

[66] R. Yin, C. Zhong, G. Yu, Z. Zhang, K.-K. Wong, and X. Chen, "Joint spectrum and power allocation for D2D communications underlaying cellular networks," *IEEE Transactions on Vehicular Technology*, vol. 65, no. 4, pp. 2182–2195, 2016.

[67] G. George, R. K. Mungara, and A. Lozano, "An analytical framework for device-to-device communication in cellular networks," *IEEE Transactions on Wireless Communications*, vol. 14, no. 11, pp. 6297–6310, 2015.

[68] X. Ma, J. Liu, and H. Jiang, "Resource allocation for heterogeneous applications with device-to-device communication underlaying cellular networks," *IEEE Journal on Selected Areas in Communications*, vol. 34, no. 1, pp. 15–26, 2016.

[69] W. Cheng, X. Zhang, and H. Zhang, "Optimal power allocation with statistical QoS provisioning for D2D and cellular communications over underlaying wireless networks," *IEEE Journal on Selected Areas in Communications*, vol. 34, no. 1, pp. 151–162, 2016.

[70] L. Song, D. Niyato, Z. Han, and E. Hossain, "Game-theoretic resource allocation methods for device-to-device communication," *IEEE Wireless Communications*, vol. 21, no. 3, pp. 136–144, Jun. 2014.

[71] L. Song, D. Niyato, Z. Han, and E. Hossain, "Game-theoretic resource allocation methods for device-to-device communication," *IEEE Wireless Communications*, vol. 21, no. 3, pp. 136–144, 2014.

[72] Z. Zhou, M. Dong, K. Ota, J. Wu, and T. Sato, "Energy efficiency and spectral efficiency tradeoff in device-to-device (D2D) communications," *IEEE Wireless Communications Letters*, vol. 3, no. 5, pp. 485–488, 2014. arXiv: 1407.1556.

[73] R. Yin, G. Yu, H. Zhang, Z. Zhang, and G. Y. Li, "Pricing-based interference coordination for D2D communications in cellular networks," *IEEE Transactions on Wireless Communications*, vol. 14, no. 3, pp. 1519–1532, 2015.

[74] W. Zhong, Y. Fang, S. Jin, K. K. Wong, S. Zhong, and Z. Qian, "Joint resource allocation for device-to-device communications underlaying uplink mimo cellular networks," *IEEE Journal on Selected Areas in Communications*, vol. 33, no. 1, pp. 41–54, 2015.

[75] H.-h. Nguyen, M. Hasegawa, and W.-j. Hwang, "Distributed resource allocation for D2D communications underlay cellular networks," vol. 20, no. 5, pp. 942–945, 2016.

[76] Y. Li, D. Jin, J. Yuan, and Z. Han, "Coalitional games for resource allocation in the device-to-device uplink underlaying cellular networks," *IEEE Transactions on Wireless Communications*, vol. 13, no. 7, pp. 3965–3977, 2014.

[77] Y. Xiao, K.-c. Chen, C. Yuen, S. Member, Z. Han, L. A. Dasilva, and S. Member, "A bayesian overlapping coalition formation game for device-to-device spectrum sharing in cellular networks," *IEEE Transactions on Wireless Communications*, vol. 14, no. 7, pp. 4034–4051, 2015.

[78] S. Maghsudi and S. Stanczak, "Hybrid centralized-distributed resource allocation for device-to-device communication underlaying cellular networks," *IEEE Transactions on Vehicular Technology*, vol. 9545, no. c, pp. 1–1, 2015.

[79] H. Min, J. Lee, S. Park, and D. Hong, "Capacity enhancement using an interference limited area for device-to-device uplink underlaying cellular networks," *IEEE Transactions on Wireless Communication*, vol. 10, no. 12, pp. 3995–4000, 2011.

[80] J. Wang, D. Zhu, C. Zhao, J. Li, and M. Lei, "Resource sharing of underlaying device-to-device and uplink cellular communications," *IEEE Communications Letters*, vol. 17, no. 6, pp. 1148–1151, 2013.

[81] W. Guo, S. Wang, and X. Chu, "Capacity expression and power allocation for arbitrary modulation and coding rates," in *IEEE Wireless Communications and Networking Conference*, China, Apr. 2013.

[82] 3. TSG-RAN, "Further advancements for E-UTRA physical layer aspects," 3GPP Technical Report, 3G TR 36.814 v9.0.0, Mar. 2010.

[83] S. Boyd and L. Vandenberghe, "Convex optimization," in. Cambridge University Press, 2004, ch. 3 Covex Function.

[84] J. Nocedal and S. J. Wright, "Numerical optimization," in, 2nd. Springer, 2006.

[85] E. Süli and D. F. Mayers, *An Introduction to Numerical Analysis*. Cambridge University Press, 2003.

[86] M. Held and R. M. Karp, "A dynamic programming approach to sequencing problems," in *Proceedings of the 16th ACM national meeting*, New York, USA, 1961, pp. 71.201–71.204.

[87] R. Ahlswede, N. Cai, S.-Y. Li, and R. Yeung, "Network information flow," *IEEE Trans. Inf. Theory*, vol. 46, no. 4, pp. 1204–1216, Jul. 2000.

[88] S. Katti, H. Rahul, W. Hu, D. Katabi, M. Medard, and J. Crowcroft, "XORs in the air: Practical wireless network coding," *IEEE/ACM Trans. Netw.*, vol. 16, no. 3, pp. 497–510, Jun. 2008.

[89] P. Gupta and P. Kumar, "The capacity of wireless networks," *IEEE Trans. Inf. Theory*, vol. 46, no. 2, pp. 388–404, Mar. 2000.

[90] J. Laneman, D. Tse, and G. W. Wornell, "Cooperative diversity in wireless networks: Efficient protocols and outage behavior," *IEEE Trans. Inf. Theory*, vol. 50, no. 12, pp. 3062–3080, Dec. 2004.

[91] B. Rankov and A. Wittneben, "Spectral efficient protocols for half-duplex fading relay channels," *IEEE J. Sel. Areas in Commun.*, vol. 25, no. 2, pp. 379–389, Feb. 2007.

[92] D.-S. Chen, R. G. Batson, and Y. Dang, *Applied Integer Programming: Modeling and Solution*. Hoboken, NJ: Wiley, 2010.

[93] M. Jünger, T. Liebling, D. Naddef, G. L. Nemhauser, W. R. Pulleyblank, G. Reinelt, G. Rinaldi, and L. A. Wolsey, *50 Years of Integer Programming 1958–2008*. Springer, 2009.

[94] Q. Ye, M. Al-Shalash, C. Caramanis, and J. G. Andrews, "A tractable model for optimizing device-to-device communications in downlink cellular networks," in *IEEE International Conf. Commun. (ICC)*, Jun. 2014, pp. 2039–2044.

[95] ——, "Resource optimization in device-to-device cellular systems using time-frequency hopping," *IEEE Transactions on Wireless Communications*, vol. 13, no. 10, pp. 5467–5480, Oct. 2014.

[96] S. Wang, W. Guo, Z. Zhou, Y. Wu, and X. Chu, "Outage probability for multi-hop D2D communications with shortest path routing," *IEEE Communications Letters*, vol. 19, no. 11, pp. 1997–2000, Nov. 2015.

[97] T. Novlan, H. Dhillon, and J. Andrews, "Analytical modeling of uplink cellular networks," *Wireless Communications, IEEE Transactions on*, vol. 12, no. 6, pp. 2669–2679, Jun. 2013.

[98] A. Carroll and G. Heiser, "An analysis of power consumption in a smartphone," in *Proceedings of the 2010 USENIX Conference on USENIX Annual Technical Conference*, ser. USENIXATC'10, Boston, MA: USENIX Association, 2010, pp. 21–21.

[99] M. Haenggi, *Stochastic Geometry for Wireless Networks*. Cambridge University Press, 2013.

[100] Y. Wu, W. Liu, S. Wang, W. Guo, and X. Chu, "Network coding in device-to-device (D2D) communications underlaying cellular networks," presented at IEEE Int. Conf. on Commun., London, U.K., 2015.

[101] S. Boyd and L. Vandenberghe, "Convex optimization," in. Cambridge University Press, 2004, ch. 3 Covex Function.

[102] W. Dinkelbach, "On nonlinear fractional programming," *Management Science*, vol. 13, no. 7, pp. 492–498, 1967.

[103] M. Ni, L. Zheng, F. Tong, J. Pan, and L. Cai, "A geometrical-based throughput bound analysis for device-to-device communications in cellular networks," *IEEE Journal on Selected Areas in Communications*, vol. 33, no. 1, pp. 100–110, Jan. 2015.

[104] A. Legout, G. Urvoy-Keller, and P. Michiardi, "Rarest first and choke algorithms are enough," in *Proceedings of the 6th ACM SIGCOMM Conference on Internet Measurement*, Rio de Janeriro, Brazil, 2006.

[105] I. Stoica, R. Morris, D. Liben-Nowell, D. R. Karger, M. F. Kaashoek, F. Dabek, and H. Balakrishnan, "Chord: A scalable peer-to-peer lookup protocol for internet applications," *IEEE/ACM Trans. Netw.*, vol. 11, no. 1, pp. 17–32, Feb. 2003.

[106] Q. Li, H. Li, J. Russell P., Z. Chen, and C. Wang, "CA-P2P: Context-aware proximity-based peer-to-peer wireless communications," *Communications Magazine, IEEE*, vol. 52, no. 6, pp. 32–41, Jun. 2014.

[107] M. Großmann, "Proximity enhanced mobile D2D video streaming," in *Proceedings of the 18th Annual International Conference on Mobile Computing and Networking (Mobicom '12)*, Istanbul, Turkey, 2012, pp. 427–430.

[108] J. Kim, F. Meng, P. Chen, H. E. Egilmez, D. Bethanabhotla, A. F. Molisch, M. J. Neely, G. Caire, and A. Ortega, "Adaptive video streaming for device-to-device mobile platforms," in *Proceedings of the 19th Annual International Conference on Mobile Computing Networking (MobiCom '13)*, USA, 2013, pp. 127–130.

[109] V. Ayadurai and M. Prytz, "Software radio platform for network-assisted device-to-device (NA-D2D) concepts," in *Proceedings of the Second Workshop on Software Radio Implementation Forum (SRIF 13')*, Hong Kong, China, 2013, pp. 53–60.

[110] M. Zulhasnine, C. Huang, and A. Srinivasan, "Exploiting cluster multicast for P2P streaming application in cellular system," in *IEEE Wireless Communications and Networking Conference (WCNC)*, Apr. 2013, pp. 4493–4498.

[111] Y. Shen, W. Zhou, P. Wu, L. Toni, P. Cosman, and L. Milstein, "Device-to-device assisted video transmission," in *Proceedings of the 20th International Packet Video Workshop (PV)*, Dec. 2013, pp. 1–8.

[112] M. Cha, H. Kwak, P. Rodriguez, Y.-Y. Ahn, and S. Moon, "I tube, you tube, everybody tubes: Analyzing the world's largest user generated content video system," in *Proceedings of the 7th ACM SIGCOMM Conference on Internet Measurement*, ser. IMC '07, San Diego, California, USA: ACM, 2007, pp. 1–14.

[113] D. W. K. Ng, E. S. Lo, and R. Schober, "Dynamic resource allocation in MIMO-OFDMA systems with full-duplex and hybrid relaying," *IEEE Transactions on Communications*, vol. 60, no. 5, pp. 1291–1304, 2012.

[114] E. J. O'neil, P. E. O'Neil, G. Weikum, and E. Zurich, "The LRU-K page replacement algorithm for database disk buffering," in *ACM SIGMOD International Conference on Management of Data*, 1993, pp. 297–306.

[115] C.-H. Lin, S.-A. Yuan, S.-W. Chiu, and M.-J. Tsai, "Progressface: An algorithm to improve routing efficiency of GPSR-like routing protocols in wireless Ad Hoc networks," *IEEE Trans. on Comput.*, vol. 59, no. 6, pp. 822–834, Jun. 2010.

[116] A. E. Gamal and Y.-H. Kim, *Network Information Theory*. Cambridge University Press, 2011.

[117] P. M. Pardalos and J. B. Rosen, *Constrained Global Optimization: Algorithms and Applications*. Springer Berlin Heidelberg, 1987.

[118] J. E. Falk and R. M. Soland, "An algorithm for separable nonconvex programming problems," *Management Science*, vol. 15, no. 9, pp. 550–569, 1969.

[119] H. P. Benson, "Separable concave minimization via partial outer approximation and branch and bound," *Operations Research Letters*, vol. 9, no. 6, pp. 389–394, Nov. 1990.

[120] 3GPP, "RP-140808: review of regulatory requirements for unlicensed spectrum," Alcatel-Lucent, Alcatel-Lucent Shanghai Bell, Ericsson, Huawei, HiSilicon, IAESI, LG, Nokia, NSN, Qualcomm, NTT Docomo, Technical Report, 2014.

[121] R. Zhang, M. Wang, L. Cai, Z. Zheng, and X. Shen, "LTE-unlicensed: The future of spectrum aggregation for cellular networks," *Wireless Communications, IEEE*, vol. 22, no. 3, pp. 150–159, Jun. 2015.

[122] Q. Ye, M. Al-Shalash, C. Caramanis, and J. Andrews, "Resource optimization in Device-to-Device cellular systems using time-frequency hopping," *IEEE Transactions on Wireless Communications*, vol. 13, no. 10, pp. 5467–5480, Jul. 2014.

[123] M. Ni, L. Zheng, F. Tong, J. Pan, and L. Cai, "A geometrical-based throughput bound analysis for device-to-device communications in cellular networks," *IEEE Journal on Selected Areas in Communications (JSAC)*, vol. 33, no. 1, pp. 100–110, Jan. 2015.

[124] S. Wang, W. Guo, Z. Zhou, Y. Wu, and X. Chu, "Outage probability for multi-hop D2D communications with shortest path routing," *IEEE Communications Letters*, Sep. 2015.

[125] G. Parissidis, M. Karaliopoulos, T. Spyropoulos, and B. Plattner, "Interference-aware routing in wireless multihop networks," *IEEE Transactions on Mobile Computing*, vol. 10, no. 5, pp. 716–733, May 2011.

[126] Y. Li, C. Song, D. Jin, and S. Chen, "A dynamic graph optimization framework for multihop device-to-device communication underlaying cellular networks," *IEEE Wireless Commun.*, vol. 21, no. 5, pp. 52–61, Oct. 2014.

[127] H. Yuan, W. Guo, and S. Wang, "Emergency route selection for D2D cellular communications during an urban terrorist attack," in *IEEE International Conference on Communications Workshops (ICC)*, Sydney, Jun. 2014, pp. 237–242.

[128] C. Lin, S. Yuan, S. Chiu, and M. Tsai, "Progressface: An algorithm to improve routing efficiency of GPSR-like routing protocols in wireless Ad hoc networks," in *IEEE Transactions on Computers*, vol. 59, Jun. 2010, pp. 822–834.

[129] Y. Wu, W. Liu, S. Wang, W. Guo, and X. Chu, "Network coding in device-to-device (D2D) communications underlaying cellular networks," in *IEEE International Conference on Communications (ICC)*, Jun. 2015, pp. 2072–2077.

[130] Y. Sanada and Q. Wang, "A co-channel interference cancellation technique using orthogonal convolutional codes on multipath Rayleigh fading channel," *IEEE Transactions on Vehicular Technology*, vol. 46, no. 1, pp. 114–128, Feb. 1997.

[131] M. O. Hasna, M. S. Alouini, A. Bastami, and E. S. Ebbini, "Performance analysis of cellular mobile systems with successive co-channel interference cancellation," *IEEE Transactions on Wireless Communications*, vol. 2, no. 1, pp. 29–40, Jan. 2003.

[132] S. Zhang, S. C. Liew, and H. Wang, "Blind known interference cancellation," *IEEE Journal on Selected Areas in Communications*, vol. 31, no. 8, pp. 1572–1582, Aug. 2013.

[133] W. Chen, K. B. Letaief, and Z. Cao, "Network interference cancellation," *IEEE Transactions on Wireless Communications*, vol. 8, no. 12, pp. 5982–5999, Dec. 2009.

[134] A. Agrawal, J. G. Andrews, J. M. Cioffi, and T. Meng, "Iterative power control for imperfect successive interference cancellation," *IEEE Transactions on Wireless Communications*, vol. 4, no. 3, pp. 878–884, May 2005.

[135] M. C. Gonzalez, C. A. Hidalgo, and A.-L. Barabasi, "Understanding individual human mobility patterns," *Nature*, vol. 453, no. 7196, pp. 779–782, Jun. 2008.